An Electron Microscopy Study into Vps1 and the role of its F-actin Binding Regions within Clathrin-mediated Endocytosis

JOHNSON, SIMEON,RICHARD

An Electron Microscopy Study into Vps1 and the role of its F-actin Binding Regions within Clathrin-mediated Endocytosis

Author: Simeon R Johnson (BSc)

Supervisors: Dr Martin W Goldberg and Dr Tim J Hawkins

Abstract: Clathrin-mediated endocytosis is a conserved process utilised by metazoans and fungi for the internalisation of cell surface receptors into vesicles upon ligand binding. This is a vital process by which cells are able to communicate with other cells and there external environment. Transmission electron microscopy of endocytic sites in F-actin binding mutants of *S. cerevisiae* suggest an absolute requirement for Vps1p to bind F-actin in order to generate directional propagation of an invaginations against the internal osmotic pressure of the cell. Structural observations of endocytic pits by electron tomography revealed a dynamin-like structure indicative of a mode of scission analogous to that carried out by dynamin-1. Following this observation similarity searches were conducted between dynamin-1 and Vps1p revealing conservation of primary and secondary structure between the two proteins within the GTPase domain, middle domain and GTPase effector domain. Supported by recent findings the observations recorded here favour a model of scission that incorporates Vps1p in a manner that is comparable with its mammalian homologue, dynamin-1.

Acknowledgments: I’d like to thank Dr Martin W Goldberg and Dr Tim J Hawkins for their supervision throughout my masters and providing myself with continuous support with my academic development. I’d further like to thank Mrs Christine Richards and Mrs Helen Grindley for providing training in electron microscopy sample preparation and imaging techniques and in particular to Mrs Christine Richards for help with development of new protocols for electron microscopy sample preparation. Thank you also to Dr Budhika Mendis for training in electron tomography image acquisition and tomogram reconstruction. Finally a thank you to Dr Ritu Mishra for initial training in yeast culture techniques and to Prof Kathryn Ayscough for providing the mutant yeast strains that made this project possible.

Contents

List of Abbreviations

Abbreviation	Definition
DC	Day culture
DO	Drop-out
FixI1	Immuno Fixative 1: 0.1%UA in acetone with 2%H2O
FixI2	Immuno Fixative 2: 0.25%GA and 0.1%UA in acetone
FixU1	Ultrastructural Fixative 1: 2%GA, 0.1%UA and 5%H2O in acetone
FixU2	Ultrastructural Fixative 2: 1%OSO4, 2%GA, 0.5%UA and 5%H2O in acetone
FS1	Freeze Substitution 1: -90˚C→0˚C at 90
FS2	Freeze Substitution 2: -90˚C→0˚C at 6˚/h
FS3	Freeze Substitution 3:-90˚C→-50˚C at 1˚C/h
FS4	Freeze Substitution 4:-90˚C→-20˚C at 1˚C/h
FS5	Freeze Substitution 5:-90˚C→-50 ˚C at 0.5˚C/h
FS6	Freeze Substitution 6:-90˚C→-20 ˚C at 2˚C/h
FS7	Freeze Substitution 7:-90˚C→-50˚C at 0.5˚C/h
FS8	Freeze Substitution 8:-90˚C→-20˚C at 2˚C/h
GA	Glutaraldehyde
GAM	Goat anti-mouse
GAR	Goat anti-rat
GED	GTPase effector domain
GFP	Green fluorescent protein
GαGFP	Goat anti-GFP
HPF	High pressure freezing
LR	Lowicryl resin
LTE1	Low Temperature Embedding: Temperature maintained at -50˚C. 10%HM20→100%HM20 serial concentration at 10%incriments/24h
LTE2	Low Temperature Embedding: Temperature maintained at -25˚C. 10%LR White→100%LR White serial concentration at 10%incriments/24h
LTE3	Low Temperature Embedding: Temperature maintained at -50˚C. 10%HM20→100%HM20 serial concentration at 20%incriments/24h
LTE4	Low Temperature Embedding: Temperature maintained at -25˚C. 10%LR White→100%LR White serial concentration at 20%incriments/24h
MαGFP	Mouse anti-GFP
NPF	Nucleation promotion factor
OD	Optical density
ONC	Overnight culture
PH	Plekstrin homology
PRD	Proline rich domain
RTE1	Room Temperature Embedding: 50%Epon for 24h→100%Epon for 24h
RTE2	Room Temperature Embedding: 50%LR White for 24h→100%LR White for 24h
RTE3	Room Temperature Embedding: 10%Epon→100% Epon serial concentration at 10%incriments/24h
RTE4	Room Temperature Embedding: 10%LR White→100% LR White serial concentration at 10%incriments/24h
SD	Selective drop-out

Abbreviation	Definition
SDS	Sodium dodecyl sulphate
SEM	Scanning electron microscope
SH3	Src homology three binding domain
TEM	Transmission electron microscope
TIRF	total internal reflection fluorescence
UA	Uranyl acetate
WASP	Wiscott-Aldritch syndrome protein

List of Figures

List of Tables

List of Tables

1.1 A Brief Overview of Clathrin-Mediated Endocytosis in *S. Cerevisiae*

Endocytosis is the process of taking in matter by a living organism via invagination of the membrane to form a vesicle. Of the many forms of endocytosis the most widely studied is clathrin-mediated endocytosis. This endocytic pathway is the dominant form observed in both fungal and metazoan species and is essential for a diverse array of processes from normal functioning nerve terminals in mammals to internalisation of alpha-factor in yeast. The system at the centre of this study is that provided by *S. cerevisiae*, utilised for its robust genetics and similarity with mammalian endocytosis; exhibiting conservation of the broad stages and use of homologous proteins. Here a general overview of the endocytic cascade within *S. cerevisiae* will be presented with reference to relevant yeast proteins, and where possible the mammalian homologues will be listed in brackets.

The endocytic cascade comprises three broad stages, aptly called early-, mid- and late-endocytosis (figure 1). These stages represent coat-assembly, invagination and scission/inward movement of the vesicle respectively (See Weinberg & Drubin, 2012 for review). The process requires the recruitment and arrangement of in excess of 50 different proteins to the plasma membrane in a spatiotemporal specific manner.

Although the various proteins thought to be involved within the endocytic cascade have been well characterised in the main, the factors that determine where and when an endocytic site will form remain ambiguous. It has been suggested that lipid signalling may be responsible as the two earliest coat proteins to arrive, Ede1p (Eps15) and Syp1p (FCho 1/2) bind to the membrane in a ubiquitin-dependant manner and via an F-BAR domain, respectively (Aguilar & Wendland, 2003). F-BAR domains confer the ability of proteins to bind the membrane lipid phosphatydylserine, linking the endocytic machinery to the plasma membrane. The F-BAR motif has also been exemplified as a membrane curving and tabulating protein when it forms complex oligomeric and polymeric structures (Itoh & De Camilli, 2006; Madsen, Bhatia, Gether, & Stamou, 2010). These characteristics explain the importance of early endocytic proteins in providing a platform on which later arriving endocytic proteins can assemble. What has been clarified through use of fluorescent alpha-factor and

fluorescently labelled endocytic proteins, is that the endocytic cargo accumulates after the arrival of Ede1p (Eps15) but before Sla1p (intersectin/CIN85) (Toshima et al., 2006).

The variable timings of the early coat proteins spent at the plasma membrane compared with the regular lifetimes of later proteins suggests a molecular checkpoint. This may well be to ensure an appropriate cargo is loaded or that the cargo is fully loaded prior to the arrival of the late coat and WASP/Myo complex which drives invagination of the membrane (Boettner et al., 2009; Sun, Martin, & Drubin, 2006; Urbanek, Smith, Allwood, Booth, & Ayscough, 2013). The mechanism implicated is still being disputed with early work favouring a ubiquitin-dependant mechanism suggested by increased internalisation of ubiquitinated cargo (Aguilar, Watson, & Wendland, 2003; Hicke & Riezman, 1996). Later work portrays a non-specific mechanism, since mutagenic analysis of ubiquitin binding motifs within early and early coat proteins revealed an overall decrease in internalisation but not specifically to ubiquitinated cargoes suggesting ubiquitin regulates a more generic step (Dores, Schnell, Maldonado-Baez, Wendland, & Hicke, 2010). The overall decrease in internalisation portrays ubiquitin to be more of a stabilising component of the coat proteins.

Accumulation of cargo is swiftly followed by acquisition of the late coat proteins producing a connection between the cargo, plasma membrane and endocytic machinery (figure 1). Among the late coat proteins to arrive is Sla1p, which forms part of the Sla1p (intersectin/ CIN85)-End3p (Eps15)-Pan1p (intersectin) complex (Mahadev et al., 2007; Warren, Andrews, Gourlay, & Ayscough, 2002; Yu & Cai, 2004; Zeng, Yu, & Cai, 2001). Sla1p provides a vital link between the coat proteins and the actin cytoskeleton via its interaction with all three yeast Arp2/3 activating proteins, linking actin dynamics to the coat proteins, driving invagination (Warren et al., 2002; Yu & Cai, 2004; Zeng et al., 2001).

The arrival of the actin nucleation promotion factor (NPF), Las17 (WASP/N-WASP) marks the transition from early to mid-endocytosis (figure 1). Mutations of this complex perturb internalisation of endocytic cargoes attributed to a loss of F-actin at the endocytic patches showing a similar phenotype to latrunculin-A treated cells (Ayscough et al., 1997; Morton, Ayscough, & McLaughlin,

2000; Sun et al., 2006; Urbanek et al., 2013; Yu & Cai, 2004). Although Las17p (WASP/N-WASP) is deemed to be the key NPF there are several other candidates including Abp1p (ABP1) and Pan1p (intersectin) for which less severe phenotypes were observed (Nannapaneni et al., 2010; Sun et al., 2006).

Actin polymerisation is generated through activation of Arp2/3p (Arp2/3) complex by the Abp1p (ABP1)-Las17p (WASP/N-WASP)-Bzz1p (syndapin) complex. This complex links the power of actin polymerisation to the coat proteins via Sla1p (intersectin/ CIN85)-End3p (Eps15)-Pan1p (intersectin) complex (Mahadev et al., 2007; Warren et al., 2002; Yu & Cai, 2004; Zeng et al., 2001). Vps1p (dynamin) has been shown to colocalize with Sla1p (intersectin/ CIN85) at endocytic sites providing an indirect link with F-actin (Mahadev et al., 2007; Smaczynska-de Rooij et al., 2010; Wang, Sletto, Tenay, & Kim, 2011).

Following invagination the scission event results from the actions of a multitude of proteins of which Rvs161/167p (amphiphysins) are thought to be of central importance. Initially it was hypothesized that Rvs161/167 (amphiphysins) heterodimer was responsible for generating the scission in cohort with forces exerted by actin polymerisation (Dawson, Legg, & Machesky, 2006a; Kishimoto et al., 2011; J. Liu, Kaksonen, Drubin, & Oster, 2006; Wang et al., 2011; Youn et al., 2010). Rvs161/167 have been demonstrated to self-assemble into a "collar" configuration at the neck of the bud via their N-BAR domains and amphipathic helices, bringing adjacent sides of the membrane into close enough proximity to induce a scission (Youn et al., 2010). Post scission the coat proteins disassemble through a variety of factors including phosphorylation of various coat proteins including the Sla1p-Pan1p-End3p complex by Ark1p and Prk1p kinases (Toret, Lee, Sekiya-Kawasaki, & Drubin, 2008; Wang et al., 2011; Yu & Cai, 2004).

(a)

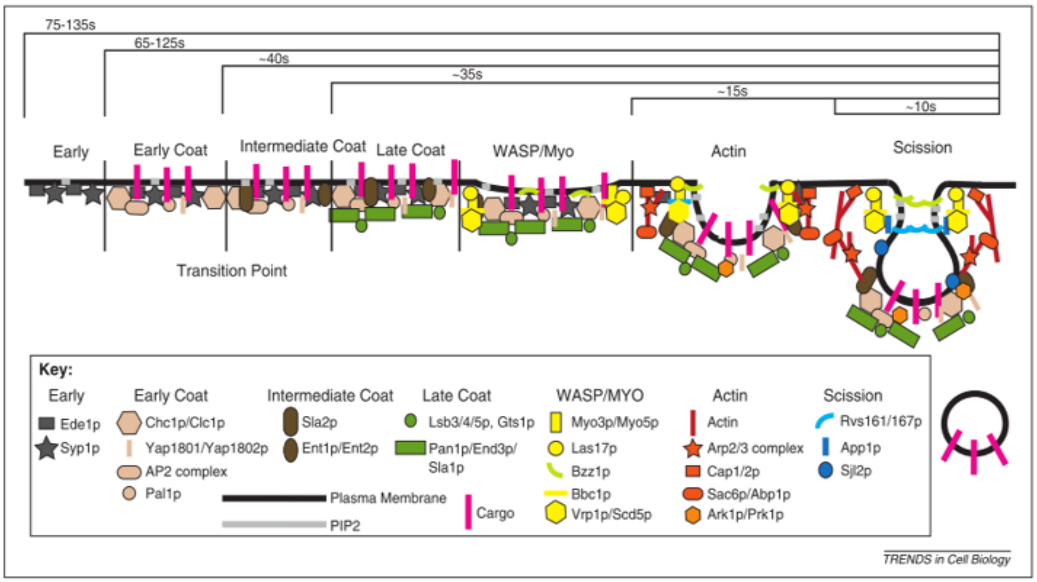

(b)

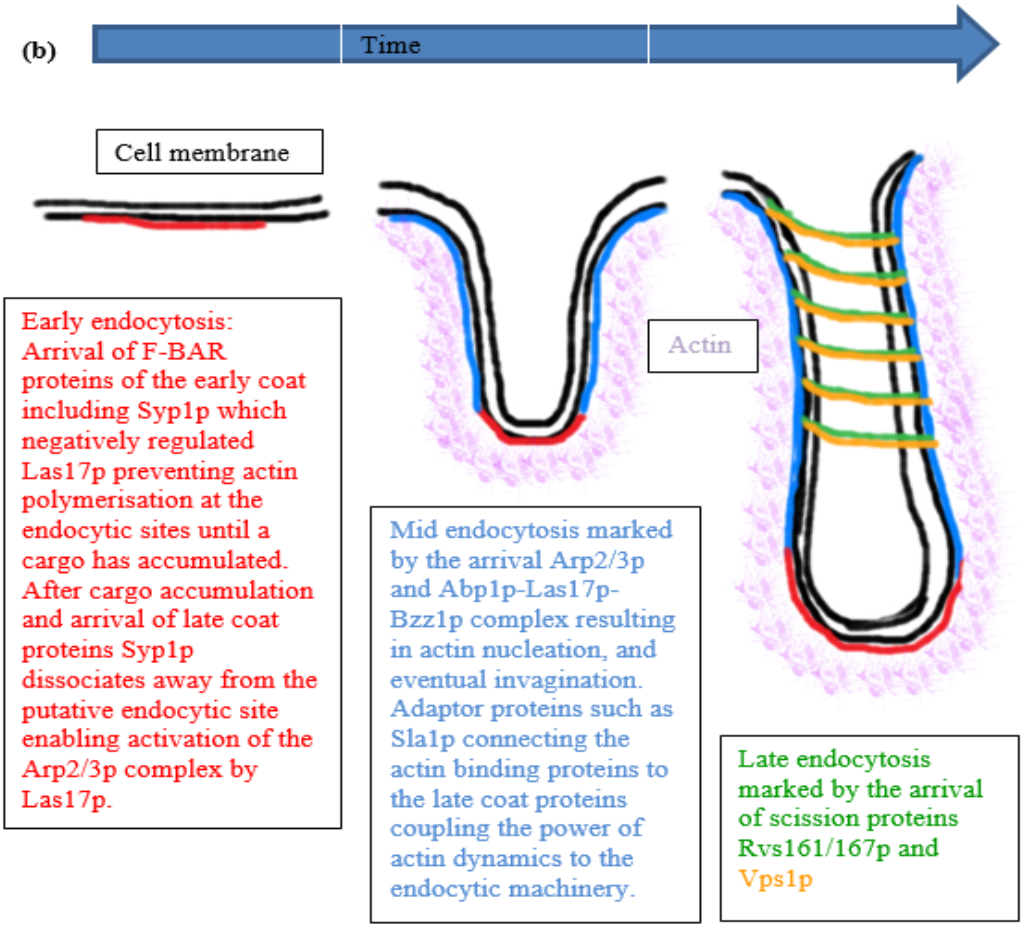

Figure 1: (a) Depicts the ordered recruitment of endocytic proteins to the plasma membrane relative to recorded occupancies. However this model omits Vps1 and acknowledges no interaction between Rvs161/167 and Sla1p or Vps1 and Sla1p. (Taken from Weinberg & Drubin 2012) **(b)** A simplified model of the complex stages illustrated above illustrating key proteins representative of the different stages with the crucial addition of Vps1 and arrangement with Rvs167 deduced from the literature. Colours of the writing correspond to colours within the schematic.

1.2 Vps1: An Endocytic Protein

Vps1p was previously characterised as a yeast dynamin involved in various cellular processes including production of peroxisomes and vacuole fusion and fission (Hoepfner, van den Berg, Philippsen, Tabak, & Hettema, 2001a; Nothwehr, Conibear, & Stevens, 1995; Röthlisberger, Jourdain, Johnson, Takegawa, & Hyams, 2009). Until recently the role of this protein within an endocytic context had been ignored or at best acknowledged as peripheral as deletion of *vps1p* did not perturb the endocytic process unlike in mammalian systems where dynamin is central to the endocytic cascade, vital for the scission of the vesicle from the membrane (Damke, 1994; Danino, Moon, & Hinshaw, 2004; Herskovits, Burgess, Obar, & Vallee, 1993; Ochoa et al., 2000; Ramachandran, 2011; Smaczynska-de Rooij et al., 2010). The basic domain structure of Vps1p is similar to that of the classical mammalian dynamins (dynamin-1 and dynamin-2) having an N-terminal GTPase and C-terminal GTPase effector domain (GED) adjoined by a central domain (figure 2). Homogeneity of domain structure would suggest an overlap in the function of Vps1 with dynamin-1. However the PRD and PH domains are absent from Vps1p which might account for some of the subtle differences between how Vps1p and dynamin-1 perform *in vito*.

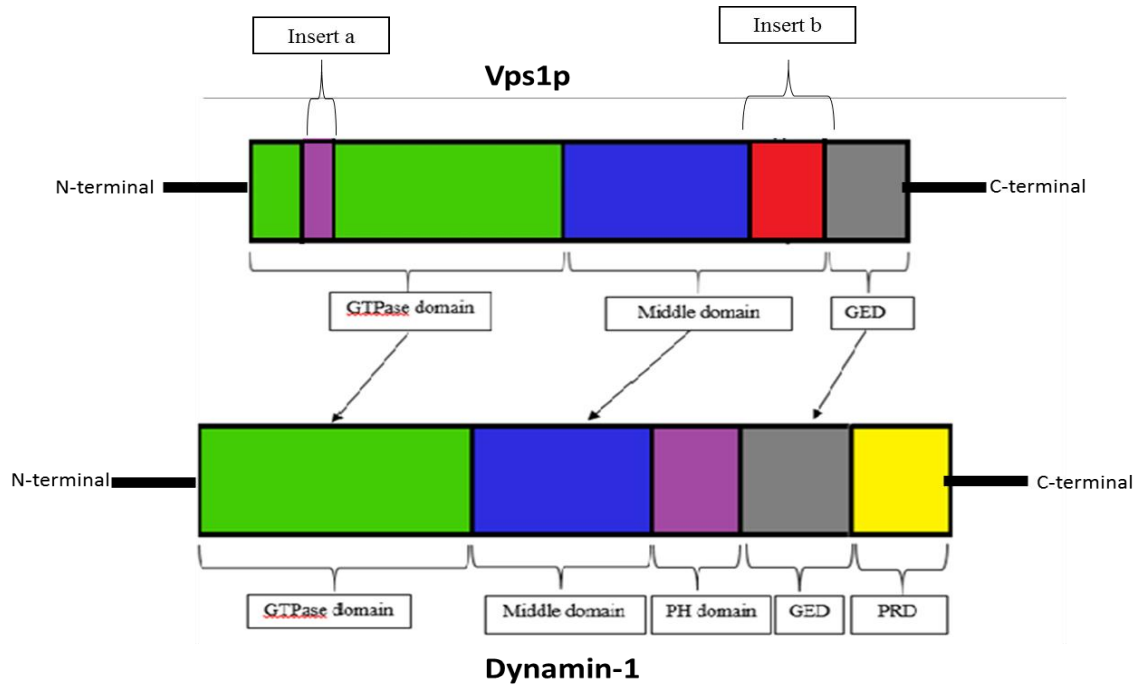

Figure 2: An illustration of the domain structure of Vps1 compared with that of dynamin to highlight conservation of key domains that provide this protein with the ability to self-assemble in a GTP-dependant manner similar to that of Dynamin-1. This configuration can help us to further speculate as

to how Vps1 could perform scission in a way that follows that of dynamin-1 in mammalian endocytosis.

Vps1p deletion mutants produced reduced rates of internalisation of the lipophilic dye FM4-64 suggested an involvement within the endocytic cascade (Smaczynska-de Rooij et al., 2010). The same study also illustrated increased occupancies at the membrane for Ent1p, Sla2p, Las17p, Abp1p, and Sac6p representative of the early, mid and late stages of endocytosis in addition to colocalisations with Abp1p and Sla1p (figure 1). The effect on residencies demonstrates an importance within the endocytic cascade whilst the colocalisations at endocytic patches confirm its direct involvement within the process. Association of Vps1p with Abp1p and Sla1p suggest an involvement within the scission event which was further supported by increased patch retraction/failure to scission in *vps1p* null mutants as indicted by kymographs tracking the coat proteins Sla1p and End3p. The yeast WASP homologue Las17p which normally resides at the membrane throughout the endocytic event was noted to invaginate and retract in conjunction with the coat proteins which suggests a failure in scission placing Vps1p as a scission related protein.

The deletion mutants provided some insight as to the role of Vps1 as it produced an increase in residency of Rvs167 at the endocytic site in addition to retraction of invagination. Rvs167 has been characterised as a scission protein as deletions or mutations of its amphipathic helices result in increased failure of cargo internalization i.e. the cargo-bearing vesicle is unable to detach from the plasma membrane producing an overall decrease in endocytosis (Smaczynska-de Rooij et al., 2012; Wang et al., 2011; Youn et al., 2010). However the persistence of endocytosis in *rvs167* mutants suggest other proteins at play can compensate for its function. The retraction of invaginations is a phenotype that has been observed in Rvs167p deletions suggesting an overlap in function with the amphiphysin proposed to be responsible for generating the scission event. Later biofluorescence complementation (BiFC) assays for Vps1p and Rvs167p demonstrated an interaction which was mapped using a yeast-two-hybrid approach and found to occur via a conserved typeI *src*-homology 3 (SH3) binding site within Vps1p confirming Vps1p as a protein implicated within the scission event (Smaczynska-de Rooij et al., 2012).

These findings place Vps1p within the scission event which is further supported by the synergistic effects observed in a double deletion of *rvs167*Δ*vps1p*Δ which produced a 60% retraction rate of invaginations compared with 39% in *vps1p*Δ and 31% in *rvs167*Δ (Smaczynska-de Rooij et al., 2010). Such a relationship is also apparent between mammalian dynamin-1 and amphiphysins suggesting Vps1p to be acting in a dynamin-1-like fashion (Itoh et al., 2005; Smaczynska-de Rooij et al., 2012; Vallis, Wigge, Marks, Evans, & McMahon, 1999).

This evidence characterises Vps1 as an endocytic protein and suggests possible roles within both elongation of the invagination and the scission event. The former by virtue of its colocalisations with over 80% of Sla1p-RFP at the cell membrane, which is linked to the actin dynamics via Sla2p that binds directly to actin via its ILEQ motifs (Smaczynska-de Rooij et al., 2010; Warren et al., 2002). Further to this, *in vitro*, Vps1 has exhibited a capacity to self-assemble and tubulate liposomes (Smaczynska-de Rooij et al., 2010, 2012). The latter is inferred through its co-localisation with Rvs167-RFP at the plasma membrane which is already widely accepted as the protein central to the scission event (Smaczynska-de Rooij et al., 2010).

1.3 A Model for Scission

Early models of scission in *S. cerevisiae* proposed Rvs161 and Rvs167 (homologues of the mammalian amphiphysins) as forming a heterodimeric complex at the neck of the bud (figure 3). *In vitro* Rvs161/167 has been shown to bind membranes in a curvature-independent manner promoting tubulation of liposomes *in vitro* (Youn et al., 2010). This observation demonstrates a capacity for Rvs161/167 to tubulate membranes but would suggest the requirement for other endocytic machinery to produce a scission. The nature of the N-BAR motifs attached to these proteins enables them to both adhere and curve membranes, bringing the adjacent sides of the membranes into close proximity resulting in scission (Kishimoto et al., 2011; J. Liu et al., 2006; Youn et al., 2010).

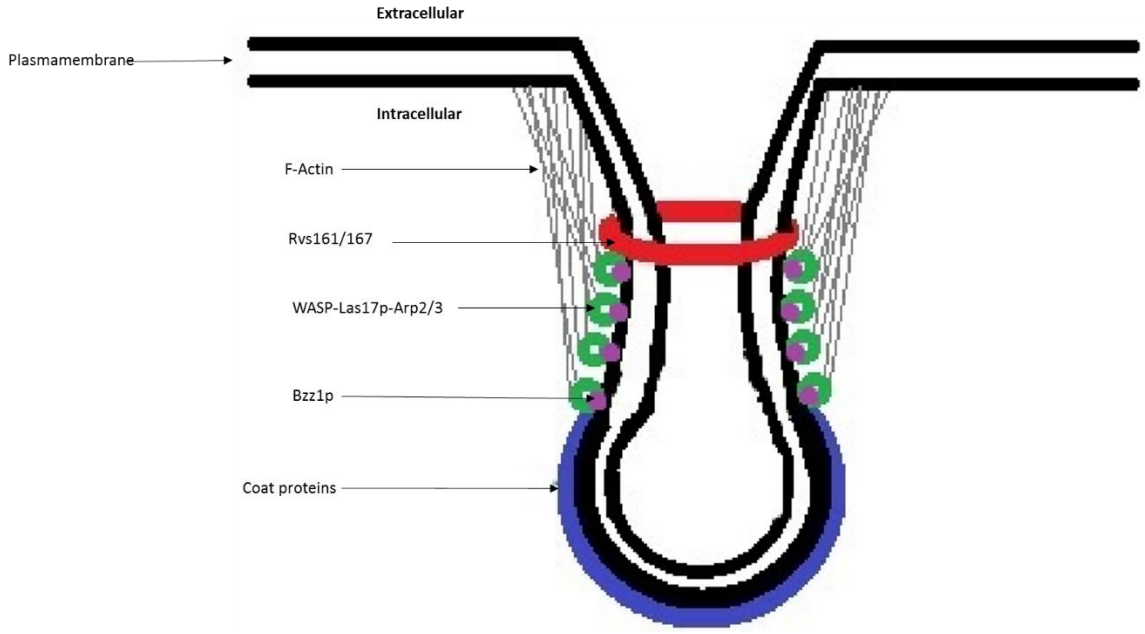

Figure 3: A depiction of a possible arrangement of the heterodimer Rvs161p/167p that could cause the walls of the invagination to become abutted engendering a fusion at the neck of the invagination, detaching the vesicle from the membrane when utilised in conjunction with actin nucleation. Actin nor Vps1p have been included at this stage as it is still not clear how these assemble in relation to Rvs161p/167p and actin dynamics. What is clear though is that all three are factors within the scission of the vesicle from the membrane. The evidence provided within this thesis will support a possible arrangement refractive of the data collected, in conjunction with existing studies carried out on Rvs161p/167p, Vps1p and actin.

However such forces were mathematically assessed as insufficient to induce a scission alone and analysis of these proteins *in vitro* did not reveal a capacity to emulsify indicative of scission but instead exhibited high levels of tubulation (Dawson et al., 2006a; Kishimoto et al., 2011; J. Liu et al., 2006; Youn et al., 2010). The lipids persist as continuous lamina (i.e. are not emulsified) and are not in droplet form from. This could be a result of cofactors required for scission being absent from the purification e.g. Vps1p, actin and the actin binding/nucleating proteins. Further to this Vps1p (dynamin) has been shown to share an overlap in function with Rvs167p (amphiphysin), and is implicated in working synergistically with Rvs167p to produce efficient scission (Smaczynska-de Rooij et al., 2012; Wang et al., 2011).What is producing this additional force and how might Vps1 be implicated within the scission event?

A theoretical model has been suggested where the transmembrane domains of the endocytic proteins act as “filters” segregating lipids based on charge (J. Liu et al., 2006). Proteins with an overall

positive charge would capture negatively charged lipids but would allow for unhindered diffusion of positive lipids along the invagination toward the bud and *vice versa*. This process can be further accelerated by intrinsic incompatibilities of lipids e.g. hydrophobic Vs hydrophilic, producing a phase separation between the lipids that form the neck and those that form the bud. The resultant line tension brings adjacent sides of the membrane at the bud-neck interface into close enough proximity for thermal fluctuations to be sufficient to initiate a fusion releasing the vesicle from the membrane. This model explains while even in the absence of key regulators of the scission event we still get endocytosis all be it at a reduced rate.

The stages of mammalian endocytosis up to the scission event show homogenity with the yeast model, exhibiting use of homologous proteins for conserved stages (see Weinberg and Drubin 2012 for review). For example although amphiphysins are utilised during the scission event in both systems their role is subordinate to that of dynamin-1 in clathrin-mediated endocytosis of mammalian systems which can be disrupted producing only small reduction in rates of cargo internalisation versus the much higher reductions observed in yeast (Dawson et al., 2006a; Vallis et al., 1999; Youn et al., 2010). Although amphiphysins contribute to membrane curvature and deformation through their association with dynamin-1, it is the mechanochemical constriction of oligomeric dynamin-1 that brings adjacent sides of the invagination into close enough proximity to produce a scission.

1.4 Actin in Endocytosis

Actin has been shown to be a key component of both mammalian and fungal clathrin-mediated endocytosis and in both systems appears to be involved in formation and shape of the invagination. In yeast cells actin has been suggested as being required to drive invagination of the membrane against the internal cellular pressure, exhibiting localisation to endocytic sites at the time point corresponding t invagination of the membrane (Aghamohammadzadeh & Ayscough, 2009). Mutational analysis of Arp2/3 binding sites within NPFs failed to perturb accumulation of actin at endocytic sites within yeast suggesting there dominant role might well be as adaptor proteins and less so as activators of the Arp2/3 complex (Galletta, Chuang, & Cooper, 2008). However mutations of the Arp2/3 complex

failed to perturb actin accumulation at endocytic sites suggesting other endocytic proteins to have actin nucleating abilities (Martin et al., 2005).

Dynamin-1 has been found to colocalize with F-actin at membrane locations where remodelling of the membrane is required for example at endocytic sites and podosomes (Bruzzaniti et al., 2005; Mooren, Kotova, Moore, & Schafer, 2009; Ochoa et al., 2000). Dynamin-1 has also been shown to colocalize with the Arp2/3 complex and its associated NPFs as has Vps1p within *S. cerevisiae* as described above (Galletta et al., 2008; Martin et al., 2005; Smaczynska-de Rooij et al., 2010; Urbanek et al., 2013). This portrays a model of cortical actin reassembly that is dependent upon a relationship between actin and regulatory proteins. However evidence has since emerged supporting a direct interaction between Dynamin-1 and F-actin.

DynK44A mutation within the G-domain of dynamin-1 produced a reduction in localisation of F-actin to the comets of podosomes suggesting a mechanism of remodelling dependent upon dynamin oligomerisation and the subsequent conformation change as a result of the GTP hydrolysis (Bruzzaniti et al., 2005). It was not clear from this study how a conformational change within dynamin could translate into cortical actin rearrangement. However a co-sedimentation assay later revealed a direct interaction between dynamin-1 and F-actin while no such interaction was revealed in the DynK44A mutant indicative of a GTP dependant mechanism of actin regulation (Gu et al., 2010). Notably though the binding of dynamin-1 to short F-actin prevents attachment of capping proteins, promoting elongation of filaments (Carreno, Engqvist-Goldstein, Zhang, McDonald, & Drubin, 2004; Merrifield, Feldman, Wan, & Almers, 2002; Merrifield, Perrais, & Zenisek, 2005). In this way dynamin-1 could be aiding the elongation of the invagination through linking actin polymerisation to the endocytic machinery. The conservation of this domain promoted research into the yeast homologue Vps1p as despite mutations within Arp2/3 or its associated NPFs, clathrin mediated endocytosis still occurs which could be explained by this association of actin with Vps1p, prompting investigation into the conserved interface.

BAR and F-BAR proteins have been proposed to not only be required to induce membrane curvature as shown *in vitro*, but to act as sensors of membrane curvature. Of the earliest endocytic proteins to be recruited to the endocytic site is Syp1p, an F-BAR domain protein. Syp1p negatively regulates WASp-Las17p-Arp2/3p complex preventing actin polymerisation at the endocytic site until after its departure (Boettner et al., 2009). This step could conceivably act as a molecular switch allowing endocytosis to propagate through its dissociation. The release of Syp1p is shortly followed by the arrival of F-BAR protein Bzz1p which interacts directly with the WASP-Las17p-Arp2/3 complex to induce actin polymerisation *in vitro* on glass beads (Arasada & Pollard, 2011; Soulard et al., 2005). The idea is that Bzz1p attaches to an already curved membrane, "sensing" the curvature, initiating actin polymerisation and subsequent invagination of the membrane.

Coupling the actin binding/nucleating complex WASP-Las17p-Arp2/3 complex to the membrane, via the F-BAR protein Bzz1p, could explain how actin polymerisation at the endocytic site could drive directional propagation of the invagination into the cytosol. Vps1p could be an integral part in the GTP-dependant organisation of F-actin to produce invagination of the membrane at the endocytic event as is the case for dyamin-1.

1.5 Domain Structure of Dynamin-1 Could Suggest a Model of Scission That Incorporates Vps1

Monomeric dynamin is a large (~100kDa) multi-domain protein comprising of five key domains; GTPase (G) domain, a bundle signalling element (BSE), a stalk domain, a plekstrin homology domain (PH) and a proline rich domain (PRD) munch like the yeast dynaminVps1p (Faelber et al., 2011; Shin et al., 1999; Vater, Raymond, Ekena, Howald-Stevenson, & Stevens, 1992). Upon assembly of the monomeric dynamin into a helical polymeric structure the basal GTPase activity was found to increase 1000 fold (Chappie, Acharya, Leonard, Schmid, & Dyda, 2010; Shin et al., 1999; Takahashi et al., 2012) resulting in conformational changes within each monomeric subunit culminating in scission of the endocytic vesicle from the membrane (Faelber et al., 2011; Hinshaw & Schmid, 1995; J. Liu et al., 2006; Mears et al., 2011). This model suggests that interactions between adjacent

dynamins produces catalytic effect on the GTPase activity, providing the energy required to drive the conformational change that brings about the scission event.

Oligomerisation of dynamin and subsequent torsion producing a constriction of the complex has been shown to occur during GTP-dependant dimerization of G-domains (Chappie et al., 2011, 2010). In the first instance this dimerization serves to stabilise dynamin-1 which appears to be in flux between three states; monomeric, dimeric and trimeric (most common form). Dimerization of said domains serves not only to stabilise the dynamin oligomer but induces a rearrangement of the catalytic GTPase domain resulting in a high increase in activity (Chappie et al., 2010). The subsequent conversion of GTP to GDP produces a torsion within the structure, reducing the overall length, constricting the membrane. Interestingly pseudo-atomic electron microscopy reconstruction-based models showed the G-domain of one monomer to interact with the GED of a dynamin in the adjacent coil of the helix providing insight into the constriction mechanism that precludes the scission of the vesicle (Chappie et al., 2011). From this it could be inferred that before constriction of the vesicle neck can take place, one complete coil must first form.

A self-assembly defective *dynamin-1*, I690K corresponding to the GED domain, was produced indicating a conserved residue necessary for self-assembly and rearrangement of the G-domain to enable interaction with the GED or for effective binding of GTP (Song, Yarar, & Schmid, 2004). An equivalent mutation (I649K) was created within the GED domain of *S. cerevisiae* resulting in a reduction in the frequency of invaginations produced. A secondary effect of this mutation within the yeast model was the production of hyper-elongated invaginations (>200nm). These findings would indicate a conserved residue that enables the binding of GTP whilst conferring an inability to hydrolyse the nucleotide through loss of interaction between the G-domain and GED. The result of which is loss of scission producing extremely long invaginations. The findings were analogous compared with those observed in the mammalian I690K mutation, which also falls within the amphipathic helix of the GED, indicative of a similar interaction occurring (Song, Yarar, et al., 2004).

Within yeast a GTP-dependant self-assembly mechanism has been resolved with Vps1p forming oligomeric structures that cause tubulation of liposomes *in vitro* (Smaczynska-de Rooij et al., 2012). *In vivo* mutations within this domain produces defective scission as indicated by increased retraction of endocytic patches toward the membrane, concomitant with reduced internalisation of cargoes and an inability to bind GTP (Nannapaneni et al., 2010; Smaczynska-de Rooij et al., 2010; Yu & Cai, 2004). The conservation of key domains required for self-assembly, GTP hydrolysis and subsequent scission would imply Vps1p to perform within the scission event in a dynamin-1-like fashion.

The stalk domain has also been shown to be instrumental in orchestrating dynamin into oligomeric assemblies in both Vps1p and dynamin-1 (Faelber et al., 2011; Mishra, Smaczynska-de Rooij, Goldberg, & Ayscough, 2011; Smaczynska-de Rooij et al., 2010; Song, Leonard, & Schmid, 2004; Song, Yarar, et al., 2004). The stalk domain which corresponds to the middle domain of Vps1p, has been predicted to associate in a cross-thatch alignments via a highly conserved interface 2, figure 4 (Faelber et al., 2011). Mutations of this interface have been shown to prevent oligomerisation of dynamin (Faelber et al., 2011; Shin et al., 1999; Song, Leonard, et al., 2004; Song, Yarar, et al., 2004). This region is rich in alpha-helices and similarly so in Vps1p creating a potential actin binding interface or possibly an actin nucleation site. It's conceivable that G-actin binding adjacent helices of oligomeric Vps1p may well be retained in close enough proximity and stably enough for F-actin assembly to ensue. Mutations within this region could therefore be affecting how stably G-actin is able to associate with Vps1p, perturbing actin nucleation and by association, the directional propagation of the invagination.

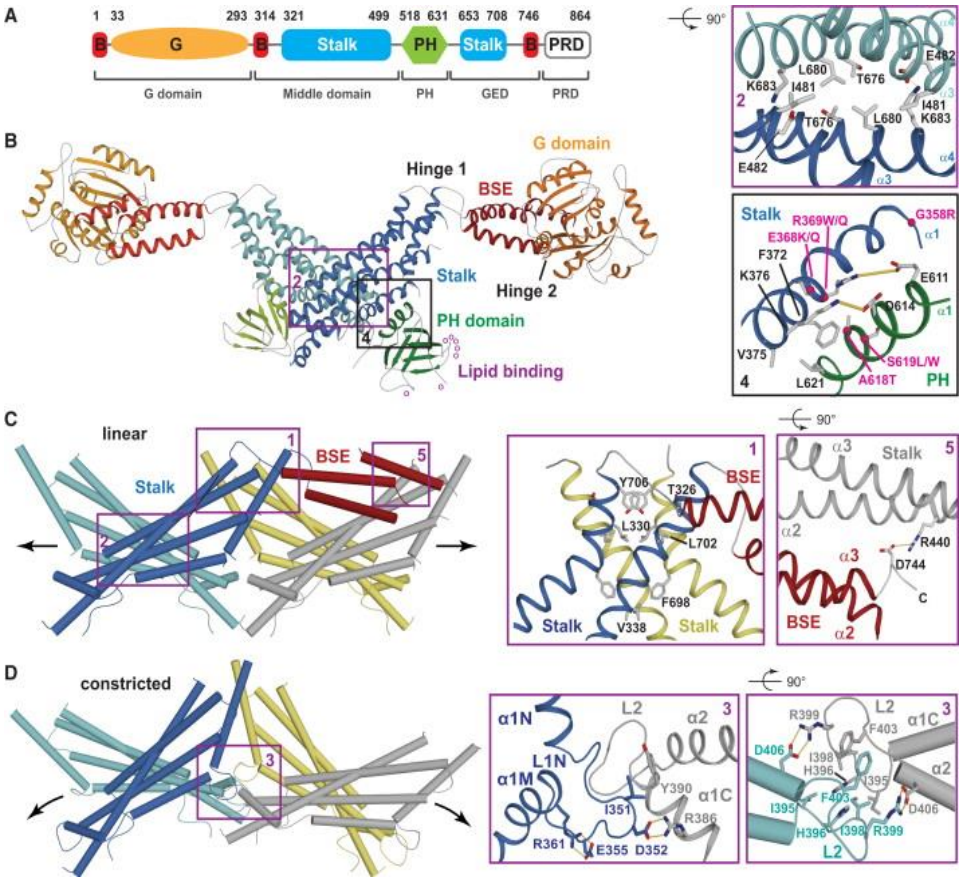

Figure 4: (A) The domain architect of dynamin-1 in a nucleotide-free conformation. (B) The dynamin dimer with the conserved interfaces-2 and -4 highlighted, show interaction of interface-2 to with PH domains folding against interface-4 of the stalk region. (C) The interface of two stalk domains via interfaces-1, and -2 to produce a linear conformation. Interaction of the BSE element within one dimer interacts with the stalk region of another dimer via interface-5. (D) Adjustment of interface-3 proposed to bring about the helical conformation in dynamin filaments. (Diagram taken from Faelber et al. 2011)

The stalk domain is further involved in regulating intramolecular, and as a consequence, intermolecular interaction via binding to a highly conserved interface-4 (figure 4) of the PH domain. This interaction occurs at an interface opposite that of the oligomerisation interfaces-1 and -2 (Faelber et al., 2011; Ford, Jenni, & Nunnari, 2011). In this conformation the lipid binding domains are oriented toward the G-domain occluding the domain from lipid membranes. This explains why dynamin is unable to bind membranes and form oligomers in its inactive state. In support of this, mutations of either the interface within the PH domain or the corresponding interface within the stalk region gave rise to increase oligomerisation rates of dynamin (Faelber et al., 2011; Kenniston & Lemmon, 2010). Crystallographic data combined with electron microscopy density models indicate

that this interface opens during lipid binding, allowing for the PH domains to interact with the membrane bilayer (Chappie et al., 2011; Faelber et al., 2011; Mears et al., 2011).

Salt bridges have been predicted to form between the BSE domain of one dynamin monomer to the GTPase domain of the adjacent monomer (figure 4) implicating this domain as a regulatory element of dynamin-mediated endocytosis. Supporting data was provided by mutagenic analysis of the BSE domain which gave significant amplification in the levels of dynamin-mediated endocytosis (Faelber et al., 2011).

The proline-rich domain (PRD) has been proposed as a further regulatory element in dynamin oligomerisation (Zhang and Hinshaw, 2001). However no direct interactions have yet been observed between the BSE and any other domain within Vps1p and so more work is required to clarify this mode of modulation.

True dynamins e.g. dynamin-1, have a PRD and PH domain which is lacking from all other dynamin-like proteins including Vps1p (figure 2). However these proteins have divergent inserts within the GTPase and between the middle and GED domain that appear to confer similar properties to that of the PH and PRD domain within dynamin-1 (figure 2) . That is the sequences appear to be important in determining the subcellular localisation and functioning of the respective dynamin-like proteins (Hinshaw & Schmid, 1995; van der Bliek, 1999). Mutation of an SH3 binding motif within insert b (figure 2) or the corresponding SH3 motif within Rvs167 prevented interaction between the two proteins at the endocytic site (Smaczynska-de Rooij et al., 2012).

As yet there is no defined structure for Vps1p at angstrom resolution or even at nanometre resolution meaning many of the structural similarities between Vps1p and dynamin-1 are speculative. Despite the focus of this study cantering around hypothesized actin binding domains within the middle domain, it should also be considered that other domains and interactions with this region may well be contributing factors to the phenotypes observed. Such a mutation might also affect how Vps1p is able to associate with nucleotides and other endocytic proteins through occlusion of interaction interfaces as a result of conformational changes. The importance of understanding the structure of dynamin will

become more apparent when comparisons of primary and secondary structure between Vps1p and dynamin-1 are carried out.

2 Material and Methods

This chapter serves to detail the procedures carried out to obtain the data presented with specific emphasis transmission electron microscopy (TEM) and associated preparation techniques.

All materials and suppliers are listed in appendix 1.

2.1 Yeast Strains

Transformed cells containing charge swap mutants of Vps1 and a null mutant were provided by Kathryn Ayscough (table 1). The charge swap mutations have been mapped in figure 5 which shows a clear clustering within the central domain. A domain speculated to be important for linkage of Vps1 to actin and actin binding and regulation of GED activity.

Table 1: Vps1p mutations analysed. The mutated residues for each of the charge swap mutants utilised. The mutated region falls within a putative actin binding site within the middle domain as confirmed by studies on dynamin-1 (Gu et al., 2010). These studies demonstrated a direct interaction between these conserved residues and actin.

Mutation
WT
Vps1 RR457-8EE (RR-EE)
Vps1 K453E:RR457-8EE (KRR-EEE)
Vps1 E461K
Vps1Δ

2.2 Culture Methods

Culture media composition is listed in table 2. Solid state cultures were produced on sterile petri dishes using a selective drop-out (SD) media with a Uracil drop-out supplement. SD agar was inoculated using disposable sterile loops inside of a sterile laminar flow cabinet minimising risk of contamination associated with the more traditional aseptic techniques of "under flame". Inoculated plates would then be incubated at 30℃ for a period of 48h to generate significant colonies which would later act as a stock for subsequent liquid cultures. Stocks were re-plated every 2-4 weeks and stored at 4℃ to ensure plasmid retention.

Table 2: Compositions of the growth media used. Appendix 2 details the stock solutions and the protocol utilised. The key difference to note between overnight cultures (ONC) and day cultures (DC) is a reduction in glucose concentration. This reduction has been suggested to prevent a build-up of glucose within the cell wall which would otherwise occlude the passage of fixatives and resins leading to poor preservation of infiltration and lack of infiltration in affected cells which will be discussed in more detail later.

Media	Composition
YPD	• 2% w/v difco peptone and 1% w/v yeast extract, 2% w/v Glucose (0.2g/100ml agar for solid state cultures)
YPD (DC)	• 2% w/v difco peptone and 1% w/v yeast extract, 1% w/v Glucose
SD (ONC)	• 0.67% w/v yeast nitrogen base without amino acids, 1X Ura DO, 2% w/v Glucose (0.2g/100ml agar for solid state cultures)
SD (DC)	• 0.67% w/v yeast nitrogen base without amino acids, 1X Ura DO, 1% w/v Glucose

Generating liquid cultures was a two stage process necessary to ensure cells could be harvest during their log phase of growth. 10ml of SD media would be inoculated in sterile 50ml falcon tubes which were angled in a cradle to provide a good surface to air ratio promoting healthy growth. The sealed tubes in their rack would be transferred to the 30℃ incubator and placed on a shaker set to 120RPM. The agitation helps to maintain an even growth rate though out the cell population ensuring an even distribution of nutrients and oxygen. Cells would be left for 18h to reach an optical density ($O.D_{600}$) in excess of 1.5. Following ONC a DC could be inoculated using the concentrated culture. Typically an initial inoculation to produce an OD_{600} of 0.1 would allow cells to reach mid- log phase in growth within an 8 hour period generating a homogenous cell culture.

2.3 Transmission Electron Microscopy (TEM)

2.3.1 Preparation

Transmission electron microscopy was carried out on a Hitachi H7600 100Kv transmission electron microscope. Due to the low penetrative capacity of electrons, propagation can only be achieved in a high vacuum. Further to this at 100Kv samples must be less than 80nm in thickness perpendicular to the direction of the electron beam to obtain sufficient transmission for a maximum resolution. Such hostile conditions require rigorous preparation of samples that in short requires dehydration and embedding within a resin that will support the sample sufficiently for ultra-thin section to be obtained using a Leica UC6 ultramicrotome. The goal of the techniques described below is to preserve the natural morphology and internal structures in their original localisations.

2.3.2 High Pressure Freezing (HPF)

High pressure freezing offers an alternative to conventional room temperature aldehyde/osmium fixation methods, providing superior preservation of ultrastructure and a reduction in artefacts such as protein clumping, loss of lipids and collapse of hydrated glycans and proteins (see Studer, Humbel, & Chiquet, 2008 for review).Using a high pressure freezer (Leica EM PACT) samples are vitrified though subjection to extreme pressure (~210MPa) and temperatures (below-196℃). Vitrification preserves macromolecular structures in situ that would be lost or moved using more conventional methods.

The high pressures prevent formation of crystalline ice (figure 5) through suppression of water expansion during freezing, and instead causes the water within the sample to form amorphous ice (see Chaplin: http://www.lsbu.ac.uk/water/). Freezing is effective to a depth of approximately 200µm pending the water-cell ratio. The poor conduction properties of water cause an exponential decrease in cooling time with increased distance from the cooling source and so even in overloaded samples, viable cells can still be retained toward the periphery. For a more uniform and reproducible initial fix,

100µm Leica membrane carriers were employed for their superior heat conduction giving a uniform vitrification thorough out the sample.

Several routes could result in formation of crystalline ice within a sample all of which result from either a reduced heat conduction or loss in pressure. Measures can be taken to avoid such scenarios and have been described in appendix 3.

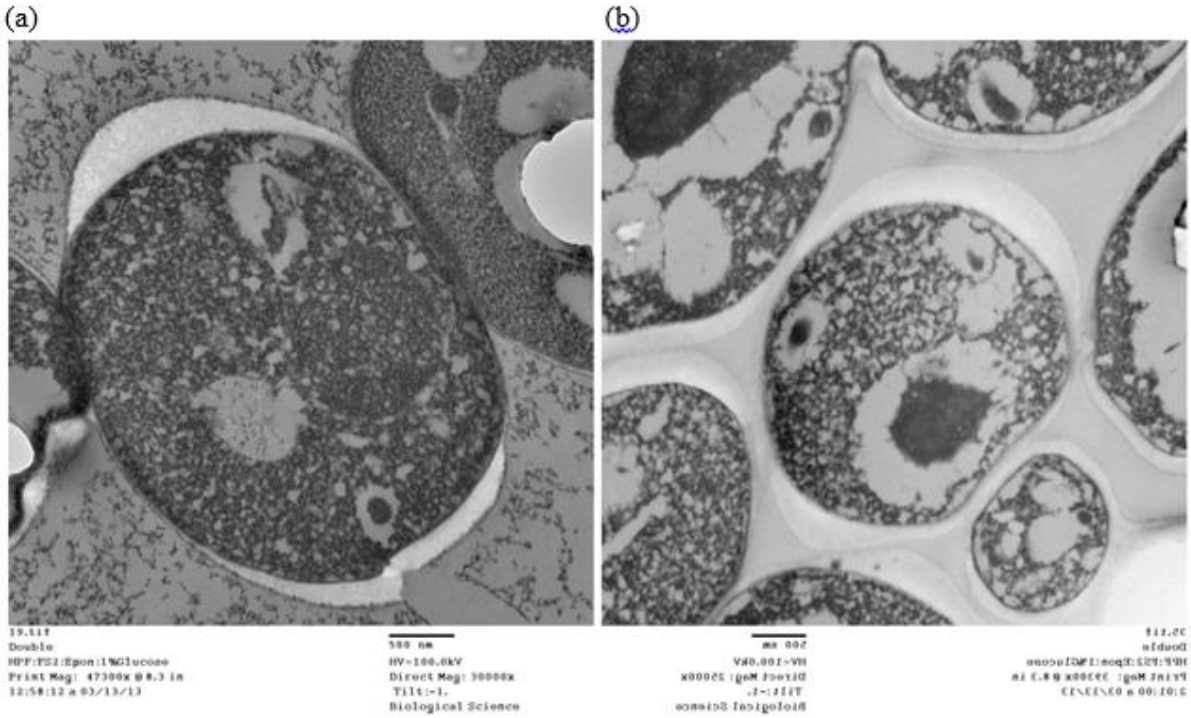

Figure 5: (a) and (b) demonstrate extensive crystallisation of water suggested by the lattice configuration of the cytosol. The precise cause of crystallisation in each of the cases cannot be definitively deduced from the images although information regarding a probable cause can be derived. This crystallisation was ubiquitous throughout the sample suggesting a pressure issue as opposed to a conduction issue which would retain some well-preserved cells and exhibit a gradient of crystallisation.

DCs would be taken from the incubator upon reaching an OD_{600} of ~0.6 and transferred to sterile 50ml syringes with a removable $2\mu m$ membrane filter. The suspension would pass through the filter under pressure causing cells to accumulate upon the surface of the membrane filter. Post filtrations the membrane filter is removed and transferred onto filter paper soaked in media from the suspension from which it has been derived. This minimalizes osmotic stresses and temperature fluctuations during transfer to membrane carriers.

Visible aggregates upon the filter paper were transferred to the 100µm Leica membrane carriers for HPF. The stages from filtering to loading can be achieved in under 2-minutes. Speed is essential to limit the time for which the cells are exposed to stress inducing conditions, ensuring a representative sample is produced.

2.3.4 The Optimal Protocol for Imaging the Endocytic Event at the Plasma Membrane

Of the fixatives, freeze-substitution protocols and reins tested I would surmise that purely for ultrastructural analysis the optimum combination is FixU2: FS1:RTE1. This combination allows for fast sample turnover while retaining high levels of ultrastructural preservation specifically at the membrane. Use of FixI1:FS6:LTE4 should also be implored it immunohistochemical analysis is required. I would further advise experimenting with shorter time periods for LR white infiltration under a low temperature embedding protocol as a recent publication has demonstrated infiltration with Agar 100 in under a 12h period (Buser & Drubin, 2013; McDonald, 2013). Even at temperatures as low as -20℃ LR white retained a level of fluidity that surpasses that of Agar 100.

Having established a good protocol for preservation of the plasma membrane and associated structures I sought to assess the structure of the invagination from a three-dimensional perspective as from simple tilts further details surrounding the invagination were documented. The morphologies of these structures cannot be properly understood within a two-dimensional capacity and so a 200Kv JEOL 2100F FEG TEM was used to achieve deeper electron penetration allowing the EM tomography.

2.4 Electron Tomography

Electron tomography was performed using a 200Kv JEOL 2100F FEG TEM with a eucentric stage which allows movement in the z direction in addition to the x and y direction. With this ability the specimen can imaged in various orientations without lateral movements as a function of lateral tilt. Simply put this retains the region of the sample being imaged in its various orientations both within the focal plane and at a constant magnification through retention of a constant rotation axis. This is achieved through servo controlled movements of the z plane with respect to the rotation axis. In this

way successive images can be compiled using the weighted-back projection algorithms to produce a three-dimensional image. Such reconstructions were carried out computationally using Gatan 3D reconstruction software.

Specimens were prepared as described above with the addition of a fine carbon coat to reduce the accumulation of electrons upon the sample. Such an accumulation is the result of the increased time periods spent in the path of the electron beam required for image acquisition.

2.5 Quantifying images

Invagintions were measured and quantified using imageJ, a free image analysis software from http://rsbweb.nih.gov/ij/. The length of an invagination was calculated through measuring the distance from the top of the invagination down the centre of the lumen of the invagination to the tip (figure 6). Angles were measured by drawing horizontal lines spanning the top of invagination. A second line would be drawn from the centre of this line to the tip of the invagination returning an angle between the invagination and membrane (figure 6).

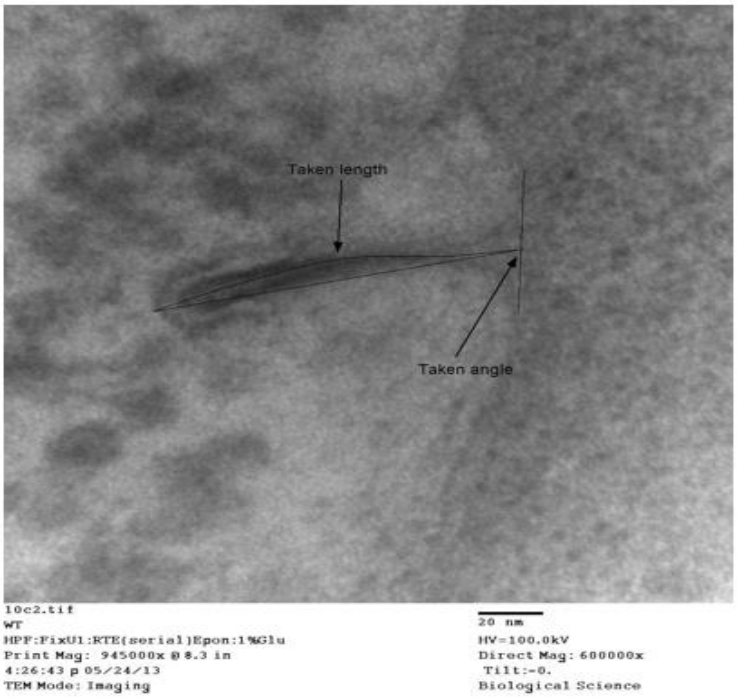

Figure 6: Using imageJ lengths of invaginations and angles were quantified as shown above. The length is a line that extends from the top of the mouth of the invagination (i.e. where the membrane begins to invaginate) to the tip of the invagination, maintaining an equidistant from the adjacent wall of the invagination.

3 Results

3.1 Imaging Invaginations and Associated Proteins

Although a biological question is at the centre of this thesis a significant technical question was also addressed: how could endocytic structures be both preserved and imaged to such a resolution that the mechanism of endocytosis might be elucidated? Three key areas of processing were optimised for imaging the ultrastructure of the endocytic invagination; fixation, embedding, and freeze substitution.

3.1.1 Fixation

HPF provides a temporary fix, which needs to be substituted for one compatible with the conditions inside the transmission electron microscope (TEM) with the exception of cryo-electron microscopy. Under a high vacuum water would simply sublime, destroying the sample and potentially damaging the TEM (Appendix 4.1). Prior to infiltration with resin which acts as the final fix, chemical fixatives can be added to help retain structural morphologies of ultrastructural components. An abundance of fixes exist that may be combined in a multitude of combinations and ratios producing great diversification in the level of preservation observed. The difficulty arises in selecting a combination of fixes appropriate for the required application.

Here the key components to be preserved are the plasma membrane and structures that form at on or around invaginations and enable imaging at high resolutions with minimal formation of artefacts. Due to the protein dense cytosol of *S. cerevisiae* the idea was to generate a fix that would not only retain structures and their localisation but also to see if emphasis could be taken away from the ribosomes enabling more clear imaging of invaginations and associated structures. Fixes that would be appropriate for immunohistochemical analysis were also produced to enable further research into localisations of various endocytic proteins to be assessed, time permitting.

FixI1 and FixI2 (table 3) pertain to weak (uranyl acetate) or low concentrations of mild (glutaraldehyde) fixatives to minimise crosslinking of epitopes. FixI1 produced the greatest

preservation of antigenicity which was evident from a trial run. However the absence of water in FixI1 gave a severe reduction in membrane preservation (figure 7 and 8) but improved nuclear membrane preservation (figure 7). Ultrastructural preservation remained consistent between both fixes however this is likely attributed to the low temperature embedding (LTE) protocols described later. Employed under room temperature conditions FixI1 samples exhibit a significant extraction with loss of many internal structures that are preserved after LTE (figure 7).

Under the low temperature embedding protocols described below, use of FixI1 produces excellent balance in contrast, revealing fine structures at the membrane and minimising alterations through crosslinking of endogenous protein structures. The presence of glutaraldehyde (GA) will cause the crosslinking of fine structure such as actin networks at the invagination that could be the primary cause of clumped extensions at the invagination (figure 8a and 9b) where an actin network supporting the invagination should be evident. However such structures are not present in the absence of GA which would suggest either an artefact or that the network is too fine for detection.

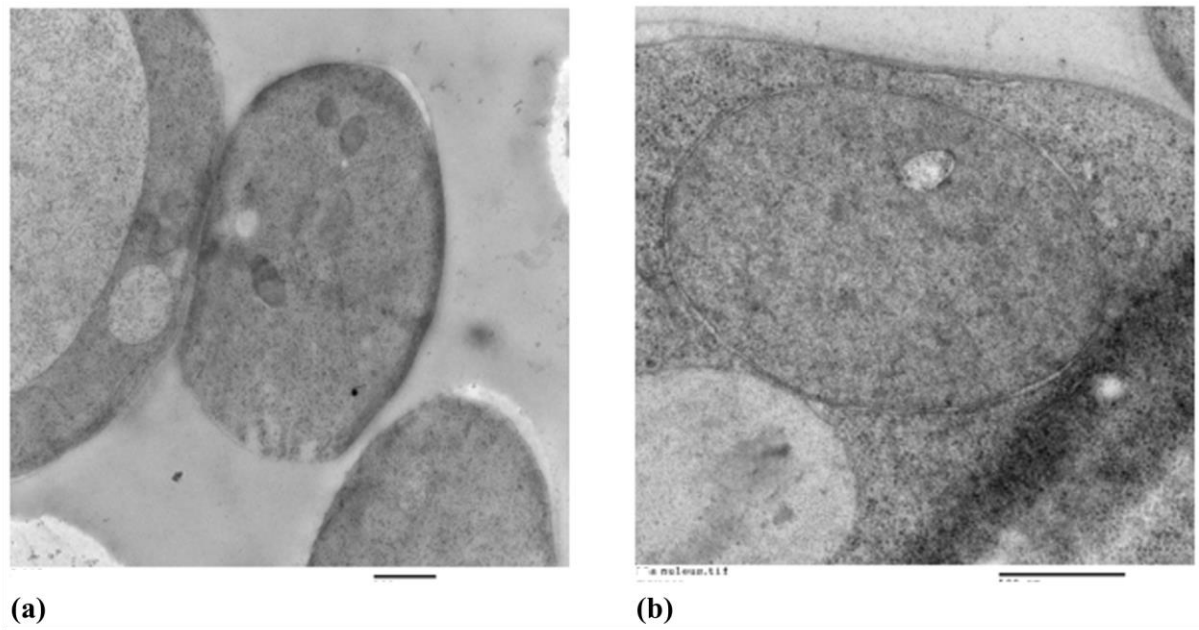

Figure 7: HPF samples subjected to FixI1: FS3:LTE6 exhibit excellent preservation of internal membranous structure, in particular the nucleus. However the contrast of the plasma membrane is limited by the absence of water making distinction of invaginations more difficult. (a) An overall image, highlighting the reduced plasma membrane contrast. (b) Cell nucleus with excellent preservation of the nuclear envelope. Both inner and outer membranes can be clearly distinguished. Scale bars represent 500nm.

Table 3: Fixatives utilised within the study: UA-Uranyl acetate, GA-glutaraldehyde, OSO_4-osmium tetroxide

Abbreviation	Definition
FixI1	Immuno Fixative 1: 0.1%UA in acetone with 2%H_2O
FixI2	Immuno Fixative 2: 0.25%GA and 0.1%UA in acetone
FixU1	Ultrastructural Fixative 1: 2%GA, 0.1%UA and 5%H_2O in acetone
FixU2	Ultrastructural Fixative 2: 1%OSO_4, 2%GA, 0.5%UA and 5%H_2O in acetone

Osmium tetroxide is well established as a lipid stain and is the dominant means for giving contrast to lipid rich structures. After assessing how water and uranyl acetate can provide good contrast to membranes but also enabling visualisation of finer structures, I was curious to see if further contrast of both internal and external membranes could be achieved in addition to retention of the finer structures by osmium tetroxide. Simultaneously it was also important to assess the effects of higher concentrations of GA upon the ultrastructural preservation. Since osmium tetroxide and glutaraldehyde act on different cellular components this is possible.

FixU1 and FixU2 were developed and revealed very different advantages. Fix U1 exhibited a greatly reduced contrast of the sample as a whole but consequently enabled visualisation of finer structures at the base of invaginations (figure 9 (c) and (d)). This could be a result of high levels of uranyl acetate deposition within the high concentration of proteins that comprise the endocytic machinery. Despite uranyl acetate being classed as a negative stain its chemical properties enable it to form bonds with uranyl ions will bind to proteins and sialic acid carboxyl groups and to lipid and nucleic acid phosphate groups (Terzakis, 1968). FixU2 returned improved membrane contrast in addition to associated components at the site of invaginations making this the preferred fix (figure 9 (a) and (b)). The increase in proportion of GA produced no obvious improvements at this magnification.

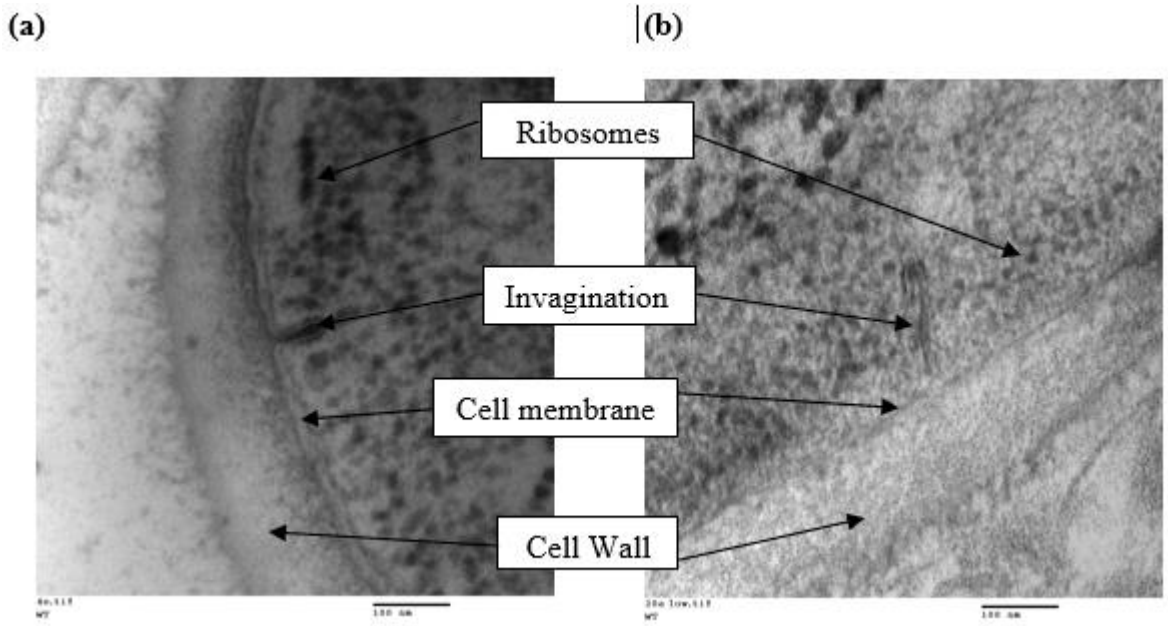

Figure 8: (a) The small percentage of water within FixI1 returns greater contrast making membranes and invaginations more visible. Both micrographs illustrate portions of wild type (WT) cells treated with different immuno fixes (b) In absence of water (FixI2) membranes are faded and difficult to distinguish often requiring tilts to reveal invagination.

Exactly why the addition of water generates better preservation of membranes can only be speculated. Interestingly though internal membranes are not as readily affected by the addition or removal of water to the fixative. Some believe a hydrosphere is required to support the membrane and structures integral to the membrane. Loss of this "sphere" causes the membranes to collapse into a monolayer, losing the intermembrane space (Buser & Drubin, 2013) . As a result no distinction can be made between the ribosome dense cytoplasm in *S. cerevisiae* and the cell membrane.

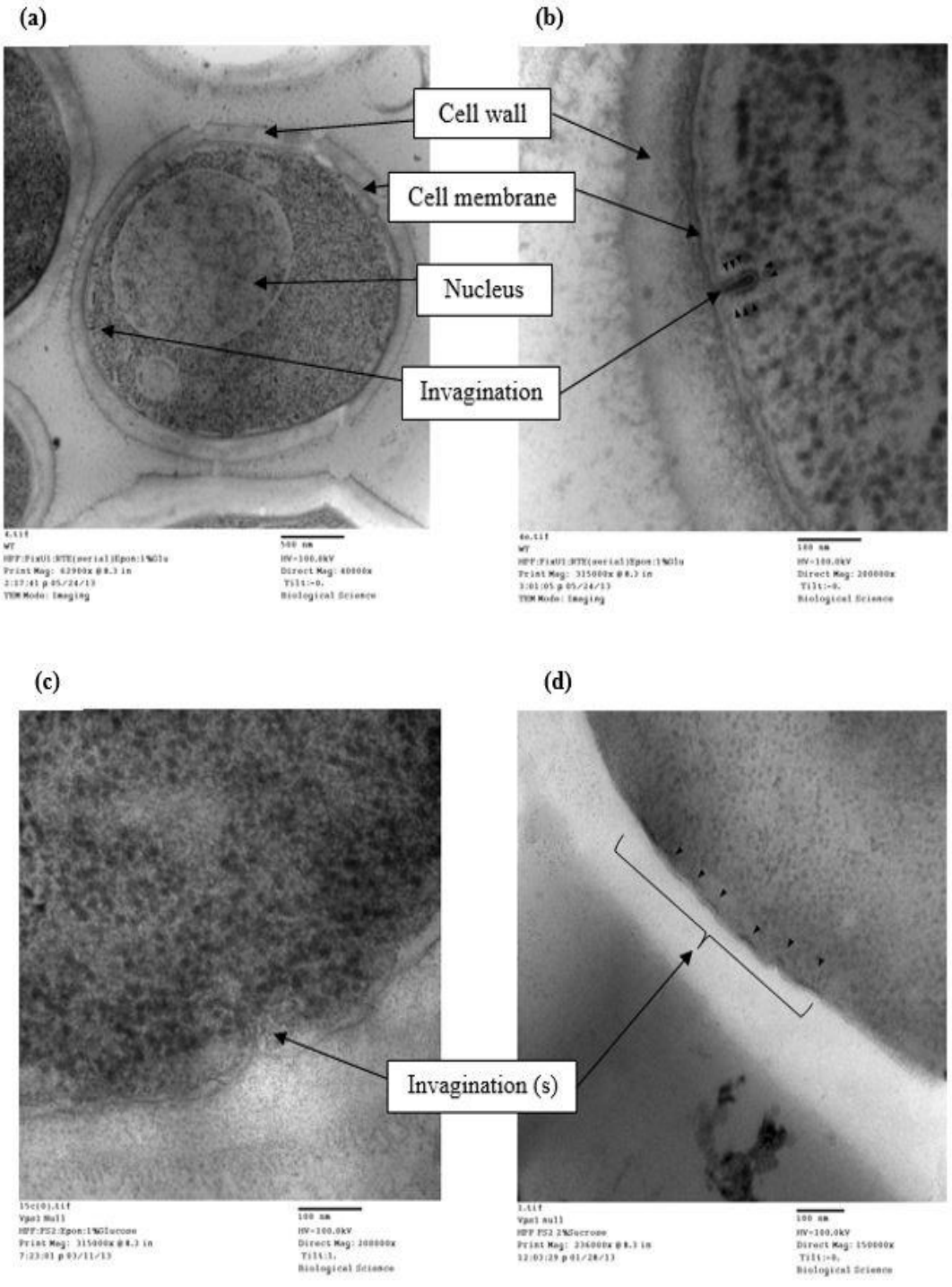

Figure 9: (a), (b) show micrographs of samples treated with FixU2 which can be distinguished by the high contrast of membranous structures. (c) and (d) were treated with FixU1 exhibit poor membrane contrast however, (d) reveals interesting electron dense regions at newly forming invaginations, indicative of the endocytic machinery.

3.1.2 Embedding

Embedding is the process of infiltration of the sample with a resin and broadly speaking encompasses two categories; low temperature embedding (LTE) and room temperature embedding (RTE). The general principal for embedding is to first substitute all the water within the sample for a solvent which would subsequently be substituted by a compatible resin. Following infiltration the resin can be polymerised which enables for ultra-thin sections (<80nm) of the sample to be collected for TEM analysis.

LTE allows for infiltration and polymerisation to take place at temperatures as low as -50, which serves to reduce kinetic movements of macromolecules during the substitution. In this way localisations and morphologies of various macromolecular structures are preserved as close as possible to their native state and the effects of free radicals is reduced (McDonald, 2013). By this sentiment these methods are more effective in preserving antigenicity compared with RTE. RTE is altogether a faster, more rigorous process ideal for structural analysis but due to the detrimental effects on antigenicity is regarded as unsuitable for immunohistochemistry.

In practice it became increasingly apparent that little difference could be distinguished between the levels of preservation observed when using the different resins at the operative magnifications (figure 10). I would suggest that changing the resin could be beneficial in improving preservation of antigenicity but exhibits no additional benefits to ultrastructural preservation. This said the increased extraction of cellular content observed in Agar 100 resin embedded samples enable the more clear distinction of structures at the membrane which would otherwise be occluded by the electron dense ribosomes however this may well be attributed to the substitution protocol.

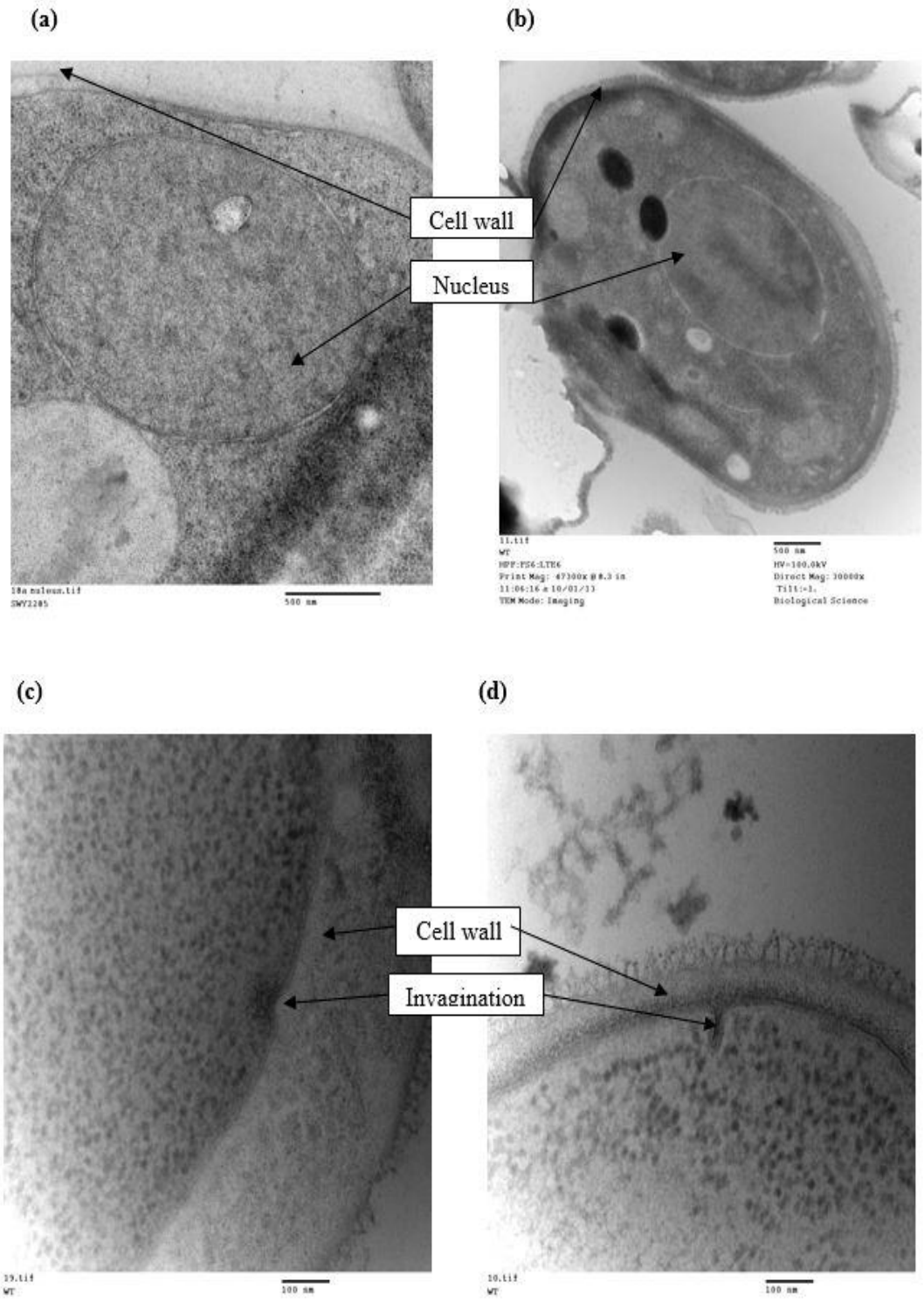

Figure 10: Examples of micrographs produced from samples embedded in LR white medium grade (a), HM20 (b), and Agar 100 resin (c and d). All samples were fixed using FixI1.

Table 4: Resin utilised and the times allowed for infiltration. LTE requires increased time for incubation due to the increased viscosity of the resins at low temperatures. Samples that were insufficiently infiltrated exhibited fragile regions that would fragment and crumble post sectioning.

RTE1	**Room Temperature Embedding: 50%Epon for 24h→100%Epon for 24h**
RTE2	Room Temperature Embedding: 50%LR White for 24h→100%LR White for 24h
RTE3	Room Temperature Embedding: 10%Epon→100% Epon serial concentration at 10%incriments/24h
RTE4	Room Temperature Embedding: 10%LR White→100% LR White serial concentration at 10%incriments/24h
LTE1	Low Temperature Embedding: Temperature maintained at -50˚C. 10%HM20→100%HM20 serial concentration at 10%incriments/24h
LTE2	Low Temperature Embedding: Temperature maintained at -25˚C. 10%LR White→100%LR White serial concentration at 10%incriments/24h
LTE3	Low Temperature Embedding: Temperature maintained at -50˚C. 10%HM20→100%HM20 serial concentration at 20%incriments/24h
LTE4	Low Temperature Embedding: Temperature maintained at -25˚C. 10%LR White→100%LR White serial concentration at 20%incriments/24h

3.1.3 Freeze Substitution

The process of substituting out water from the sample for a solvent carrying the fixative, stain or both is known as freeze substitution. Following HPF we are presented with a sample that is fixed by amorphous ice which needs to be substituted for a solvent combined with a fixative, stain or both. In this manner as the water is replaced the structures are simultaneously fixed in position through cross-linking of various structures to retain their localisations at the point of freezing. With fixing samples comes alteration in structures and production of artefacts, arguably returning a less representative sample. In response to this protocols were devised that altogether omit fixatives and simply substitute for a solvent followed by a resin and as previously described.

The freeze substitution protocols in table 5 were devised with respects the limitation of the resin being used. All freeze substitution was carried out in a Leica automated freeze substitution machine (AFS) which enables for programming of gradual stepped warming of the sample. To avoid formation of ice

crystals the AFS is precooled to -90℃ at which time samples can be transferred from cryo-storage to the chamber without formation of ice crystals. Acetone with an appropriate cocktail of fixative and stains is added to each cryovile which first serves to lift the sample from the membrane carrier enabling 360° infiltration while solubilising the amorphous ice while carrying the fixatives and stains into the specimen. In conjunction with this the sample will undergo gradual warming to promote further solubilisation of the vitreous ice while ensuring complete infiltration by the fixatives and negative stains.

The Agar 100 resin requires a room temperature conditions to infiltrate the specimen or extensive time scales at temperatures approaching 0℃ due to the increase in viscocity. Sub-zero temperature infiltration is not possible due to solidification of the resin. Thus fixatives are advisable when utilising Agar 100 resin as structural collapse may be evident upon dehydration of the sample. Excellent preservation was exhibited in both FS1 and FS2 when combined with FixU2 making Agar 100 the optimal choice for ultrastructural analysis. Ironically this was uncovered through a programming error. Previous runs utilised much more gradual cooling and showed no significant improvement with the faster run. These finding coincide with the recent publication by Christopher Buser and David Drubin (Buser & Drubin, 2013). Prior to the addition of Agar 100 the samples were rinsed 3 times in 100% EtOH for 30 minutes each to ensure all acetone is removed as Agar 100 will not fully polymerise if contaminated with acetone.

FS3, FS5 and FS7 (table 5) are compatible with HM20 that remains liquid at temperatures as low as -50℃. The idea in using this was to ascertain a sample that has had a more minimal opportunity for movement of internal structures and macromolecules through reducing the kinetic energy via cooling. Reducing movement of macromolecules is of great importance when performing immunohistochemical analysis to ensure representative localisations are preserved. Taking this a step further it seemed that the reduced temperature could also allow for a sample to be infiltrated by a resin without the requirement for fixatives which was evident from the data collected (figure 29b). The advantage of this process for ultrastructural analysis is overshadowed by the daunting time scales

required. It should be noted that this LTE method showed more consistent infiltration compared with RTE protocols which exhibited poorly infiltrated regions toward the centre of the sample.

Table 5: A summary of freeze substitution protocols utilised within this study

FS1	**Freeze Substitution 1: -90˚C→0˚C at 90℃/h**
FS2	Freeze Substitution 2: -90˚C→0˚C at 6˚/h
FS3	Freeze Substitution 3:-90˚C→-50˚C at 1˚C/h
FS4	Freeze Substitution 4:-90˚C→-20˚C at 1˚C/h
FS5	Freeze Substitution 5:-90˚C→-50 ˚C at 0.5˚C/h
FS6	Freeze Substitution 6:-90˚C→-20 ˚C at 2˚C/h
FS7	Freeze Substitution 7:-90˚C→-50˚C at 0.5˚C/h
FS8	Freeze Substitution 8:-90˚C→-20˚C at 2˚C/h

LR white (medium grade) exhibits a much reduced viscosity compared with HM20 allowing for more rapid infiltration and reduced extraction at low temperature. Unlike HM20 LR white is only operable from temperature exceeding -20℃ and so FS4, FS6 and FS8 were tested. No significant improvements in ultrastructural preservation were observed. However in using LR white with minimal fixatives, as with HM20, the option to perform immunohistochemical analysis is available.

3.2 Predicted secondary structure reveals possible actin binding domains demonstrating analogity with dynamin-1

SIM is an online tool that compares a protein sequence to those already within the SWISS-PROT database and searches for similarity in sequence conservation (http:@expasy.hcuge.ch/). Using SIM sequences were compared by subjection to the linear-space local similarity algorithm (Huang & Miller, 1991) within a BLOSUM 62 matrix (figure 11). This particular algorithm is capable of discerning regions of similarity between two similar proteins without considering the entire amino acid sequence as a whole, i.e. it can identify regions that have a high or low levels of alignment, generating a score for that specific region that would not affect that of an adjacent region of higher or lower similarity.

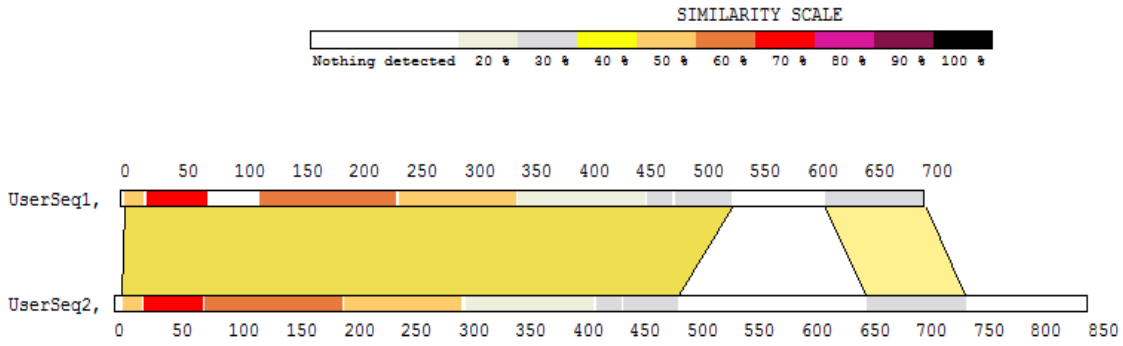

Figure 11: A comparison between the amino acid sequence of Vps1p (UserSeq1) and mammalian dynamin-1 (UserSeq2) generated using SIM (http://web.expasy.org/cgi-bin/sim, appendix 5). Levels of similarity upward of 30% can be observed for the GTPase, middle and GED domains with the highest region of similarity represented in the GTPase domain that exhibits 60% and 70% conservation.

The initial comparison yielded a high similarity between regions corresponding to the GTPase domain (60%-80%), middle (30%-50%) and GED (30%-40%) (Figure 2). Such similarity is synonymous with an overlap in function between the domains of Vps1p and Dynamin-1. Despite inference that this protein is not dissimilar to its mammalian homologue few steps have been taken to assess the similarity at the ultrastructural level and so many questions regarding commonalities between the domain structures still remain. That is to say, is the level of similarity sufficiently high for Vps1p to act in a manner that partially or fully mirrors Dynamin-1?

The mutant strains assed within this study (table 1) were provided by the Ayscough lab and carry mutations within a putative actin binding region of Vps1p that exhibits dwindling similarity to dynamin-1, at around 30%. The main goal here was to assess how F-actin might be implicated in the directional propagation of an invagination via it association with Vps1p via these putative actin binding sites. However the mutated residues also correspond to conserved helices within the stalk region of dynamin-1 which act as a switch that regulates the activity of the GED (Faelber et al., 2011; Ford et al., 2011). Oligomerisation of dynamin-

1 enables interaction of the GED with the GTPase domain, catalysing the GTPase activity, providing the energy that drives the scission process (Chappie et al., 2010; Marks et al., 2001; Tuma, Stachniak, & Collins, 1993). Thus a possible duality exists where in an inactive state these helices perturb GED activity but in an active state couple the endocytic machinery to the power of actin dynamics.

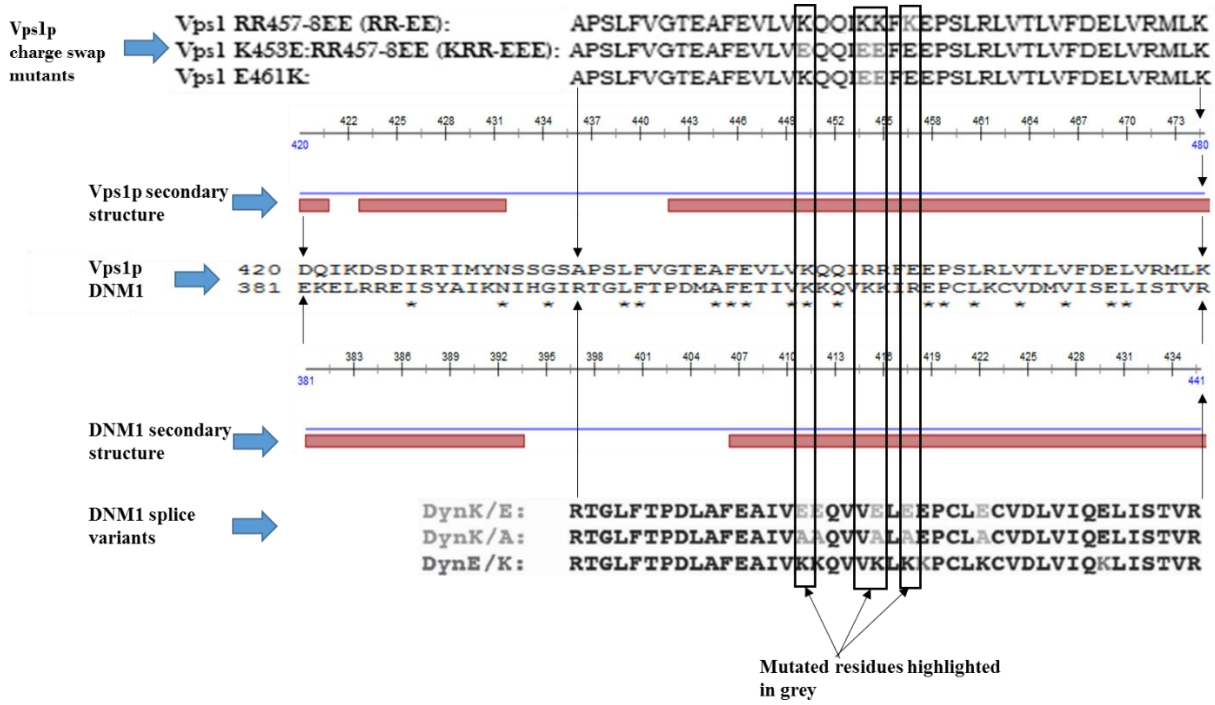

Figure 12: A previous study demonstrated a direct interaction of dynamin-1 (DNM1) middle domain with actin through mutagenic analysis. The splice variants are listed above with the altered residues in grey. The red bars overlap the residues that are predicted to form an alpha-helix as predicted by Predict Protein (www.predictprotein.org). The position of the mutations fall within putative, and since proven (Gu et al., 2010) actin binding regions within an alpha-helix of the middle domain of DNM1. Using alignment data it becomes clear why these mutations within vps1p were produced (top) for this study since they correspond to the residues mutated in dnm1 that produced defects in actin binding as shown in Gu et al., 2010. The predicted secondary structures also shows the mutations within *vps1p* to fall within the alpha-helix of the middle domain suggesting homognity of secondary structure between DNM1 and Vps1p within the mutated region.

An array of helical structures have been resolved within dynamin-1's crystal structure (figure 13, b) (including alpha-, pi- and 3_10-helix) that are concentrated within the middle domain and plextrin homology domain (figure 2). The predicted secondary structure of Vps1p was derived using PROFsec (www.predictprotein.org) revealing a similar concentration of helices

within the middle domain of Vps1 (figure 13, a). These helical motifs could represent potential actin binding sites as their solvency shows the majority to be exposed and not embedded within the secondary structure. In support of this broad suggestion is a study on these residues within the corresponding location in dynamin-1. A direct interaction between F-actin and the helical motifs of the middle domain suggesting these helices likely perform a similar role in Vps1p (Gu et al., 2010). As previously mentioned such evidence would support a duel role for the helices within this region, both as switch, controlling GED activity and an actin binding motif.

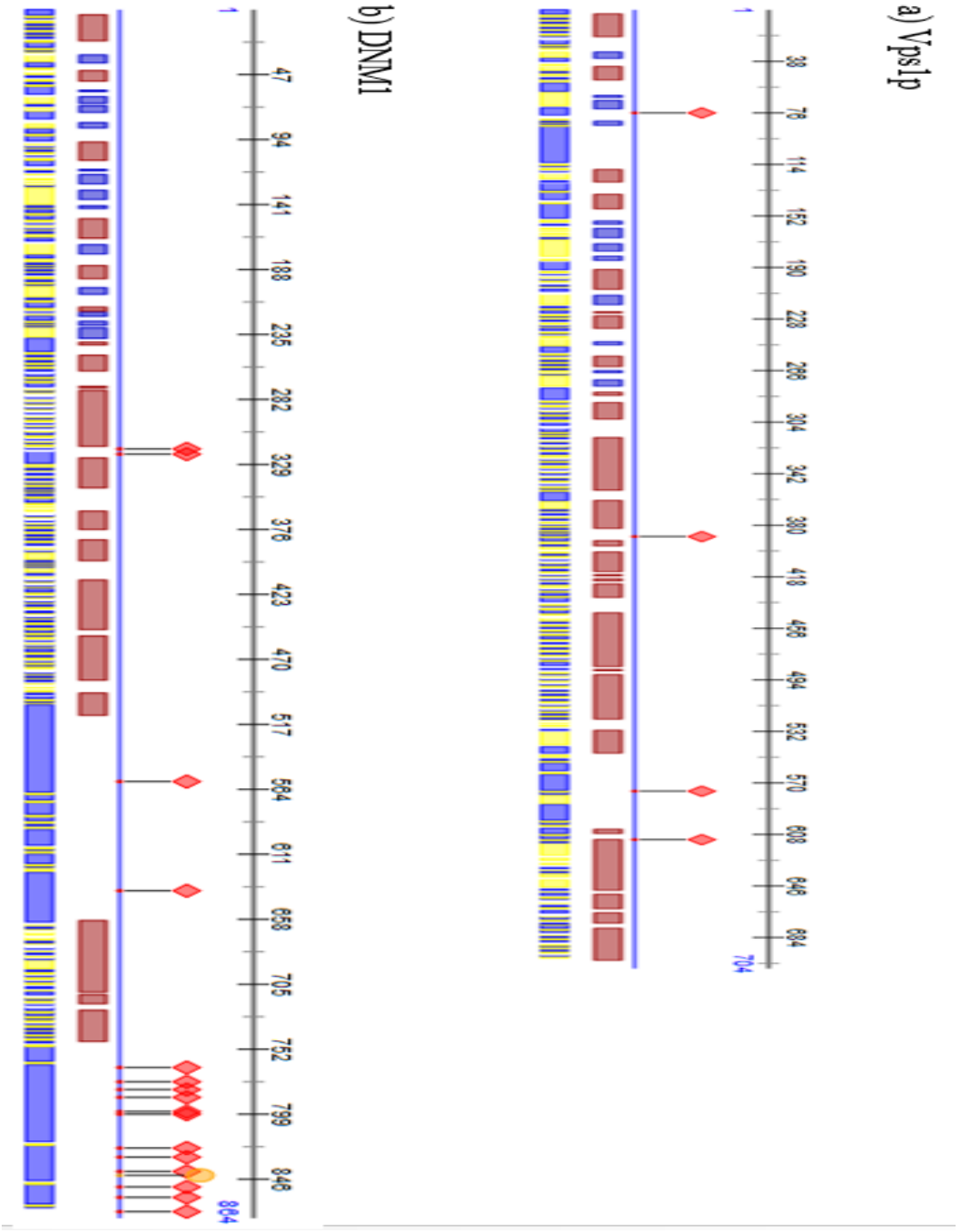

Figure 13: (a) Predicted secondary structure within Vps1 obtained using PROFsec (www.predictprotein.org) returning a 74% accuracy level (appendix 6). Red and blue bars represent helix (including alpha-, pi- and 3_10-helix) and beta-strand (extended strand in beta-sheet conformation of at least two residues length) respectively. (b) Secondary structure f Dynamin-1 derived from its crystal structure obtained from the Protein Data Bank (http://www.rcsb.org/). In both solvency is represented by the lower blue and yellow bars representing exposed and embedded motifs respectively. The sticks with diamonds atop represent potential protein-protein interaction sites.

3.3 TEM tomography reveals a dynamin-like structure

Primary and secondary structural conservations between dynamin-1 and Vps1p would suggest Vps1p could effectuate as if dynamin-1. Dynamin-1 has been described as a protein that self-assembles, encircling the invagination, which undergo constriction inducing the scission event in a GTP-dependant manner (figure 14) (Chappie et al., 2010; Danino et al., 2004; Kenniston & Lemmon, 2010; Marks et al., 2001; Sever, 2002; Wenger et al., 2013). *In vitro* Vps1 has been shown to self-assemble and tubulate membranes in a GTP-bound-dependant manner, much like dynamin-1 (Y.-W. Liu, Mattila, & Schmid, 2013; Smaczynska-de Rooij et al., 2010). A spiral structure that encircles the invagintions has been resolved for dynamin-1 by x-ray crystallography and cryo-electron microscopy (Chappie et al., 2011).

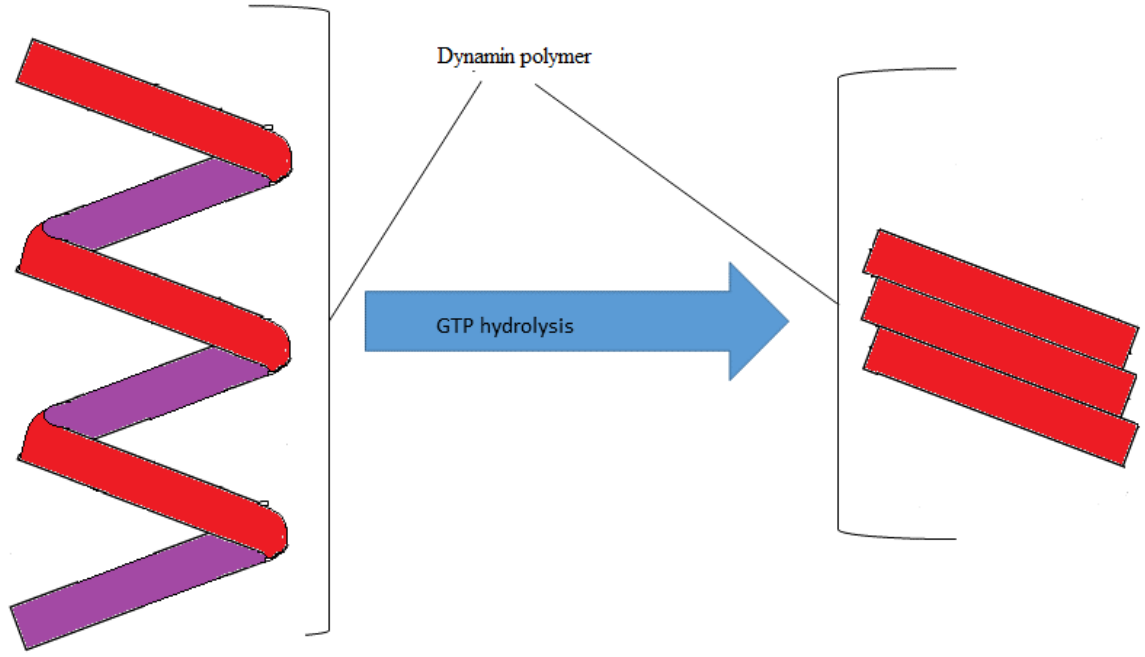

Figure 14: 17 dynamin monomers comprise each turn of the helix that encompasses the neck of an invagination post GTP binding. The subsequent interaction of the GED with the GTPase domain drives the GTP hydrolysis which in turn provides the energy giving rise to twist in each dynamin monomer. Cumulatively these twists result in a shortening of the polymeric dynamin which condenses the helix, constricting the neck of the invagination, aiding the scission process. These schematics were derived from the predicted crystal structures of polymeric dynamin as put forward by Faelber et al., 2011. In the tomograms generated during this study a structure can be seen that has a strong likeness to the structure depicted by Faelber et al, 2011 *of* dynamin in its GTP bound state.

TEM tomography was carried out on JOEL2100F field emission electron microscope at 200kV from -60 to +60 degrees tilt. Images were manually aligned using Gattan 3D reconstruction software utilising weighted back-projection algorithms. Specimen were high pressure frozen, embedded in epoxy resin and sectioned to 100nm. The images shown are in silico slices from the tomograms produced. The reconstructions clearly portray a helical structure that spans the length of the invagination which has extraordinary likeness to the structure of dynamin-1 (figure 15). To see the full tomogram please visit http://www.youtube.com/watch?v=ftzpj3GtSDE . When assessing two dimensional images electron dense region at regular intervals are visible at uniform intervals of ~3-4nm indicative of a helical structure that forms along the length of the invagination (figure 16).

Dynamin-1 has been described at a pseudoatomic level as forming a helical structure that encircles the invagination neck which would suggest to me that the structure seen here is likely to be Vps1p (Chappie et al., 2011). Other proteins that are likely contributing to the density of this structure would include the actin regulatory protein Arp2/3 and its NPFs Las17p, Abp1p and Pan1p, all of which colocalise with Vps1p either directly or indirectly via the linker protein Sla1p (Smaczynska-de Rooij et al., 2010, 2012; Warren et al., 2002). Rvs167 may well form part of the complex too having membrane binding and bending abilities in addition to its direct interaction with Vps1p at the invagination (Smaczynska-de Rooij et al., 2012; Youn et al., 2010).

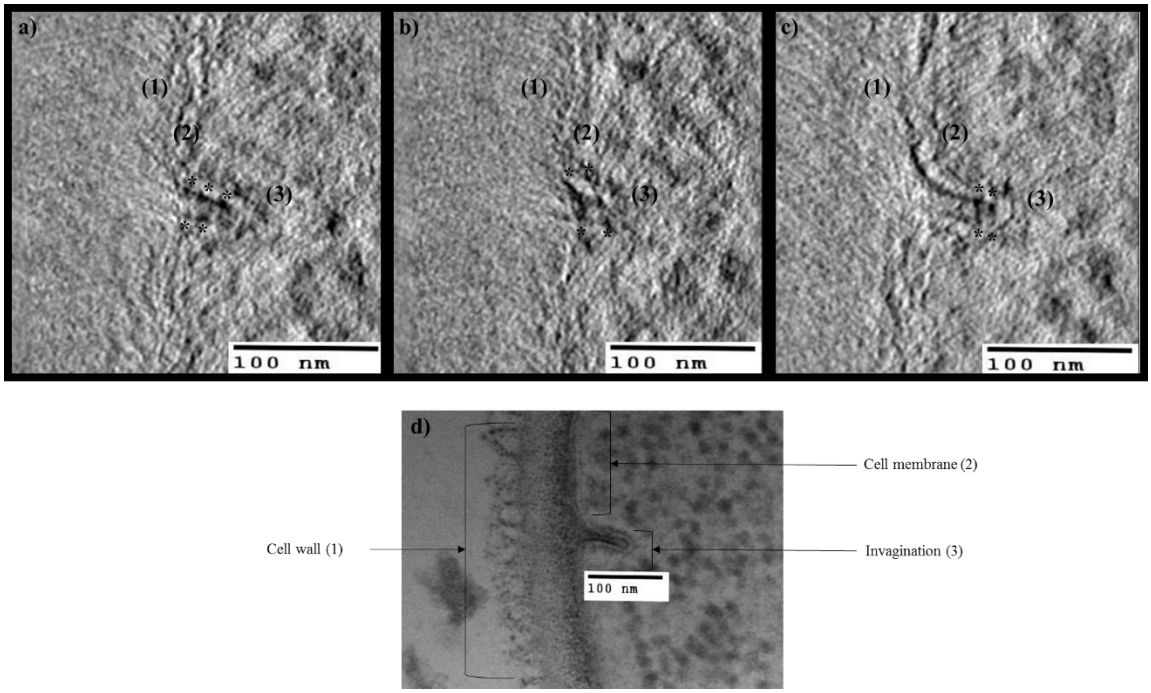

Figure 15: In silico images from tomographic reconstructions (a-c) with a micrograph of the target area illustrated below (d). The locations of the cell wall (1), cell membrane (2) and invagination (3) have been numbered in each of the silico images. A structure with a strong structural likeness to that of the predicted polymeric, GTP bound crystal structure for dynamin can be seen in images 1-3 (*). It must be stressed that to fully appreciate the likeness it is imperative to observe the full tomogram.

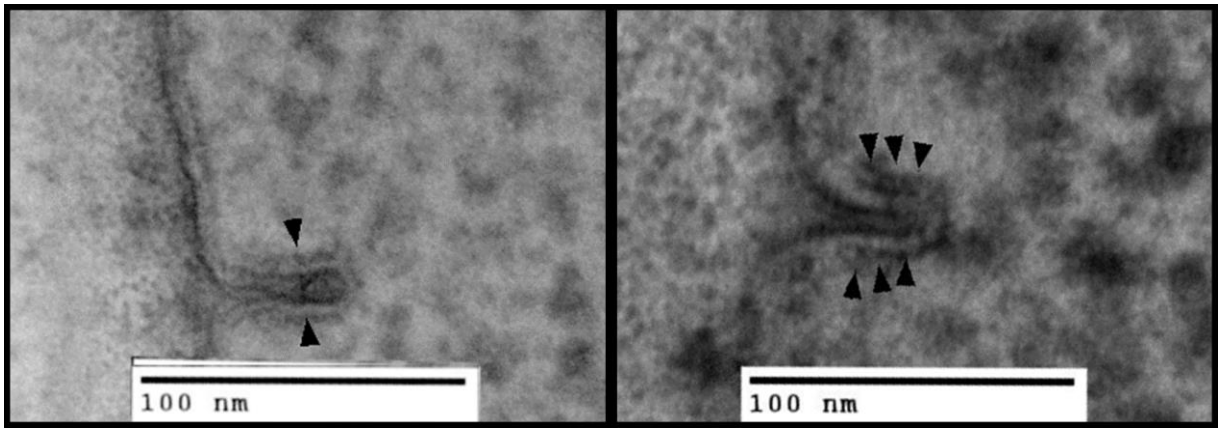

Figure 16: Electron micrographs from unlabelled WT cells displaying electron dense regions indicative of a dynamin-like structure that forms along the length of the invagination. (Left) A clear electron dense region can be seen extending cross the width of the invagination not dissimilar to the structures revealed by tomographic reconstruction. (Right) Electron dense regions at regular intervals suggest the presence of a helical structure.

Upon elucidating a potential oligomeric dynamin-like structure the vision was to test if the structure contained Vps1p using immunoelectron microscopy. The labelling was unsuccessful (not shown) which might be explained by the occlusion of Vps1p by a dense F-actin network that is believed to radiate from the structure and form along the length of the invagination. Alternatively the conformational change of Vps1 within its oligomeric form may well make it unrecognisable to the anti-Vps1p. Although the structure was not identified within this study it must still be acknowledged that this is the first high resolution tomographic reconstruction of an endocytic invagination within *S. cerevisiae* and when compared with the predicted polymeric GTP bound dynamin-1 structure (Faelber et al., 2011) it can't be denied that the structures encircling the invagination bares a strong morphological resemblance to dynamin-1; forming rungs evenly spaced apart that can be more clearly seen in the full tomogram. This morphological likeness to dynamin-1 would suggest that the structure here could be polymeric Vps1p in its GTP bound state. This is purely speculative until the structure can be successfully labelled.

3.4 Alterations of invagination trajectory provide evidence for a requirement of F-actin binding for normal invagination formation.

To investigate how Vps1p and its relation with F-actin could be contributing to invagination formation, the angle of each invagination relative to the plasma membrane was recorded in the wild type (WT) and for each of the actin binding mutants (figure 17). All strains were assessed both pre- and post- sorbitol treatment. The concentration of sorbitol was calculated to create a media which has a water potential equal to that of the cytosol. This creates an osmotically neutral environment, equalizing the pressures either side of the membrane. This allows assessment of weather the F-actin binding and Vps1p is simply required to overcome the pressure created by the cells hypotonic cytosol or if their roles are more intrinsic to the endocytic event, in particular the scission event.

To record angles a horizontal line would be drawn that would span the void created by the invagination at the plasma membrane. Following this a second line would be drawn that extends from the centre of the first to the tip of the invagination returning an angle between the membrane and tip between 0 and 90.

Statistically RR-EE (table 7, figure 18b) was the only transfected cell line to exhibit a significant difference compared with the WT, producing extremely low angles of invagination (figure 18). This might suggest a reduction in F-actin binding, and so reducing the support required for the invagination to form perpendicular to the membrane against the osmotic pressure within the cell. Equally F-actin might be required for the assembly of Vps1p at the invagination. To test this idea further the experiment was repeated for cells treated with sorbitol 15 minutes prior to being high pressure frozen. A significant return to the normal phenotype was observed (figure 17 and18b) demonstrating a need for F-actin to produce invaginations perpendicular to the membrane.

Although the remaining specimens exhibited no significant difference from the WT (table 7) the presence of extremely low angles in all mutants suggesting the other mutations could result in more transient/unstable interactions with F-actin. Hence fewer abnormal angles were recorded but non-the-less remain present. Although not of statistical significance there is still a strong suggestion that F-actin is required for directional control of invagination formation against the internal pressure of the cell. In the presence of sorbitol KRR-EEE and E461K (figure 18,c and d) demonstrate an increase in number of invaginations that fall between 80° and 90° to the plasma membrane supporting the notion of F-actin being a structural requirement for directional formation of invaginations against the internal pressure of the cell.

Table 6: The average angle of invagination for yeast strains cultured in SD media versus those cultured in SD media with sorbitol

Strain	Average Angle	Average Angle (Sorbitol)
Wt	76.72	76.58
RR-EE	65.39	77.70
KRR-EEE	80.58	85.34
E461K	79.09	82.70
Vps1 Null	82.76	80.90

Table 7: t-test and f-test results to test the significance of angle variation from the WT in untreated cells

	t-test		f-test	
	P value	Significant?	P value	Significant?
WT Vs RR-EE	0.0039	Yes	< 0.0001	Yes
WT Vs KRR-EEE	0.1664	No	0.0126	Yes
WT Vs E461K	0.5068	No	0.7808	No
WT Vs Vps1 Null	0.0724	No	0.1245	No

Table 8: t-test and f-test results to test the significance of angle variation between untreated and sorbitol treated cells.

Angle	t-test		f-test	
	P value	Significant?	P value	Significant?
WT Vs WT+Sorbitol	0.9616	No	0.868	No
RR-EE Vs RR-EE+Sorbitol	0.0202	Yes	0.0001	Yes
KRR-EEE Vs KRR-EEE+Sorbitol	0.0701	No	0.1588	No
E461K Vs E461K + Sorbitol	0.2969	No	0.3081	No
Vps1 Null Vs Vps1 Null+Sorbitol	0.4863	No	0.1311	No

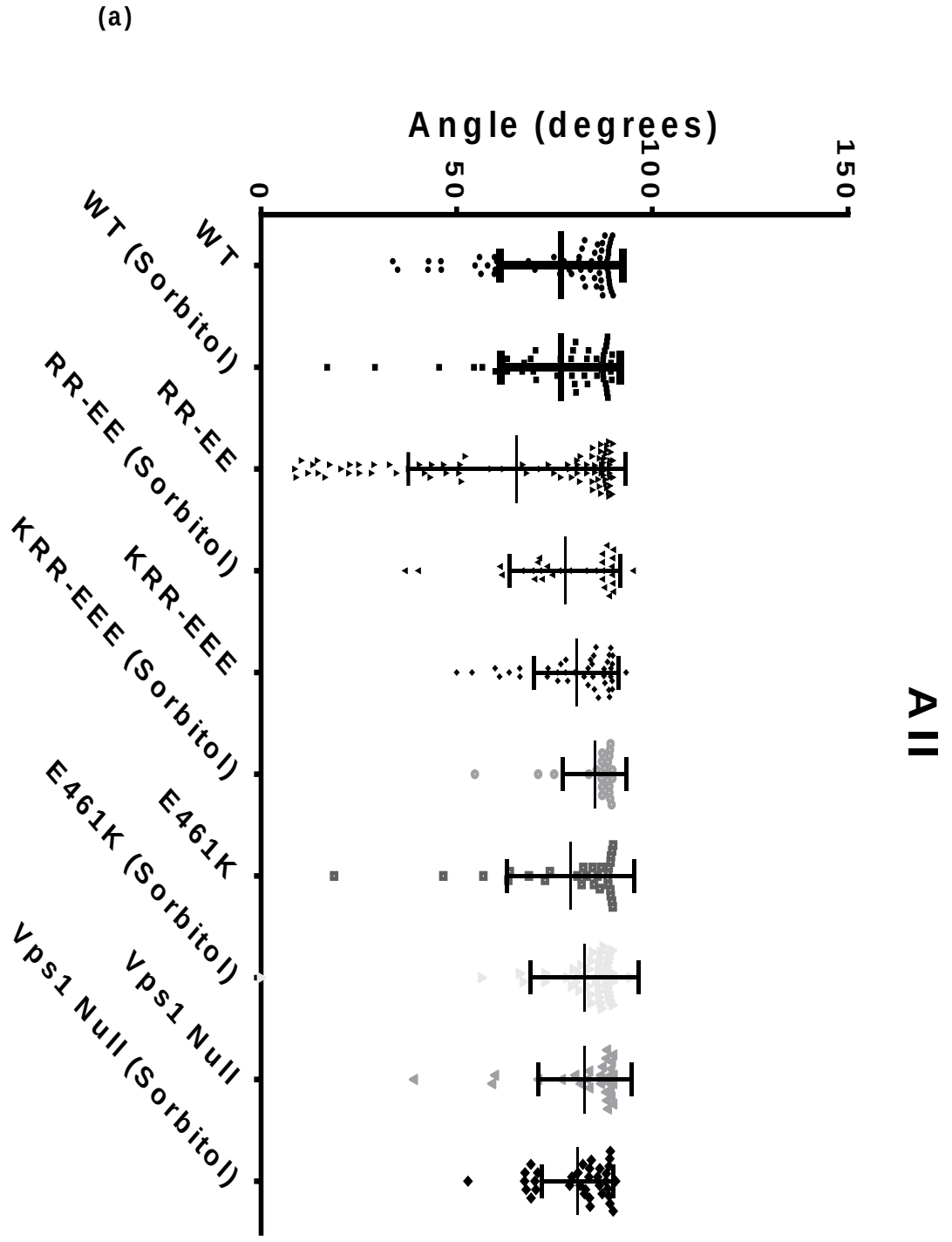

Figure 17: The angles of each individual invagination recorded for each cell line in both untreated and treated cells. The bars represent the mean plus and minus the standard deviation. These data points illustrate two populations of invaginations within the RR-EE cell lines: those that fall within the 70 degrees and over and those that fall into the 50 degrees and under category.

(a)

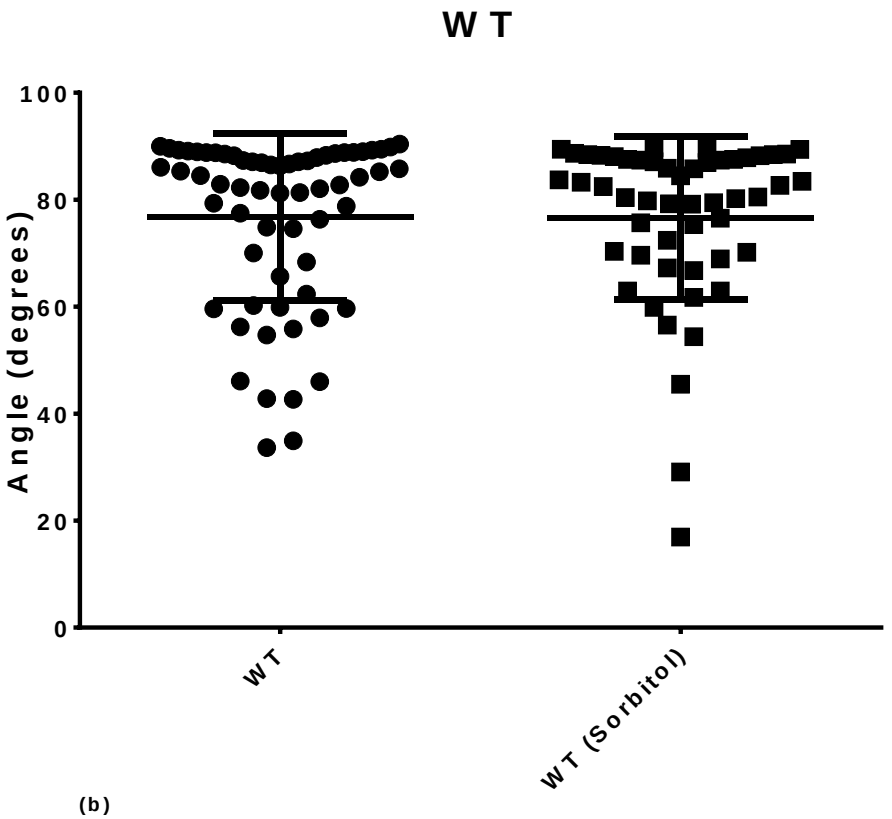
WT
Angle (degrees)
100
80
60
40
20
0
WT
WT (Sorbitol)

(b)

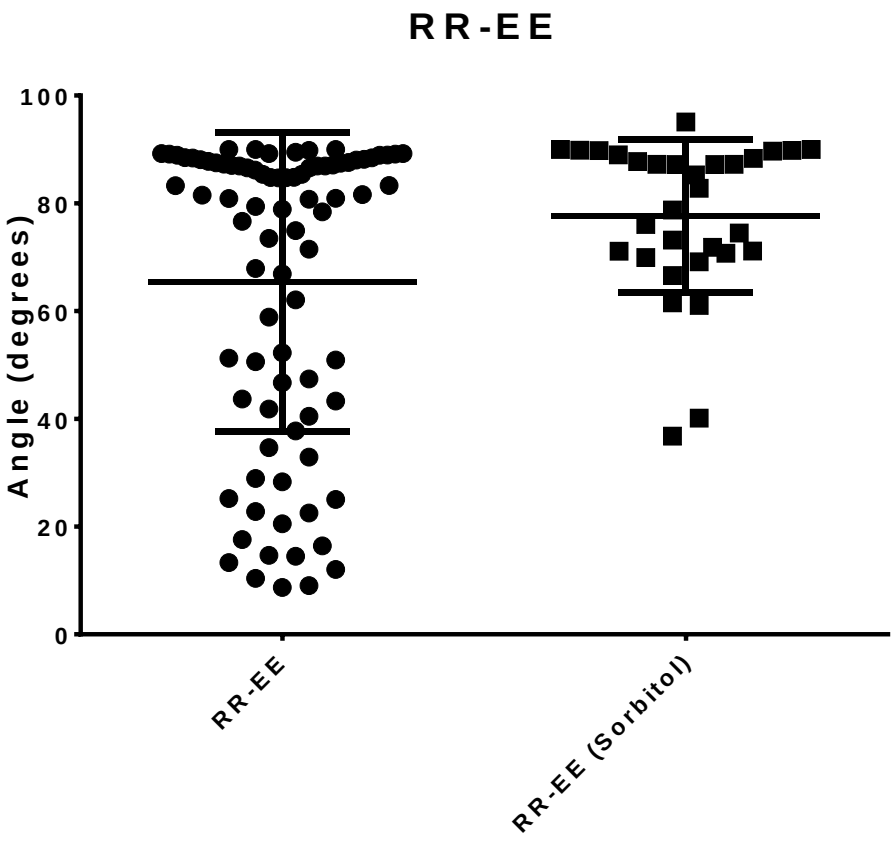
RR-EE
Angle (degrees)
100
80
60
40
20
0
RR-EE
RR-EE (Sorbitol)

(c)

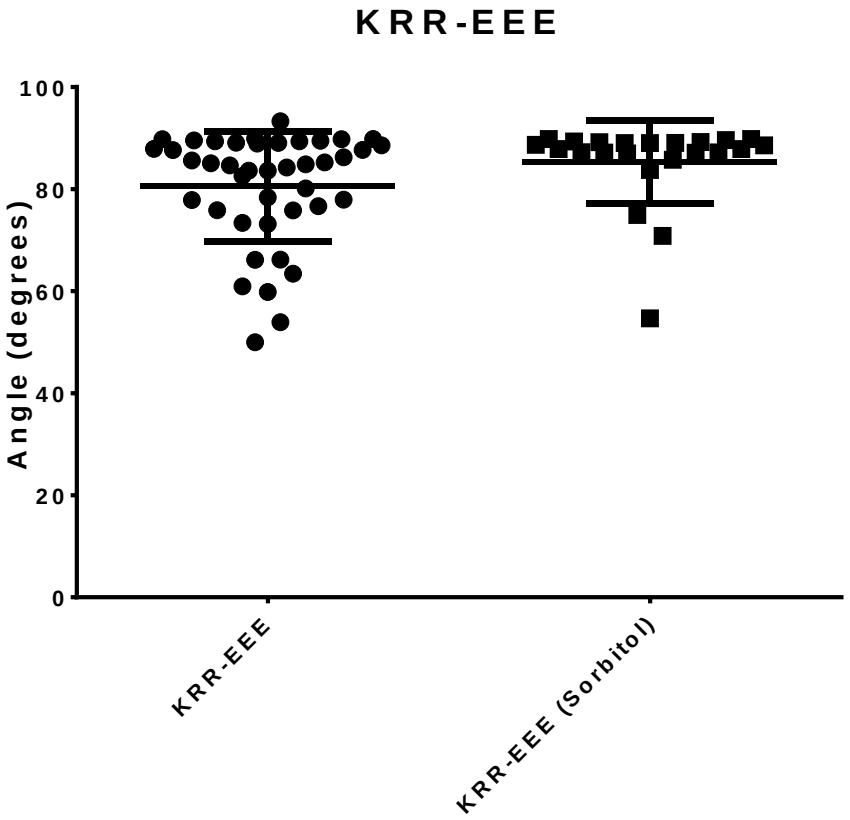
KRR-EEE
Angle (degrees)
100
80
60
40
20
0
KRR-EEE
KRR-EEE (Sorbitol)

(d)

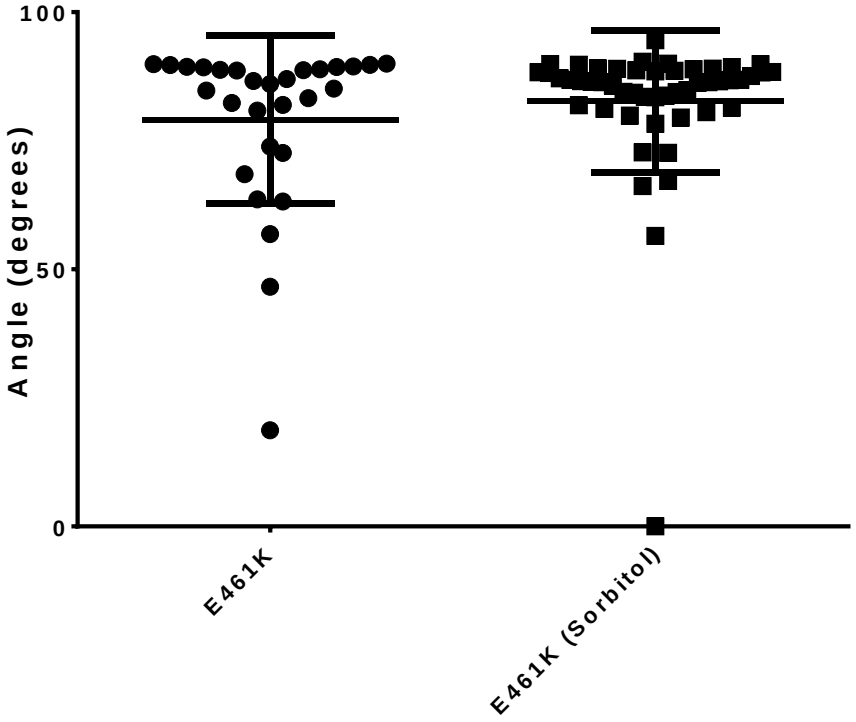
E461K
Angle (degrees)
100
50
0
E461K
E461K (Sorbitol)

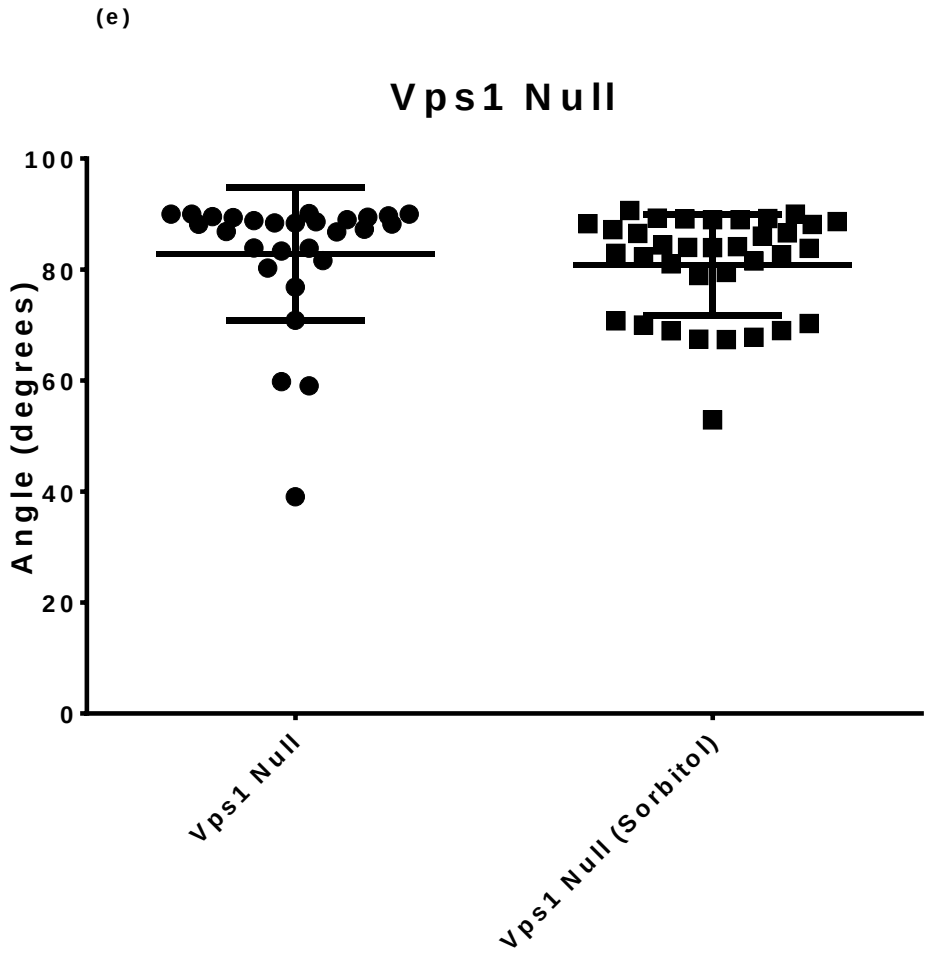

Figure 18: The angle of invagination relative to the plasma membrane in cells treated with sorbitol vs non-treated cells. Each data point illustrates the individual angles obtained for treated and untreated cells with the bars representing the mean (central bar) plus and minus the standard deviation: (a) WT; (b) RR-EE; (c) KRR-EEE; (d) E461K; (e) Vps1 Null

3.5 Vps1p/F-actin interaction dictates invagination length.

To test the whether the interaction of vps1 with F-actin is involved in elongation or scission, we studied invagination length in the actin binding mutants (figure 19). A key step that occurs prior to the scission of vesicles from the membrane in both mammalian and yeast systems is accumulation of F-actin at the site of invagination (Kishimoto et al., 2011; Ramachandran, 2011). The use of sorbitol will again be incorporated to assess whether Vps1 binding F-actin is implicated in formation of an

invagination against the internal pressure of a yeast cell or if other factors may be able to compensate for this loss of F-actin binding.

Both RR-EE and KRR-EEE length showed a significant difference to the WT length (table 10) but for very different reasons. RR-EE cell types exhibit invagination lengths far beyond the normal range of invaginations (figure 20e and f) which suggest regulatory role for RR457-8. Although it was not found to be significant this hyper-elongation of invaginations was also evident in E461K which may also act as a regulatory site for the disassembly of oligomeric Vps1p. These finding are analogous to those observed within the self-assembly defective mutants I469K indicative of defective nucleotide-hydrolysis (Mishra et al., 2011). It not only suggest a defect in scission but also stabilised actin growth to provide the driving force to extend the membrane so far into the cytosol.

Table 9: The average length of invagination for yeast strains cultured in SD media versus those cultured in SD media with sorbitol

Strain	Average Length	Average Length (Sorbitol)
Wt	76.72	76.58
RR-EE	65.39	77.70
KRR-EEE	80.58	85.34
E461K	79.09	82.70
Vps1 Null	82.76	80.90

Table 10: t-test and f-test results to test the significance of the length of mutant invaginations compared with the WT invaginations.

Length	t-test		f-test	
	P value	Significant?	P value	Significant?
WT Vs RR-EE	< 0.0001	Yes	< 0.0001	Yes
WT Vs KRR-EEE	0.0489	Yes	0.0701	No
WT Vs E461K	0.2251	No	< 0.0001	Yes
WT Vs Vps1 Null	0.8028	No	0.5925	No

Table 11: t-test and f-test results to test the significance of the length of invaginations for untreated cells compared with sorbitol treated cells.

Length	t-test		f-test	
	P value	Significant?	P value	Significant?
WT Vs WT+Sorbitol	0.0154	Yes	< 0.0001	Yes
RR-EE Vs RR-EE+Sorbitol	0.0033	Yes	< 0.0001	Yes
KRR-EEE Vs KRR-EEE+Sorbitol	0.0442	Yes	< 0.0001	Yes
E461K Vs E461K + Sorbitol	0.4284	No	0.1906	No
Vps1 Null Vs Vps1 Null+Sorbitol	0.0199	Yes	0.2974	Yes

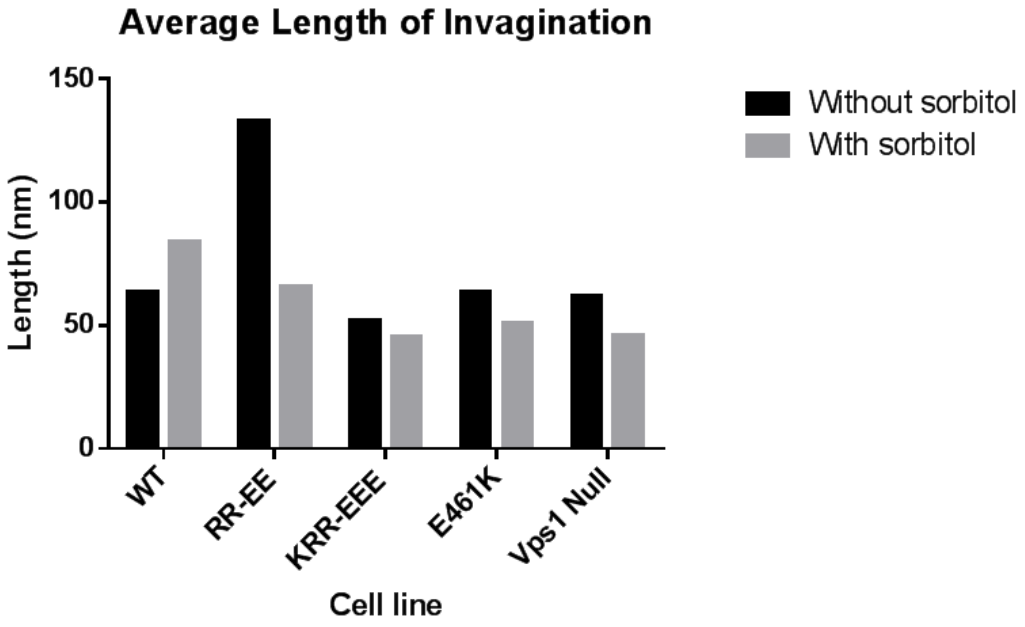

Figure19: Average length of invagintions for untreated cells Vs sorbitol treated cells

KRR-EEE produced an increase in the percentage of shorter invaginations (<50nm) suggestive of a destabilisation of the endocytic machinery causing retraction of the invagination (figure 20g and 21g). There was also an increase in proportion of abnormally long (>150nm) This could be through a lack of contact with F-actin which in turn could promote dissociation of Vps1 and its associated proteins resulting in failed internalisation. Alternatively the propensity to produce shorter invaginations could be down to reduced polymerisation of F-actin. Similar mutations within dynamin-1 were suggested as preventing dynamin-1 from interacting with the capping proteins on short pieces of F-actin, required to invaginate the membrane in podosomes (Gu et al., 2010; Ochoa et al., 2000). To this end K453:RR457-8 (KRR-EEE) it would seem are essential residues for the formation of an invagination under normal osmotic condition but it is also conceivable that these residues important in enabling Vps1p to interact with capping proteins promoting actin polymerisation.

To test whether the resultant phenotypes of hyperelongated invaginations (>200nm) or increased proportion of short invaginations (<50nm), were attributed to a loss of F-actin binding or a structural alteration within Vps1 perturbing GED activity sorbitol was added 15 minutes prior to high-pressure

freezing. This should create an osmotically neutral environment, removing the internal pressure of the cell and so the requirement for F-actin dynamics to generate the force required to produce an invagination of the membrane. RR-EE showed a significant improvement (table 11) exhibiting a distribution analogous to that of the WT (figures 20e,f and 21e, f). Such results would suggest that F-actin is not present at the invagination after addition of sorbitol as the hyper-elongation was no longer evident. Alternatively a pressure-mediated regulatory pathway not yet known could be the source of control.

Post treatment with sorbitol and subsequent HPF WT cells exhibit an increase in the proportion of abnormally long invagination (>120nm) recorded with a shift of the Gaussian distribution to the right indicative of an increased proportion of longer invaginations (figure 20a, b and 21a, b). If F-actin were required for Vps1p assembly at the invagination, it might be expected that a similar reduction in length of invagination would be observed if F-actin was absent. If F-actin is present then that the reduction in length observed in RR-EE cells treated with sorbitol is possibly attributed to pressure-dependant mechanism of Vps1p.

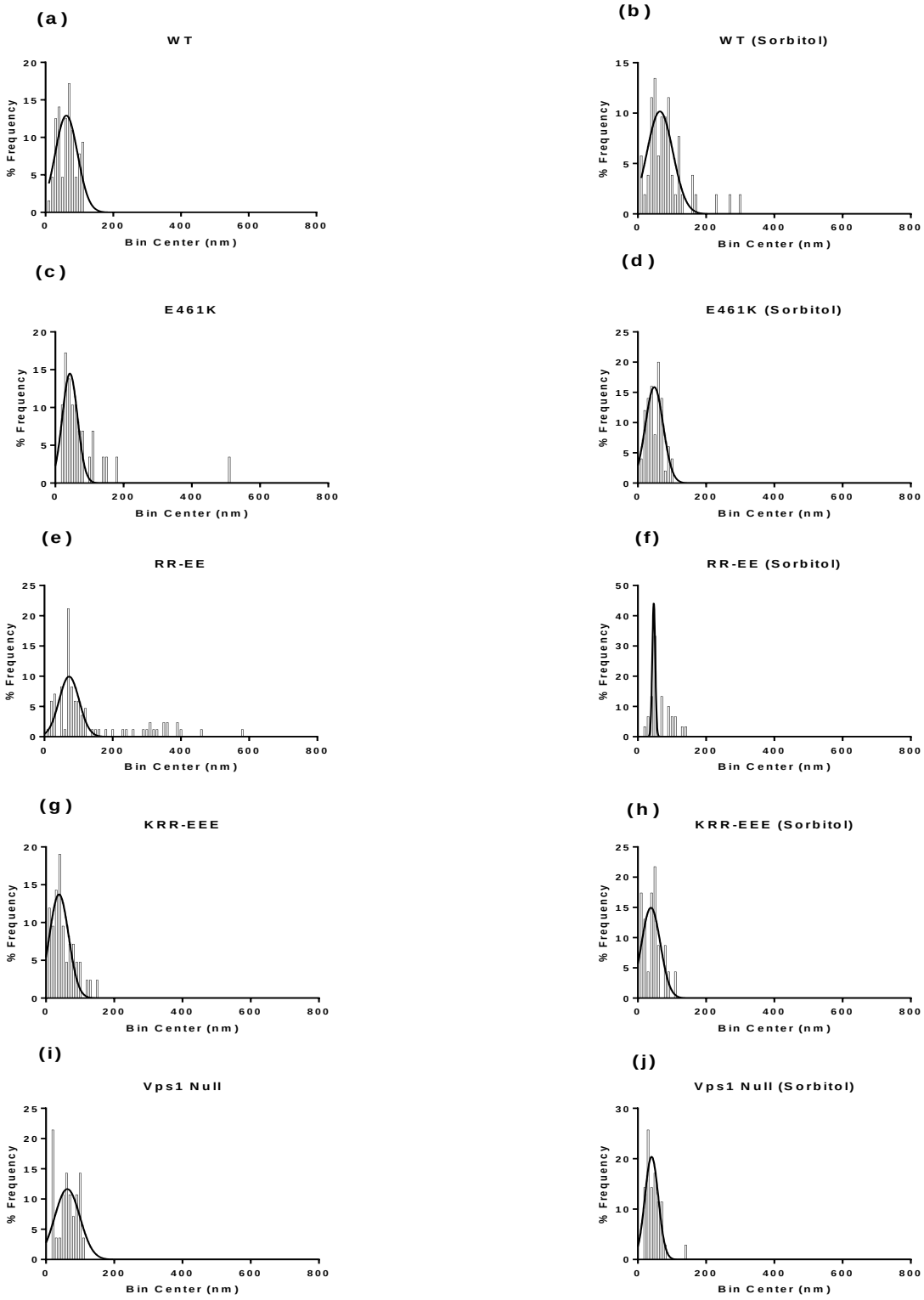

Figure 20: Frequency distribution of invaginations taken as percentage of the total number of invaginations recorded for each stain untreated and sorbitol treated cell with the Gaussian distribution overlaid.

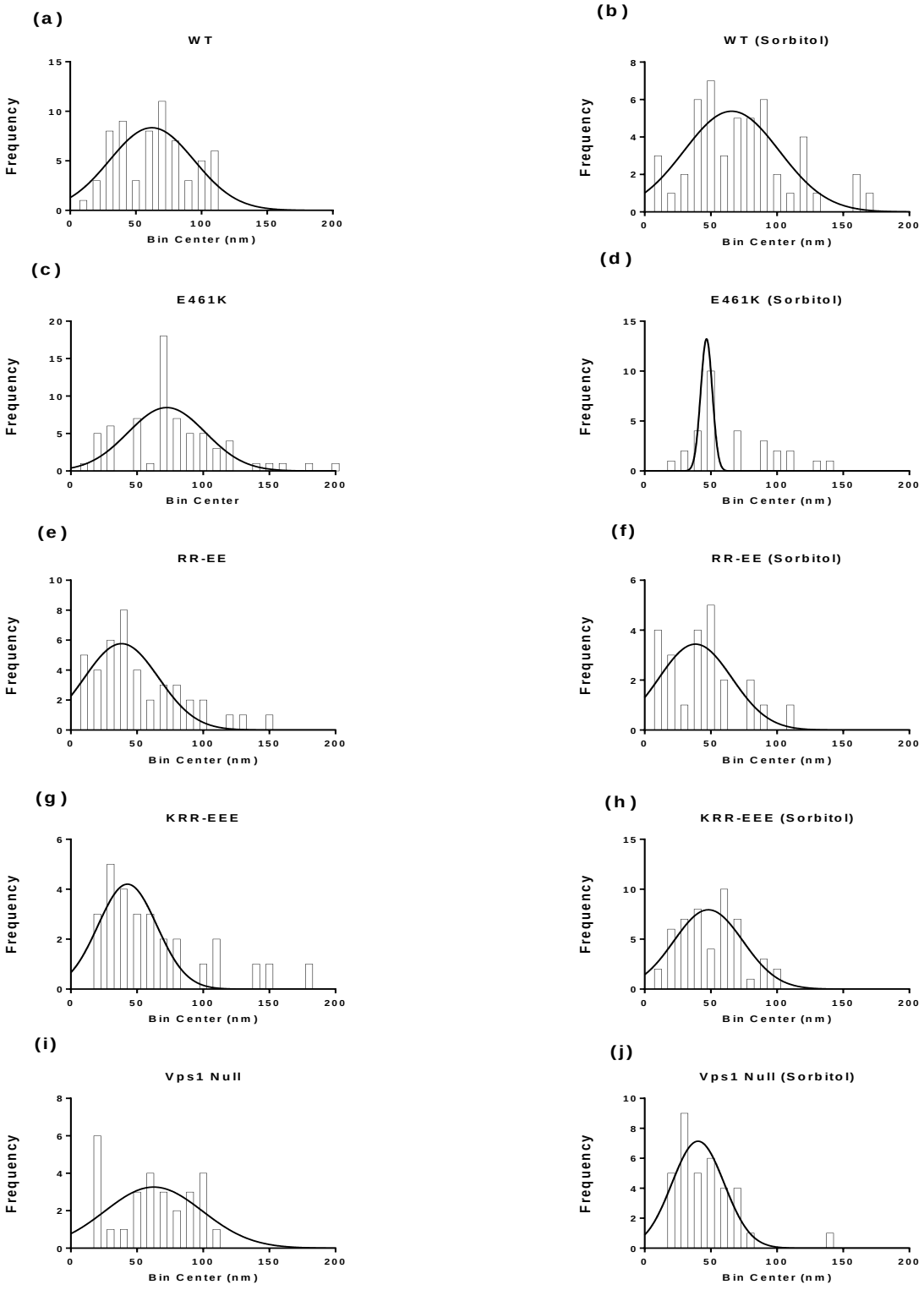

Figure 21: Frequency distribution of invaginations taken as percentage of the total number of invaginations recorded for each stain untreated and sorbitol treated cell with the Gausion distribution overlaid. These graphs show the above data excluding the high end extreme values allowing observation of the more subtle effects on the Gaussian distribution produced in data sets that exhibit a less extreme phenotype.

KRR-EEE cell types showed a high proportion of short invagination (<50nm) compared with the WT but still produced a population of abnormally long invaginations (>150nm) (figure 20, a,e). After treatment with sorbitol the proportion of shorter invaginations decreased and no abnormally long invagintions were recorded (figure 21, h). This was a significant improvement toward a WT distribution which would support arguments for the mechanism of Vps1p assembly as being pressure dependant but also a need for F-actin as a pressure sensor, conferring mechanical stresses to Vps1p, orchestrating its assembly at the invagination. Not only this, but the results suggest how a mutated Vps1 could be detrimental to the endocytic event through improper binding to F-actin that might prevent proper action of the GED. This in turn could induce an impromptu disassembly of Vps1 producing a knock-on effect resulting in retraction of the endocytic invagination.

The premise behind the pressure dependant assembly of Vps1p is hinged on its interaction with F-actin which acts to mechano-sense, transducing a force to Vps1p inducing conformational changes that allow for nucleotide binding and hydrolysis. Alternatively the pressure within the cell may well be the source of support for the invagination, much like a boat in water. If you remove the supporting elements within the hull of the boat you would induce collapse of the hull. By the same premise, defective endocytic components could produce an instability within the endocytic machinery inducing failure of all other associated endocytic component, resulting in retraction of the invagination.

3.6 F-actin binding to Vps1 necessary to generate invaginations perpendicular to the membrane.

The majority of invaginations between 0-120nm produce angles between 85 and 90 degrees in untreated cells. Those falling outside of this range have a propensity to develop more extreme angles ranging between 0 and 50 degrees (figure 17, 22). When angle and length are considered in conjunction with one another it introduces a possible pattern whereby a reduction in angle is attributed to an increase in length, symptomatic of the structural limitations of F-actin to support an invagination (figure 24). Treatment with sorbitol produced a shift in the distribution of invagintions with the majority falling between 50 and 90 degrees and lengths between 0nm and 150nm (figure 24). The general trend of decreased angle with increase in length is diminished compared with untreated cells.

The persistence of abnormal angles (<80 degrees) would support the argument that Vps1p requires interaction with F-actin to produce a directional propagation of F-actin against the internal pressure of the cells. The overall reduction in length and angle in the presence of sorbitol adds support to F-actins interaction with Vps1p being of regulatory nature, perhaps mechano-sensing membrane invagination causing conformational changes within oligomeric Vps1p to enable effective nucleotide binding and hydrolysis.

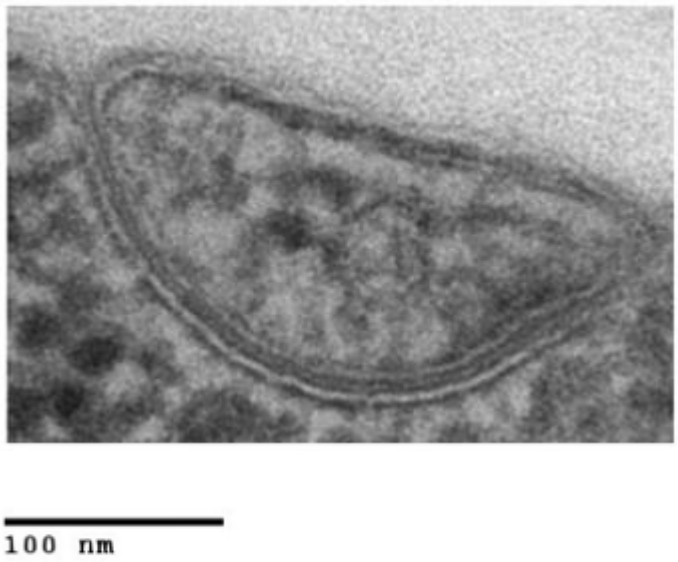

Figure 22: Hyper-elongated invagination found in RR-EE mutation illustrates clearly how these abnormally long invaginations are also subject to extreme curvature with the base of the invagination almost contacting the membrane.

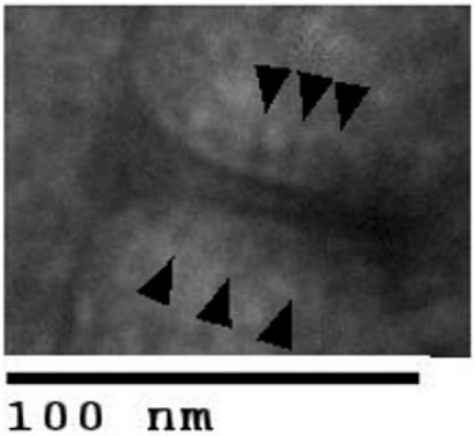

Figure 23: After addition of sorbitol KRR-EEE exhibited an increase in proportion of invaginations falling between 50nm-120nm, and a reduction in those falling between 0nm-50nm. Interestingly filaments radiating away from the invagination resembling F-actin (indicated by the black arrows) can be seen which could suggesting F-actin binding is retained. Therefore the phenotype observed may well be a result of a structural alteration in Vps1p preventing the action of pressure mediated disassembly.

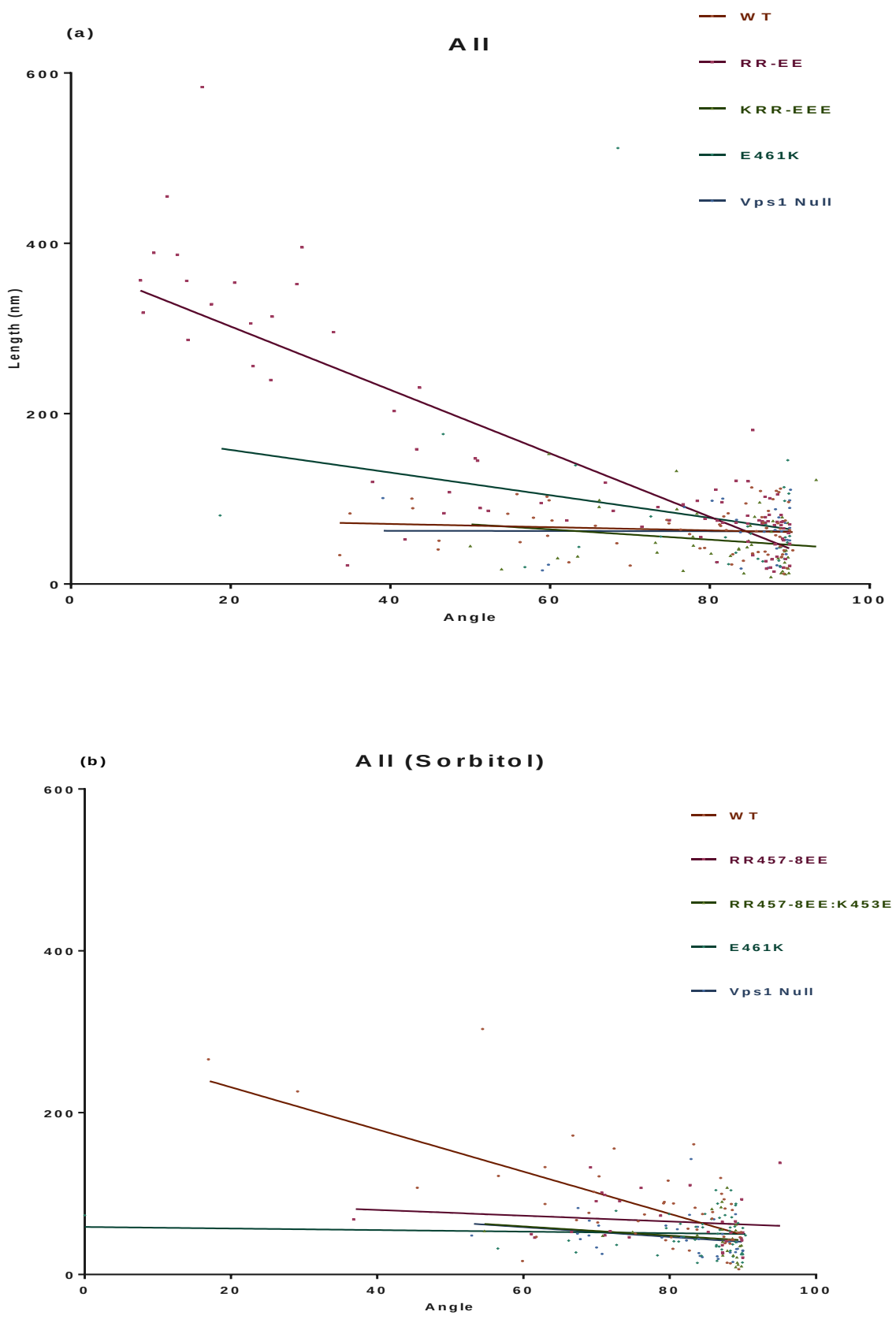

Figure 24: (a) Angle Vs length for WT and mutant strains of *S. cerevisiae* treated with 0.5M sorbitol (final concentration 0.5M). **(b)** Angle Vs length for WT and mutant strains of *S. cerevisiae*.

3.7 Frequency of invaginations suggests a destabilisation of the endocytic machinery through lack of association with F-actin via Vps1

The significant reduction of invagination frequency in all mutants compared with the WT (table 13) would suggest a destabilisation of the endocytic machinery increasing the frequency of the failed endocytic events. However a significant improvement after the addition of sorbitol was only apparent within E461K and Vps1 null (table 14). Although not statistically significant figure 25 shows a clear increase in the frequency of invaginations exhibited within the different mutant cell lines lending favour to two conclusions previously suggested. The first that the scission event is a pressure mediated process reliant upon interaction of Vps1 with F-actin to sense the pressure within the cell initiating scission upon reaching approximately 120nm. The second conclusion is that F-actin acts to stabilise the endocytic machinery against the internal pressure enabling formation of stable invaginations against the internal pressure and hence defective binding results in a decrease in frequency of invaginations.

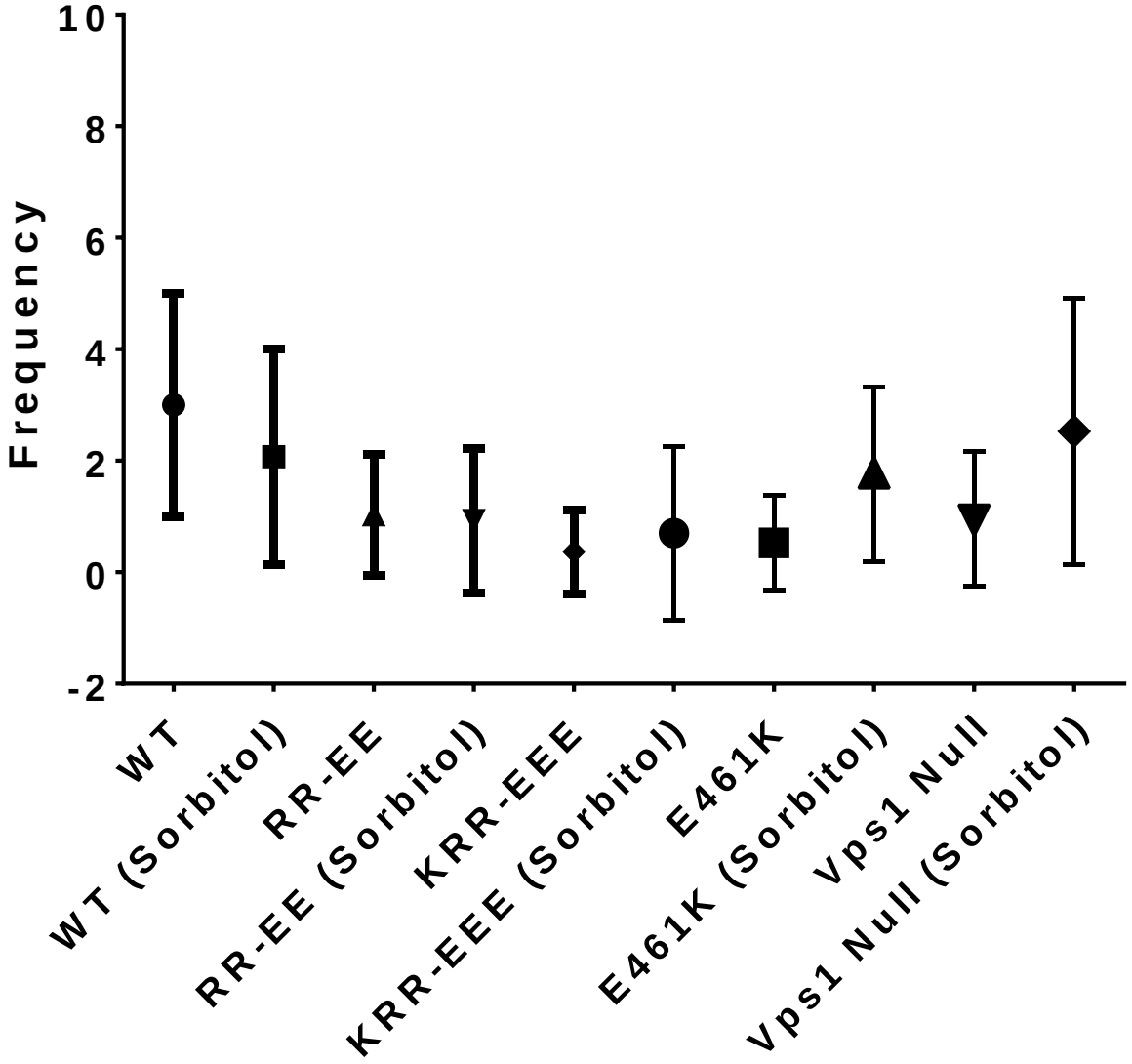

Figure 25: Average frequency of invagination for WT and mutant strains of *S. cerevisiae* in untreated cells and cells treated with 0.5M sorbitol. Error bars represent plus and minus the standard deviation either side of the average for each data set.

Table 12: The average frequency of invaginations for yeast strains cultured in SD media versus those cultured in SD media with sorbitol

Strain	Average Frequency	Average Frequency (Sorbitol)
Wt	2.073171	3
RR-EE	0.926829	1.029703
KRR-EEE	0.7	0.367347
E461K	1.757576	0.528736
Vps1 Null	2.526316	0.96

Table 13: t-test and f-test results to test the significance of average invagination frequency per cell against the average frequency per WT cell.

Frequency	t-test		f-test	
	P value	Significant?	P value	Significant?
WT Vs RR-EE	< 0.0001	Yes	< 0.0001	Yes
WT Vs KRR-EEE	< 0.0001	Yes	< 0.0001	Yes
WT Vs E461K	< 0.0001	Yes	< 0.0001	Yes
WT Vs Vps1 Null	< 0.0001	Yes	0.0147	Yes

Table 14: t-test and f-test results to test the significance of average invagination frequency per cell of untreated cells against sorbitol treated cells.

Frequency of invagination	t-test		f-test	
	P value	Significant?	P value	Significant?
WT Vs WT+Sorbitol	0.0577	No	0.8195	No
RR-EE Vs RR-EE+Sorbitol	0.6303	No	0.1788	No
KRR-EEE Vs KRR-EEE+Sorbitol	0.1121	No	< 0.0001	No
E461K Vs E461K + Sorbitol	< 0.0001	Yes	< 0.0001	Yes
Vps1 Null Vs Vps1 Null+Sorbitol	0.0069	Yes	0.0022	Yes

4 Discussion

4.1 A Dynamin-Like Protein

Vps1p shares a significant homogeneity with dynamin-1 as revealed by similarity searches and secondary structure comparisons (figure 13). The presence of key conserved residues within the G-domain, middle domain, and GED have directed much of the mutational analysis on this protein. The data from such studies would suggest a conservation of function for these residues supporting a mode of action for Vps1p to be analogous to that of mammalian dynamin-1.

Mutations within conserved residues of the G-domain and GED domain have produced defects in both self-assembly of Vps1p and its role within the scission. Such defects have been manifested as hyper-elongated invaginations and reduced rates of endocytosis *in vivo* (Mishra et al., 2011; Nannapaneni et al., 2010; Smaczynska-de Rooij et al., 2010). As previously discussed such defects were recorded by electron microscopy, tracking of fluorescently labelled endocytic proteins and use of fluorescent lipid dyes (FM4-64) (Chappie et al., 2010; Mishra et al., 2011; Nannapaneni et al., 2010; Smaczynska-de Rooij et al., 2010; Wang et al., 2011; Wenger et al., 2013). Similarly corresponding mutations within dynamin-1 produced failures in self-assembly and conferred an inability to hydrolyse GTP, preventing scission. Solving of the crystal structure combined with biochemical assays monitoring orthophosphate (Pi) concentration demonstrated either an inability to bind GTP or an inability to hydrolyse GTP as a result of these mutations (Chappie et al., 2010; Y.-W. Liu et al., 2013; Marks et al., 2001; Wenger et al., 2013). In both systems these domains have been demonstrated as essential to the self-assembly mechanism of dynamins and in producing the mechano-constriction that results in scission.

In vitro Vps1p is functionally undifferentiated from dynamin-1 displaying a propensity to self-assemble and tubulate membranes in a nucleotide-bound dependant fashion, independent of membrane curvature, causing tubulation of membranes (Smaczynska-de Rooij et al., 2010, 2012). Mammalian dynamin-1 has also been well characterised as a protein that assembles in a nucleotide-bound-dependant fashion and similarly mutations within the conserved residues of the G-domain and

GED result in failure to self-assemble or perform scission (Chappie et al., 2010; Song, Yarar, et al., 2004). From these data it would be reasonable to infer that both Vps1p and dynamin-1 share both structural and functional characteristics.

The crystal structure for dynamin-1 has also been resolved and pseudoatomic models for its polymeric structure have been resolved suggesting a possible structure for Vps1 by virtue of its structural and functional homogeneity with dynamin-1 (Chappie et al., 2011; Faelber et al., 2011). With this structure in mind I set about using electron tomography to assess invagination morphology and subsequently revealed a spiral structure that encircles the invagination. The structure localises to the neck of the invagination being absent from the bud, much like the model for dynamin-1 put forward. Although interesting it is not possible at this stage to discern unequivocally what protein(s) produce the structure in question. The similarity in predicted secondary structure of Vps1p with dynamin-1 combined with the *in vitro* dynamics observed would strongly suggest Vps1 to be able to produce the structure resolved. Further to this the charge swap mutant RR-EE produced a phenotype sharing strong likeness with that observed in the assembly-defective mutants in both yeast and mammalian cells (Mishra et al., 2011; Smaczynska-de Rooij et al., 2012; Song, Yarar, et al., 2004).

Extrapolating from what is known about how dynamin self-assembles, the phenotype observed in the RR-EE mutant would implicate the middle domain of Vps1p in conformational change that enables the conversion from a GTP-bound state to a GDP-bound state, driving the scission process. Previous work has positioned the GED as a key regulator/effector of self-assembly much like in Dynamin 1 (Chappie et al., 2011; Klinglmayr, Wenger, Mayr, Bossy-Wetzel, & Puehringer, 2012; Y.-W. Liu et al., 2013; Mishra et al., 2011; Smaczynska-de Rooij et al., 2012). Supporting this further was the concomitant production in reduced frequency of invagination indicative of reduced scission. Such conformational changes have been suggested to be central to the scission process within mammalian clathrin-mediated endocytosis and more recently within yeast (Chappie et al., 2011, 2010; Ford et al., 2011; Mishra et al., 2011; Smaczynska-de Rooij et al., 2012; Vallis et al., 1999; Wenger et al., 2013).

The RR-EE mutation in yeast falls within a helical-motif of the middle domain of Vps1p, unlike the I649K self-assembly mutations which fell within the GED. For dynamin-1 the stalk (middle) domain

has been characterised predominantly as a regulatory element for its self-assembly. When dynamin-1 is in a nucleotide-free state, the stalk interacts with the PH domain via a conserved helical motif, orienting the lipid binding domain inward to occlude the GED, preventing self-assembly (Chappie et al., 2011, 2010; Faelber et al., 2011). In a nucleotide-bound state the stalk domains are thought to associate in a crosshatched alignment promoting interaction of adjacent GED and G-domains increasing the GTPase activity providing the energy required for the scission. Although the RR-EE mutation is predicted to fall within a putative actin binding helical motif we cannot dismiss a possible duality of function exhibited for this helical motif. In addition to its function as an actin binding site it might also share functional analogity with the stalk domain of dynamin-1. It could be that the RR-EE mutation may produce a conformational change that alters the orientation of the GED, preventing interaction of GED and adjacent GTPases perturbing GTP hydrolysis. The result of such a defect extrapolated from the dynamin-1 mode of function, would be stable interactions between Vps1p molecules and an inability of polymeric Vps1p to perform scission. Consequently we get this unusual hyper-elongation of invaginations and an overall reduction in the number of invagintions generated.

A limitation of the similarity search performed earlier is manifested as an unrepresentative score of 30% homogeneity between the actin binding domains of Vps1p and dynamin-1. What is not considered is how alternate residues with similar biochemical properties might be substituted in enabling for the regions to form similar structures across the different kingdoms giving rise to a conservation of function. The alignment data clearly shows a stronger similarity of ~60% for this region (figure 11), twice that suggested by the similarity search. A key consideration is that amino acids can substitute for one another provided they share a similar biochemical profile. Hence dynamins in both Animalia and Fungi kingdoms exhibit similar modes of action in similar contexts (Ford et al., 2011; Mishra et al., 2011; Ramachandran, 2011; Smaczynska-de Rooij et al., 2010). To test if these residues truly are interchangeable mutant yeast strains could be produced with residues substituted in that correspond to the like-amino acids (figure 26).

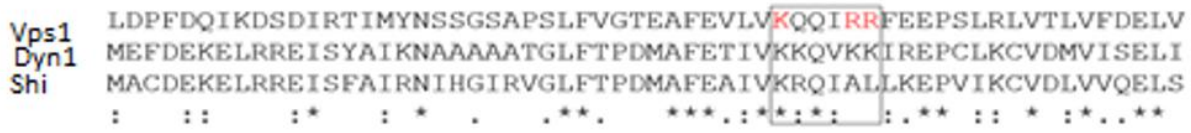

Figure 26: Alignment data corresponding to the putative actin binding domains with the respective organisms. The mutated residues have been highlighted in red: VPS1 [Saccharomyces cerevisiae] (line 2; Nucleotide-free Human Dynamin-1 [Homosapiens] (line 2); dynamin [Drosophila melanogaster] (line 3). Within the boxed region although the only mutated residue that is conserved across all three is K, but interestingly R, and K are both positively charged and have similar biochemichal properties. Therefore it might be possible for these residues to substitute for one another in the respective organisms. The mutation fall wihtin a region that shows strong similarity between the three different kingdoms with like-amino acids indicated by (:) and identical amino aids idenfied with an (*).

The ultimate goal of this study was to develop a high resolution spatial-localisation map of the different endocytic proteins and to combine this with tomographic analysis. In this way the true nature of the spiral structure could be fully concluded. Kymographs and residency times (Smaczynska-de Rooij et al., 2010, 2012)provide limited information with respects to localisation at the resolution of an invagination, and so there is a need to combine localisations at higher resolutions with this data to begin to understand how the various endocytic components interact at the level of an invagination.

4.2 A Revised Model for Scission in s. Cerevisiae

Vps1p has been reported as associating with Rvs167p at cortical actin patches and invaginations in a synergistic manner producing significantly higher levels of endocytosis compared with either $\Delta vps1p$ or $\Delta rvs167$p (Smaczynska-de Rooij et al., 2010, 2012). This relationship is reported to be mediated via a type I SH3 binding motif within Vps1p that binds Rvs167p's SH3 motif (Smaczynska-de Rooij et al., 2012). Either a direct or indirect oligomerisation of Vps1p to Rvs167p could confer the ability to bind curved membranes i.e. in a curvature dependant manner, to Vps1p. Potentially Rvs167p is more instrumental in initiating the invagination of the membrane and upon oligomerisation with another amphiphysin exposes its SH3 domain that is then bound by Vps1p. This idea is supported by the reduced residency of Rvs167p-GFP upon mutation of the SH3 motif within Rvs167p, combined with data from the BiFC assay in which both Vps1p and Rvs167p exhibit a colocalisation at cortical actin patches (Smaczynska-de Rooij et al., 2012).

Although some groups have suggested that Rvs161/167p form a heterodimeric complex at the neck of the bud this might not necessarily be the case by virtue of the *in vitro* findings which demonstrated the heterodimer as depolymerising oligomeric Vps1p (Smaczynska-de Rooij et al., 2012). Purification by GST-pull down was not successful for Rvs167p alone and so this remains inconclusive (Smaczynska-de Rooij et al., 2012). It might be possible that Rvs167p can both homo- and hetero-oligomerise and is able to interact with, and positively regulate oligomeric Vps1p when it homo-oligomerises. It might be possible to discern if the complex associates with Vps1p in a heterodimeric form or as a homo-oligomer through generating several recombinant proteins for BiFC assays: 1) Rvs167p-N-terminal label and C-terminal label; 2) Rvs161p-N-terminal and C-terminal 3) Vps1p-N or C-terminal tag complimentary to Rvs161p-tag and another strain complementary to Rvs167p-tag. With these it could be tested for homo- verses hetero-oligomerisation and which if not both associate with Vps1. If the interaction rate was compared with the level of localisation for each of these individual proteins to the membrane it might become clearer as to whether these proteins exist as a heterodimer at the endocytic event.

The production of hyper-elongated invaginations within the RR-EE mutants suggests that the interaction of Vps1p with F-actin promotes polymerisation of F-actin at the endocytic site, driving invagination of the membrane. It also infers that F-actin binding to Vps1p could promote nucleotide hydrolysis, driving the scission event which appears to malfunction in this mutant, producing hyper-elongated invaginations. KRR-EEE produced a higher proportion of shorter invaginations with significant reduction in the frequency of invaginations recorded suggesting the F-actin binding might also be required to assemble Vps1p at the invagination. It could be possible F-actin aids in orienting Vps1p into a conformation that either promotes or allows nucleotide binding and hydrolysis to bring about scission.

In vitro Vps1p has been shown to self-assemble on liposomes causing there tubulation, in a nucleotide-bound dependant manner, but not to produce scission (Smaczynska-de Rooij et al., 2010). This model was lacking the presence of F-actin, which might explain the high level of membrane tubulation, and a lack of scission observed. This could be demonstrated by: 1) A repetition of the *in*

vitro experiment utilising isolated Vps1p and liposomes both in the presence of GTP and F-actin. This would demonstrate weather the reduced tubulation and increased emulsification of liposomes is attributed to Vps1p's interaction with F-actin. 2) Repetition of the same experiment with G-actin in place of F-actin to determine if Vps1p requires preformed F-actin to oligomerise in a conformation that promotes GTP hydrolysis. Organophosphate concentrations could also be quantified in both systems to discern if F-actin increases the GTPase activity of Vps1p, promoting scission.

As previously discussed a similar interaction with F-actin has been demonstrated for dynamin-1 but there is uncertainty concerning the relationship of dynamin-1 with F-actin (Gu et al., 2010). It is not possible from this study to say unequivocally that F-actin is required for the assembly of the respective dynamins to assemble at the invagination as it could be that the dynamins have an actin nucleating capacity as suggested by the finding for dynamin-1. When the Arp2/3 complex and respective activators were mutated there was still actin nucleation to podosome comet tails. If actin nucleating factors and NPFs are disrupted there should be little or no F-actin nucleation occurring at the podosomes. One explanation is that unknown actin nucleators are present or that dynamin-1 has an actin nucleating capacity. Alternatively it could be that dyanamin-1 interacts with short pre-existing F-actin to remove the capping proteins, promoting polymerisation, driving inward movement of the invagination as suggested by studies on actin distribution in podosomes (Gu et al., 2010; Ochoa et al., 2000).

Figure 27 illustrates a possible arrangement of Vps1p, Rvs171p/167p, sla1p and actin at the invagination during endocytosis. This model was constructed based on the evidence collected not only in this study, but also based on the data collected from the various other studies considered.

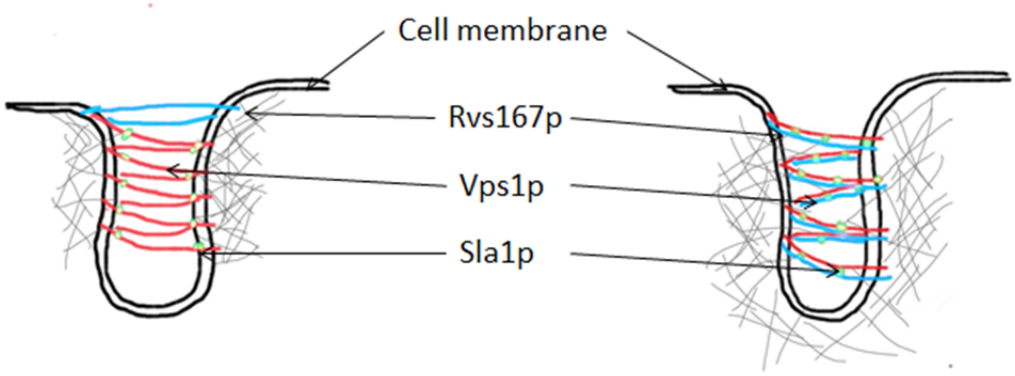

Figure 27: Suggested composition of the spiral structures observed in the tomograms obtained. The left model has been previously suggested however the right model depicts more recent findings which depict an interaction between Rvs167p-Vps1p-Sla1p at the invagination. Rvs167p-Vps1p complex being central to scission with Sla1p linking the actin dynamics to the scission apparatus aiding in elongation of the invagination against the internal osmotic pressure.

4.3 A requirement for F-actin to carry out endocytosis

An absolute requirement for F-actin in normal yeast endocytosis distinguishes the yeast endocytic cascade from that of mammals (Ayscough et al., 1997; Kaksonen, Sun, & Drubin, 2003; Kaksonen, Toret, & Drubin, 2006; Morton et al., 2000). Although a requirement for actin bundling proteins Sac6 and Scp1 at the endocytic event has been demonstrated the same study highlighted a possible need for F-actin alone as complete rescue was not observed upon the addition of sorbitol in cells treated with latrunculin-A and low levels of endocytosis were still observed in cells carrying the $\Delta Sac6\Delta Scp1$ mutation (Aghamohammadzadeh & Ayscough, 2009). Similar observations have been recorded for mutants of the key actin nucleation-promotion factors including yeast Las17p(WASP/Myo) and yeast Arp2/3p (Arp2/3) complex, Abp1p (ABP1) (Dawson et al., 2006a; Doyle & Botstein, 1996; Garcia, Stollar, & Davidson, 2012; Jonsdottir & Li, 2004; Spiess et al., 2013; Urbanek et al., 2013; Wong, Meng, Rajmohan, Yu, & Thanabalu, 2010).

Although these mutations suggest F-actin to be a requirement for endocytosis they infer no specific role. Current data suggests F-actin to be necessary to produce consistent invaginations against the internal pressure but also a role in organising endocytic proteins as complete rescue was not observed in the presence of sorbitol, analogous to the findings within this study. Here I have provided evidence

at the ultrastructural level for the requirement of an intrinsic link between Vps1p and F-actin to provide directional propagation of an invagination against the osmotic pressure of the cell. The phenotypes produced also offer an explanation as to why complete rescue is not observed in the presence of sorbitol when considering what is already known.

The hyperelongated invaginations observed in the RR-EE mutation would imply an impaired ability to hydrolyse GTP and therefore perform scission. I would suggest that the F-actin provides a scaffold to which Vps1p can adhere via its conserved helical domains. This anchorage could hold Vps1p in a conformation that enables the GED domain of one Vps1p molecule to interact with the GTPase domain of another Vps1p molecule in adjacent rungs of the helix producing a conversion of GTP to GDP. The energy derived from the conversion of GTP to GDP would provide the chemical energy needed to drive the conformational change that produces a torsion within Vps1p, causing constriction of the oligomeric complex and bringing about scission.

Observations within mammalian systems would suggest an alternate explanation. Perhaps the actin is nucleated from the conserved helices within the middle domain of Vps1p since in both dynamin-1 and Vps1p invagination of the membrane is still able to occur at reduced levels when the Arp2/3 complex is disrupted (Gu et al., 2010; Kim et al., 2006; Yu & Cai, 2004). It could equally be due to an interaction of Vps1p with pre-existing F-actin. The mutated F-actin binding region within Vps1p could be implicated in stabilising F-actin and promoting its polymerisation through removal of capping proteins as has been shown for dynamin-1 (Gu et al., 2010). Stabilisation and subsequent removal of capping proteins could enable actin polymerisation to continue that in turn would extend against the cell membrane, driving inward movement of the plasma membrane, producing the invagination.

Reduced frequency of invagination evident in RR-EE, KRR-EEE and E461K cell lines suggest an interaction of Vps1p with F-actin is required for normal endocytosis. When considering a reduced frequency and increased proportion of shorter invaginations (<50nm) in KRR-EEE it would seem that Vps1p is reliant on its interaction with F-actin to assemble at the invagination as a similar phenotype is also recorded for the *vps1p null* mutant. Loss of interaction with F-actin could cause a dissociation

of Vps1p and by association with other key endocytic proteins such as Sla1p and Rvs167p resulting in retraction of the invagination. Such retractions have been reported in cells lacking Vps1p but more so in those lacking actin nucleating and actin bundling proteins essential to the endocytic process (Carreno et al., 2004; Dawson, Legg, & Machesky, 2006b; Garcia et al., 2012; Gheorghe et al., 2008; Hoepfner, van den Berg, Philippsen, Tabak, & Hettema, 2001b; Vizeacoumar et al., 2006; Wang et al., 2011; Yu & Cai, 2004).

This data suggest that F-actin is first required to assemble Vps1p at the endocytic site, as indicated by increase proportion of shorter invagination in KRR-EEE, E461K and Vps1 null (figure 19). Secondly this association of F-actin with Vps1p may well lead to promotion of actin polymerisation, producing the energy required to invaginate the membrane against the internal pressure of the cell. But more than this, Vps1p could require F-actin as a scaffold to help retain conformations that produce high G-domain activity to provide the energy that drives the scission.

4.4 Concluding remarks

Clathrin-mediated endocytosis is a highly conserved process throughout *Animalia* with homologous proteins being required for each of the broad stages from patch formation to scission and inward movement of the vesicle. The model can now more than ever be extended to yeast which is a valuable system in assessing the key regions of conserved domains required for specific interactions with various other endocytic proteins and cytoskeletal components.

Vps1p is intrinsically involved within the endocytic cascade suggested by the aberrant localisations of other endocytic proteins in its absence (Smaczynska-de Rooij et al., 2010, 2012; Warren et al., 2002; Yu & Cai, 2004). It has been shown to directly interact with both Sla1p and Rvs167p which suggests Vps1p to be involved within the scission event, linking the rest of the endocytic proteins to the F-actin scaffold along with Arp2/3 and Abp1-Bzz1p-Las17p (Smaczynska-de Rooij et al., 2012; Warren et al., 2002). The nucleotide-bound self-assembly and capacity to tubulate membranes suggest a dynamin like mode of scission highlighting conservation of key structural components required to execute mechanoconstriction to produce a scission (Mishra et al., 2011; Smaczynska-de Rooij et al., 2010).

The mutations analysed here suggest F-actin is required for Vps1p to either oligomerise at the membrane or to activate GTP hydrolysis as indicated by the hyper-elongated invaginations. I would also propose that Vps1p is a promoter of actin polymerisation as suggested by the formation of hyper-elongated invaginations. Equally though by the reduced lengths of invagination in E461K mutant and the KRR-EEE, it is not unreasonable to suggest that Vps1p interferes with the binding of capping proteins to F-actin promoting there polymerisation. I would suggest RR457-8 to be important for binding actin and orientating the protein in a conformation that enables nucleotide binding and hydrolysis to drive the scission process. Hence in the K453E:RR457-8EE mutant, there is a significant increase in the proportion of shorter invaginations, implicating K453 as a key residue required for F-actin binding to enable assembly at the invagination.

In yeast it is still not fully clear how this mechanism works. Conservation of domain structures within the GTPase domain, middle and GED would place bias toward a mode of action analogous to that of dynamin-1. The data and arguments put forward in this study would support a model of scission similar to that observed in mammalian systems. What remains to be assessed is to what extent the homogeneity between Vps1p and dynamin-1 extends with respects to functionality and structure.

Appendix

2 Yeast Media: Protocol and stocks:

All containers, instruments and tools used were supplied as sterile sealed units or autoclaved prior to use. Gloves should always be implemented to remove the chance of bacterial infection and all handling of yeast should be performed within a sterile biological cabinet to prevent contamination of samples.

1L YPD:

- To 950ml of dH_2O add 20g difco peptone (2% w/v), 10g yeast extract (1% w/v) (20g agar for solid state cultures) and autoclave at 121℃ for 15 minutes.
- 40% w/v glucose stock typically produced 100ml at a time. Dissolve 40g f glucose powder into 100ml of dH_2O and filter sterilise. This stock should be stored at 4℃ and kept for no longer than one week.
- ONCs were generated as 20ml cultures in sterile 50ml falcon tubes and would comprise
    - 9.5ml of YPD stock
    - 0.5ml of 40% glucose stock→final concentration of 2%
    - Place at angle on shaker for 18h (sufficient for ODs to reach at least 1.3
- DCs were generated as 50ml cultures in 100ml sterile conical flasks and would comprise
    - 47.5ml YPD stock
    - 2.5ml 40% glucose stock→final concentration of 1%.
    - Incubate resultant media at 30℃ on a shaker for 30min prior to use to ensure even distribution of nutrients and to avoid inducing shock genes through sudden temperature change.

3 HPF: Operating Notes

- The ideal consistency of the sample within the membrane carrier for a successful freeze is one analogous to that of “apple sauce”. This consistency retains an optimal water-cell ratio for minimal formation of crystalline ice.
- When using the HPF samples must remain submerged in liquid N_2 post freezing to avoid recrystalisation of water within sample
- Test the machine prior to use such that the pressure can be adjusted if necessary
- Have labelled cryo viles to hand and an LN_2 bath to hand to store samples for transport to cryo storage. Ensure cryo viles are filled with LN_2 as this will act as a temperature buffer while moving your samples from the HPF to the LN_2 bath and eventually into cryo storage.
- Checking the pressure after each firing is essential to ensure at least 2000bar is achieved. Less will allow for recrystallization of water. Samples that achieve less should be discarded to save further wasting of resources.
- Prime the machine immediately after firing to give quicker cycling i.e. time taken to HPF successive samples
- When loading the membrane carriers use of a curved needle is a good way to scrape away excess sample, preventing overloading.

4 Fixation

4.1

- Fixation is essential to substitute out water for solvent. Water left within the sample would sublime under the high vacuum of the TEM destroying the sample and potentially damaging the microscope. At best the microscope would shut down to protect the getter pump and use

would be prohibited until a high enough vacuum was returned for the getter pump to cope with. Further to this the column may require cleaning due to debris which may now obstruct the beam.

-

5 Sequence Alignment with SIM

Sequences:

```
>gi|347447634|pdb|3SNH|A Chain A, Crystal Structure Of Nucleotide-free
Human Dynamin1
GPMEDLIPLVNRLQDAFSAIGQNADLDLPQIAVVGGQSAGKSSVLENFVGRDFLPRGSGIVTRRPLVLQL
VNATTEYAEFLHCKGKKFTDFEEVRLEIEAETDRVTGTNKGISPVPINLRVYSPHVLNLTLVDLPGMTKV
PVGDQPPDIEFQIRDMLMQFVTKENCLILAVSPANSDLANSDALKVAKEVDPQGQRTIGVITKLDLMDEG
TDARDVLENKLLPLRRGYIGVVNRSQKDIDGKKDITAALAAERKFFLSHPSYRHLADRMGTPYLQKVLNQ
QLTNHIRDTLPGLRNKLQSQLLSIEKEVEEYKNFRPDDPARKTKALLQMVQQFAVDFEKRIEGSGDQIDT
YELSGGARINRIFHERFPFELVKMEFDEKELRREISYAIKNAAAAATGLFTPDMAFETIVKKQVKKIREP
CLKCVDMVISELISTVRQCTKKLQQYPRLREEMERIVTTHIREREGRTKEQVMLLIDIELAYMNTNHEDF
IGFANAQQRSNQMNKKKTSGNQDEILVIRKGWLTINNIGIMKGGSKEYWFVLTAENLSWYKDDEEKEKEY
MLSVDNLKLRDVEKGFMSSKHIFALFNTEQRNVYKDYRQLELACETQEEVDSWKASFLRAGVYPERVGDK
EKASETEENGSDSFMHSMDPQLERQVETIRNLVDSYMAIVNKTVRDLMPKTIMHLMINNTKEFIFSELLA
NLYSCGDQNTLMEESAEQAQRRDEMLRMYHALKEALSIIGDIN
```

```
>gi|486405|emb|CAA82071.1| VPS1 [Saccharomyces cerevisiae]
MDEHLISTINKLQDALAPLGGGSQSPIDLPQITVVGSQSSGKSSVLENIVGRDFLPRGTGIVTRRPLVLQ
LINRRPKKSEHAKVNQTANELIDLNINDDDKKKDESGKHQNEGQSEDNKEEWGEFLHLPGKKFYNFDEIR
KEIVKETDKVTGANSGISSVPINLRIYSPHVLTLTLVDLPGLTKVPVGDQPPDIERQIKDMLLKYISKPN
AIILSVNAANTDLANSDGLKLAREVDPEGTRTIGVLTKVDLMDQGTDVIDILAGRVIPLRYGYIPVINRG
QKDIEHKKTIREALENERKFFENHPSYSSKAHYCGTPYLAKKLNSILLHHIRQTLPEIKAKIEATLKKYQ
NELINLGPETMDSASSVVLSMITDFSNEYAGILDGEAKELSSQELSGGARISYVFHETFKNGVDSLDPFD
QIKDSDIRTIMYNSSGSAPSLFVGTEAFEVLVKQQIRRFEEPSLRLVTLVFDELVRMLKQIISQPKYSRY
PALREAISNQFIQFLKDATIPTNEFVVDIIKAEQTYINTAHPDLLKGSQAMVMVEEKLHPRQVAVDPKTG
KPLPTQPSSSKAPVMEEKSGFFGGFFSTKNKKKLAALESPPPVLKATGQMTERETMETEVIKLLISSYFS
IVKRTIADIIPKALMLKLIVKSKTDIQKVLLEKLYGKQDIEELTKENDITIQRRKECKKMVEILRNASQI
VSSV
```

```
>gi|7831|emb|CAA42067.1| dynamin [Drosophila melanogaster]
MDSLITIVNKLQDAFTSLGVHMQLDLPQIAVVGGQSAGKSSVLENFVGKDFLPRGSGIVTRRPLILQLIN
GVTEYGEFLHIKGKKFSSFDEIRKEIEDETDRVTGSNKGISNIPINLRVYSPHVLNLTLIDLPGLTKVAI
GDQPVDIEQQIKQMIFQFIRKETCLILAVTPANTDLANSDALKLAKEVDPQGVRTIGVITKLDLMDEGTD
ARDILENKLLPLRRGYIGVVNRSQKDIEGRKDIHQALAAERKFFLSHPSYRHMADRLGTPYLQRVLNQQL
TNHIRDTLPGLRDKLQKQMLTLEKEVEEFKHFQPGDASIKTKAMLQMIQQLQSDFERTIEGSGSALVNTN
ELSGGAKINRIFHERLRFEIVKMACDEKELRREISFAIRNIHGIRVGLFTPDMAFEAIVKRQIALLKEPV
IKCVDLVVQELSVVVRMCTAKMSRYPRLREETERIITTHVRQREHSCKEQILLLIDFELAYMNTNHEDFI
GFANAQNKSENANKTGTRQLGNQVIRKGHMVIQNLGIMKGGSRPYWFVLTSESISWYKDEDEKEKKFMLP
LDGLKLRDIEQGFMSMSRRVTFALFSPDGRNVYRDYKQLELSCETVEDVESWKASFLRAGVYPEKQETQE
NGDEEGQEQKSASEESSSDPQLERQVETIRNLVDSYMKIVTKTTRDMVPKAIMMLIINNAKDFINGELLA
HLYASGDQAQMMEESAESATRREEMLRMYRACKDALQIIGDVSMATVSSPLPPPVKNDWLPSGLDNPRLS
PPSPGGVRGKPGPPAQSSLGGRNPPLPPSTGRPAPAIPNRPGGGAPPLPGGRPGGSLPPPMLPSRR
```

Results of SIM with:

- Sequence 1: Vps1, (1406 residues)
- Sequence 2: Dynamin (850 residues)

Using the parameters:

- Comparison matrix: BLOSUM62
- Number of alignments computed: 20
- Gap open penalty: 12
- Gap extension penalty: 4

6 Secondary Structure Pediction Using PROFsec

“PROFsec predicts secondary structure elements and solvent accessibility using evolutionary information from multiple sequence alignments and a multi-level system (Rost & Sander 1993). Three states of secondary structure are predicted: helix (H; includes alpha-, pi- and 3_10-helix), (beta-)strand (E = extended strand in beta-sheet conformation of at least two residues length) and loop (L). Secondary structure is predicted by a system of neural networks with an expected average accuracy of more than 72% (Rost & Sander, Proteins, 1994; evaluation of accuracy).”

7 Alignment Data-Clustral Omega

Alignment data obtained using Clustral Omega online analysis package (Goujon et al., 2010; McWilliam et al., 2013; Sievers et al., 2011).

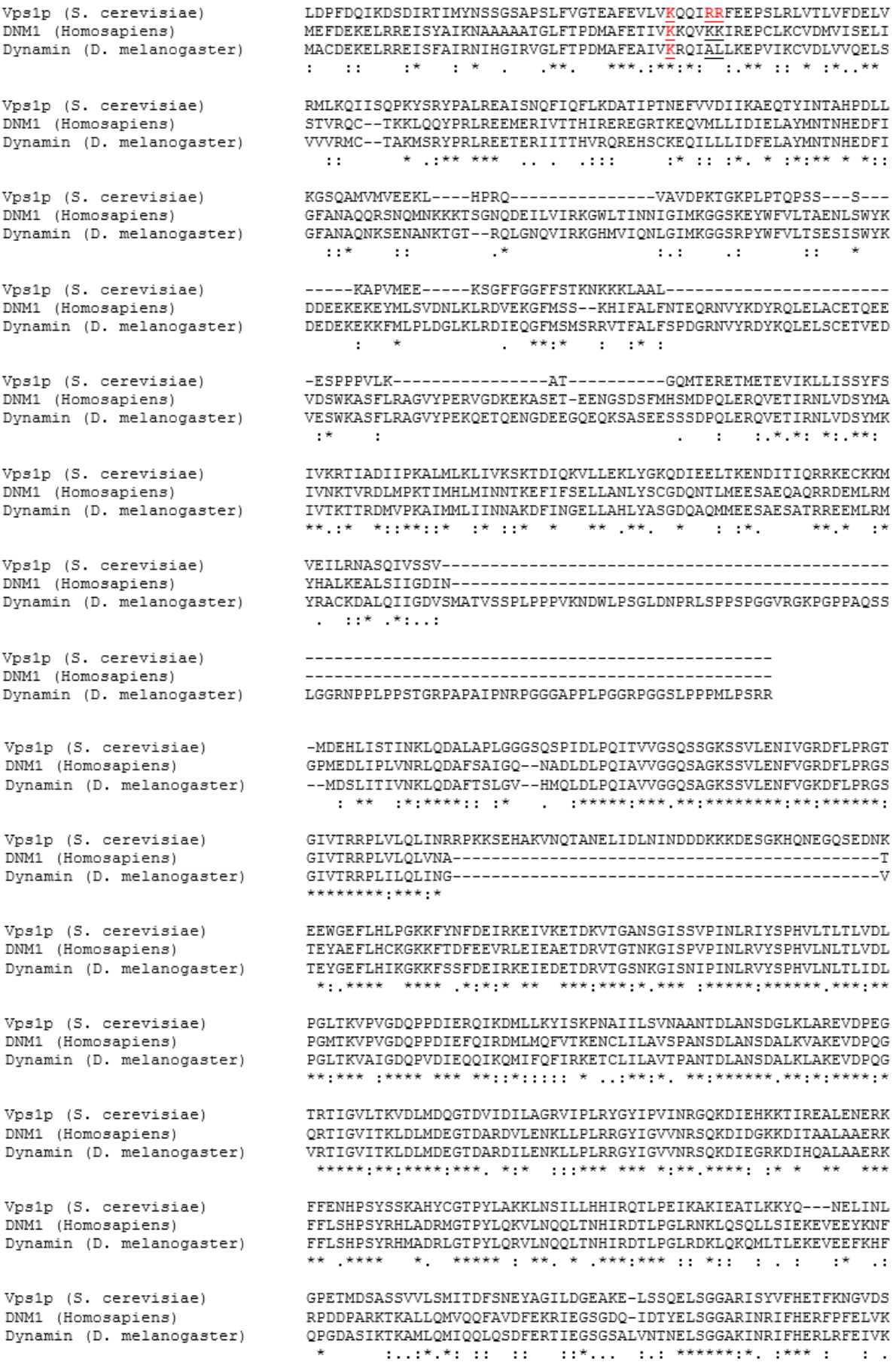
Vps1p (S. cerevisiae)
DNM1 (Homosapiens)
Dynamin (D. melanogaster)

9 Materials

PRODUCT	MANUFACTURE
ACETONE	BDH
AGAR	Melford Laboratories Ltd
AMMONIUM PERSULPHATE	Fischer Sdcientific
BACTERIOLOGICAL PEPTONE	Lab M Ltd
BOVINE SYRUM ALBUMIN	Sigma-Aldrich
CHLOROFORM	VWR
COOMASSIE BLUE	Agar
D-GLUCOSE ANHYDROUS	Fischer Sdcientific
D-SORBITOL	Sigma-Aldrich
EPON	Agar
FM4-64	Invitrogen
GAM 10NM GOLD	Nanoprobes
GLUTARALDEHYDE	Agar
GAGFP	BBInternational
HM20	Polysciences Inc
LECITHIN	Applichem
LR WHITE	Agar
METHACYCLOHEXANE	MERCK
METHANOL	Sigma-Aldrich

MINIMAL SD BASE	Clontech Laboroaries Inc
MAGFP	BBInternational
NACL	Fischer Sdcientific
NAOH	Fischer Sdcientific
OSMIUM TETROXIDE	Agar
POTASSIUM PHOSPHATE BUFFER	Sigma-Aldrich
PROSIEVE 50 GEL SOLUTION	Lonza
RAG 10NM GOLD	BBInternational
SDS	Sigma-Aldrich
SUCROSE	Fischer Sdcientific
TEMED	Fischer Sdcientific
TRIS	Fischer Sdcientific
URA DO SUPPLIMENT	Clontech Laboroaries Inc
URANYL ACETATE	BDH
YEAST EXTRACT POWDER	Lab M Ltd

References

Aghamohammadzadeh, S., & Ayscough, K. R. (2009). Differential requirements for actin during yeast and mammalian endocytosis. *Nature Cell Biology*, *11*(8), 1039–42.

Aguilar, R. C., Watson, H. A., & Wendland, B. (2003). The yeast Epsin Ent1 is recruited to membranes through multiple independent interactions. *The Journal of Biological Chemistry*, *278*(12), 10737–43.

Aguilar, R. C., & Wendland, B. (2003). Ubiquitin: not just for proteasomes anymore. *Current Opinion in Cell Biology*, *15*(2), 184–90.

Arasada, R., & Pollard, T. D. (2011). Distinct roles for F-BAR proteins Cdc15p and Bzz1p in actin polymerization at sites of endocytosis in fission yeast. *Current Biology : CB*, *21*(17), 1450–9.

Ayscough, K. R., Stryker, J., Pokala, N., Sanders, M., Crews, P., & Drubin, D. G. (1997). High rates of actin filament turnover in budding yeast and roles for actin in establishment and maintenance of cell polarity revealed using the actin inhibitor latrunculin-A. *The Journal of Cell Biology*, *137*(2), 399–416.

Boettner, D. R., D'Agostino, J. L., Torres, O. T., Daugherty-Clarke, K., Uygur, A., Reider, A., … Goode, B. L. (2009). The F-BAR protein Syp1 negatively regulates WASp-Arp2/3 complex activity during endocytic patch formation. *Current Biology : CB*, *19*(23), 1979–87.

Bruzzaniti, A., Neff, L., Sanjay, A., Horne, W. C., De Camilli, P., & Baron, R. (2005). Dynamin forms a Src kinase-sensitive complex with Cbl and regulates podosomes and osteoclast activity. *Molecular Biology of the Cell*, *16*(7), 3301–13.

Buser, C., & Drubin, D. G. (2013). Ultrastructural imaging of endocytic sites in Saccharomyces cerevisiae by transmission electron microscopy and immunolabeling. *Microscopy and Microanalysis : The Official Journal of Microscopy Society of America, Microbeam Analysis Society, Microscopical Society of Canada*, *19*(2), 381–92.

Carreno, S., Engqvist-Goldstein, A. E., Zhang, C. X., McDonald, K. L., & Drubin, D. G. (2004). Actin dynamics coupled to clathrin-coated vesicle formation at the trans-Golgi network. *The Journal of Cell Biology*, *165*(6), 781–8.

Chappie, J. S., Acharya, S., Leonard, M., Schmid, S. L., & Dyda, F. (2010). G domain dimerization controls dynamin's assembly-stimulated GTPase activity. *Nature*, *465*(7297), 435–40.

Chappie, J. S., Mears, J. A., Fang, S., Leonard, M., Schmid, S. L., Milligan, R. A., … Dyda, F. (2011). A pseudoatomic model of the dynamin polymer identifies a hydrolysis-dependent powerstroke. *Cell*, *147*(1), 209–22.

Damke, H. (1994). Induction of mutant dynamin specifically blocks endocytic coated vesicle formation. *The Journal of Cell Biology*, *127*(4), 915–934.

Danino, D., Moon, K.-H., & Hinshaw, J. E. (2004). Rapid constriction of lipid bilayers by the mechanochemical enzyme dynamin. *Journal of Structural Biology*, *147*(3), 259–67.

Dawson, J. C., Legg, J. A., & Machesky, L. M. (2006a). Bar domain proteins: a role in tubulation, scission and actin assembly in clathrin-mediated endocytosis. *Trends in Cell Biology*, *16*(10), 493–8.

Dawson, J. C., Legg, J. A., & Machesky, L. M. (2006b). Bar domain proteins: a role in tubulation, scission and actin assembly in clathrin-mediated endocytosis. *Trends in Cell Biology*, *16*(10), 493–8.

Dores, M. R., Schnell, J. D., Maldonado-Baez, L., Wendland, B., & Hicke, L. (2010). The function of yeast epsin and Ede1 ubiquitin-binding domains during receptor internalization. *Traffic (Copenhagen, Denmark)*, *11*(1), 151–60.

Doyle, T., & Botstein, D. (1996). Movement of yeast cortical actin cytoskeleton visualized in vivo. *Proceedings of the National Academy of Sciences of the United States of America*, *93*(9), 3886–91.

Faelber, K., Posor, Y., Gao, S., Held, M., Roske, Y., Schulze, D., … Daumke, O. (2011). Crystal structure of nucleotide-free dynamin. *Nature*, *477*(7366), 556–60.

Ford, M. G. J., Jenni, S., & Nunnari, J. (2011). The crystal structure of dynamin. *Nature*, *477*(7366), 561–6.

Galletta, B. J., Chuang, D. Y., & Cooper, J. A. (2008). Distinct roles for Arp2/3 regulators in actin assembly and endocytosis. *PLoS Biology*, *6*(1), e1.

Garcia, B., Stollar, E. J., & Davidson, A. R. (2012). The importance of conserved features of yeast actin-binding protein 1 (Abp1p): the conditional nature of essentiality. *Genetics*, *191*(4), 1199–211.

Gheorghe, D. M., Aghamohammadzadeh, S., Smaczynska-de Rooij, I. I., Allwood, E. G., Winder, S. J., & Ayscough, K. R. (2008). Interactions between the yeast SM22 homologue Scp1 and actin demonstrate the importance of actin bundling in endocytosis. *The Journal of Biological Chemistry*, *283*(22), 15037–46.

Goujon, M., McWilliam, H., Li, W., Valentin, F., Squizzato, S., Paern, J., & Lopez, R. (2010). A new bioinformatics analysis tools framework at EMBL-EBI. *Nucleic Acids Research*, *38*(Web Server issue), W695–9. doi:10.1093/nar/gkq313

Gu, C., Yaddanapudi, S., Weins, A., Osborn, T., Reiser, J., Pollak, M., … Sever, S. (2010). Direct dynamin-actin interactions regulate the actin cytoskeleton. *The EMBO Journal*, *29*(21), 3593–606.

Herskovits, J. S., Burgess, C. C., Obar, R. A., & Vallee, R. B. (1993). Effects of mutant rat dynamin on endocytosis. *The Journal of Cell Biology*, *122*(3), 565–78.

Hicke, L., & Riezman, H. (1996). Ubiquitination of a yeast plasma membrane receptor signals its ligand-stimulated endocytosis. *Cell*, *84*(2), 277–87.

Hinshaw, J. E., & Schmid, S. L. (1995). Dynamin self-assembles into rings suggesting a mechanism for coated vesicle budding. *Nature*, *374*(6518), 190–2.

Hoepfner, D., van den Berg, M., Philippsen, P., Tabak, H. F., & Hettema, E. H. (2001a). A role for Vps1p, actin, and the Myo2p motor in peroxisome abundance and inheritance in Saccharomyces cerevisiae. *The Journal of Cell Biology*, *155*(6), 979–90.

Hoepfner, D., van den Berg, M., Philippsen, P., Tabak, H. F., & Hettema, E. H. (2001b). A role for Vps1p, actin, and the Myo2p motor in peroxisome abundance and inheritance in Saccharomyces cerevisiae. *The Journal of Cell Biology*, *155*(6), 979–90.

Huang, X., & Miller, W. (1991). A time-efficient, linear-space local similarity algorithm. *Advances in Applied Mathematics*, *12*(3), 337–357.

Itoh, T., & De Camilli, P. (2006). BAR, F-BAR (EFC) and ENTH/ANTH domains in the regulation of membrane-cytosol interfaces and membrane curvature. *Biochimica et Biophysica Acta*, *1761*(8), 897–912.

Itoh, T., Erdmann, K. S., Roux, A., Habermann, B., Werner, H., & De Camilli, P. (2005). Dynamin and the actin cytoskeleton cooperatively regulate plasma membrane invagination by BAR and F-BAR proteins. *Developmental Cell*, *9*(6), 791–804.

Jonsdottir, G. A., & Li, R. (2004). Dynamics of yeast Myosin I: evidence for a possible role in scission of endocytic vesicles. *Current Biology : CB*, *14*(17), 1604–9.

Kaksonen, M., Sun, Y., & Drubin, D. G. (2003). A pathway for association of receptors, adaptors, and actin during endocytic internalization. *Cell*, *115*(4), 475–87.

Kaksonen, M., Toret, C. P., & Drubin, D. G. (2006). Harnessing actin dynamics for clathrin-mediated endocytosis. *Nature Reviews. Molecular Cell Biology*, *7*(6), 404–14.

Kenniston, J. A., & Lemmon, M. A. (2010). Dynamin GTPase regulation is altered by PH domain mutations found in centronuclear myopathy patients. *The EMBO Journal*, *29*(18), 3054–67.

Kim, K., Galletta, B. J., Schmidt, K. O., Chang, F. S., Blumer, K. J., & Cooper, J. A. (2006). Actin-based motility during endocytosis in budding yeast. *Molecular Biology of the Cell*, *17*(3), 1354–63. doi:10.1091/mbc.E05-10-0925

Kishimoto, T., Sun, Y., Buser, C., Liu, J., Michelot, A., & Drubin, D. G. (2011). Determinants of endocytic membrane geometry, stability, and scission. *Proceedings of the National Academy of Sciences of the United States of America*, *108*(44), E979–88.

Klinglmayr, E., Wenger, J., Mayr, S., Bossy-Wetzel, E., & Puehringer, S. (2012). Purification, crystallization and X-ray diffraction analysis of human dynamin-related protein 1 GTPase-GED fusion protein. *Acta Crystallographica. Section F, Structural Biology and Crystallization Communications*, *68*(Pt 10), 1217–21.

Liu, J., Kaksonen, M., Drubin, D. G., & Oster, G. (2006). Endocytic vesicle scission by lipid phase boundary forces. *Proceedings of the National Academy of Sciences of the United States of America*, *103*(27), 10277–82.

Liu, Y.-W., Mattila, J.-P., & Schmid, S. L. (2013). Dynamin-catalyzed membrane fission requires coordinated GTP hydrolysis. *PloS One*, *8*(1), e55691.

Madsen, K. L., Bhatia, V. K., Gether, U., & Stamou, D. (2010). BAR domains, amphipathic helices and membrane-anchored proteins use the same mechanism to sense membrane curvature. *FEBS Letters*, *584*(9), 1848–55.

Mahadev, R. K., Di Pietro, S. M., Olson, J. M., Piao, H. L., Payne, G. S., & Overduin, M. (2007). Structure of Sla1p homology domain 1 and interaction with the NPFxD endocytic internalization motif. *The EMBO Journal*, *26*(7), 1963–71.

Marks, B., Stowell, M. H., Vallis, Y., Mills, I. G., Gibson, A., Hopkins, C. R., & McMahon, H. T. (2001). GTPase activity of dynamin and resulting conformation change are essential for endocytosis. *Nature*, *410*(6825), 231–5.

Martin, A. C., Xu, X.-P., Rouiller, I., Kaksonen, M., Sun, Y., Belmont, L., … Drubin, D. G. (2005). Effects of Arp2 and Arp3 nucleotide-binding pocket mutations on Arp2/3 complex function. *The Journal of Cell Biology*, *168*(2), 315–28.

McDonald, K. L. (2013). Out with the old and in with the new: rapid specimen preparation procedures for electron microscopy of sectioned biological material. *Protoplasma*.

McWilliam, H., Li, W., Uludag, M., Squizzato, S., Park, Y. M., Buso, N., … Lopez, R. (2013). Analysis Tool Web Services from the EMBL-EBI. *Nucleic Acids Research*, *41*(Web Server issue), W597–600.

Mears, J. A., Lackner, L. L., Fang, S., Ingerman, E., Nunnari, J., & Hinshaw, J. E. (2011). Conformational changes in Dnm1 support a contractile mechanism for mitochondrial fission. *Nature Structural & Molecular Biology*, *18*(1), 20–6.

Merrifield, C. J., Feldman, M. E., Wan, L., & Almers, W. (2002). Imaging actin and dynamin recruitment during invagination of single clathrin-coated pits. *Nature Cell Biology*, *4*(9), 691–8.

Merrifield, C. J., Perrais, D., & Zenisek, D. (2005). Coupling between clathrin-coated-pit invagination, cortactin recruitment, and membrane scission observed in live cells. *Cell*, *121*(4), 593–606.

Mishra, R., Smaczynska-de Rooij, I. I., Goldberg, M. W., & Ayscough, K. R. (2011). Expression of Vps1 I649K a self-assembly defective yeast dynamin, leads to formation of extended endocytic invaginations. *Communicative & Integrative Biology*, *4*(1), 115–7.

Mooren, O. L., Kotova, T. I., Moore, A. J., & Schafer, D. A. (2009). Dynamin2 GTPase and cortactin remodel actin filaments. *The Journal of Biological Chemistry*, *284*(36), 23995–4005.

Morton, W. M., Ayscough, K. R., & McLaughlin, P. J. (2000). Latrunculin alters the actin-monomer subunit interface to prevent polymerization. *Nature Cell Biology*, *2*(6), 376–8.

Nannapaneni, S., Wang, D., Jain, S., Schroeder, B., Highfill, C., Reustle, L., … Kim, K. (2010). The yeast dynamin-like protein Vps1:vps1 mutations perturb the internalization and the motility of endocytic vesicles and endosomes via disorganization of the actin cytoskeleton. *European Journal of Cell Biology*, *89*(7), 499–508.

Nothwehr, S. F., Conibear, E., & Stevens, T. H. (1995). Golgi and vacuolar membrane proteins reach the vacuole in vps1 mutant yeast cells via the plasma membrane. *The Journal of Cell Biology*, *129*(1), 35–46.

Ochoa, G. C., Slepnev, V. I., Neff, L., Ringstad, N., Takei, K., Daniell, L., … De Camilli, P. (2000). A functional link between dynamin and the actin cytoskeleton at podosomes. *The Journal of Cell Biology*, *150*(2), 377–89.

Ramachandran, R. (2011). Vesicle scission: dynamin. *Seminars in Cell & Developmental Biology*, *22*(1), 10–7.

Röthlisberger, S., Jourdain, I., Johnson, C., Takegawa, K., & Hyams, J. S. (2009). The dynamin-related protein Vps1 regulates vacuole fission, fusion and tubulation in the fission yeast, Schizosaccharomyces pombe. *Fungal Genetics and Biology : FG & B*, *46*(12), 927–35.

Sever, S. (2002). Dynamin and endocytosis. *Current Opinion in Cell Biology*, *14*(4), 463–7.

Shin, H. W., Takatsu, H., Mukai, H., Munekata, E., Murakami, K., & Nakayama, K. (1999). Intermolecular and interdomain interactions of a dynamin-related GTP-binding protein, Dnm1p/Vps1p-like protein. *The Journal of Biological Chemistry*, *274*(5), 2780–5.

Sievers, F., Wilm, A., Dineen, D., Gibson, T. J., Karplus, K., Li, W., … Higgins, D. G. (2011). Fast, scalable generation of high-quality protein multiple sequence alignments using Clustal Omega. *Molecular Systems Biology*, *7*, 539.

Smaczynska-de Rooij, I. I., Allwood, E. G., Aghamohammadzadeh, S., Hettema, E. H., Goldberg, M. W., & Ayscough, K. R. (2010). A role for the dynamin-like protein Vps1 during endocytosis in yeast. *Journal of Cell Science*, *123*(Pt 20), 3496–506.

Smaczynska-de Rooij, I. I., Allwood, E. G., Mishra, R., Booth, W. I., Aghamohammadzadeh, S., Goldberg, M. W., & Ayscough, K. R. (2012). Yeast dynamin Vps1 and amphiphysin Rvs167 function together during endocytosis. *Traffic (Copenhagen, Denmark)*, *13*(2), 317–28.

Song, B. D., Leonard, M., & Schmid, S. L. (2004). Dynamin GTPase domain mutants that differentially affect GTP binding, GTP hydrolysis, and clathrin-mediated endocytosis. *The Journal of Biological Chemistry*, *279*(39), 40431–6.

Song, B. D., Yarar, D., & Schmid, S. L. (2004). An assembly-incompetent mutant establishes a requirement for dynamin self-assembly in clathrin-mediated endocytosis in vivo. *Molecular Biology of the Cell*, *15*(5), 2243–52.

Soulard, A., Friant, S., Fitterer, C., Orange, C., Kaneva, G., Mirey, G., & Winsor, B. (2005). The WASP/Las17p-interacting protein Bzz1p functions with Myo5p in an early stage of endocytosis. *Protoplasma*, *226*(1-2), 89–101.

Spiess, M., de Craene, J.-O., Michelot, A., Rinaldi, B., Huber, A., Drubin, D. G., … Friant, S. (2013). Lsb1 is a negative regulator of las17 dependent actin polymerization involved in endocytosis. *PloS One*, *8*(4), e61147.

Studer, D., Humbel, B. M., & Chiquet, M. (2008). Electron microscopy of high pressure frozen samples: bridging the gap between cellular ultrastructure and atomic resolution. *Histochemistry and Cell Biology*, *130*(5), 877–89.

Sun, Y., Martin, A. C., & Drubin, D. G. (2006). Endocytic internalization in budding yeast requires coordinated actin nucleation and myosin motor activity. *Developmental Cell*, *11*(1), 33–46.

Takahashi, K., Otomo, M., Yamaguchi, N., Nakashima, H., & Miyoshi, H. (2012). Replacement of Arg-386 with Gly in dynamin 1 middle domain reduced GTPase activity and oligomer stability in the absence of lipids. *Bioscience, Biotechnology, and Biochemistry*, *76*(12), 2195–200.

Terzakis, J. A. (1968). Uranyl acetate, a stain and a fixative. *Journal of Ultrastructure Research*, *22*(1), 168–84.

Toret, C. P., Lee, L., Sekiya-Kawasaki, M., & Drubin, D. G. (2008). Multiple pathways regulate endocytic coat disassembly in Saccharomyces cerevisiae for optimal downstream trafficking. *Traffic (Copenhagen, Denmark)*, *9*(5), 848–59.

Toshima, J. Y., Toshima, J., Kaksonen, M., Martin, A. C., King, D. S., & Drubin, D. G. (2006). Spatial dynamics of receptor-mediated endocytic trafficking in budding yeast revealed by using fluorescent alpha-factor derivatives. *Proceedings of the National Academy of Sciences of the United States of America*, *103*(15), 5793–8.

Tuma, P. L., Stachniak, M. C., & Collins, C. A. (1993). Activation of dynamin GTPase by acidic phospholipids and endogenous rat brain vesicles. *The Journal of Biological Chemistry*, *268*(23), 17240–6.

Urbanek, A. N., Smith, A. P., Allwood, E. G., Booth, W. I., & Ayscough, K. R. (2013). A novel actin-binding motif in Las17/WASP nucleates actin filaments independently of Arp2/3. *Current Biology : CB*, *23*(3), 196–203.

Vallis, Y., Wigge, P., Marks, B., Evans, P. R., & McMahon, H. T. (1999). Importance of the pleckstrin homology domain of dynamin in clathrin-mediated endocytosis. *Current Biology : CB*, *9*(5), 257–60.

Van der Bliek, A. M. (1999). Functional diversity in the dynamin family. *Trends in Cell Biology*, *9*(3), 96–102.

Vater, C. A., Raymond, C. K., Ekena, K., Howald-Stevenson, I., & Stevens, T. H. (1992). The VPS1 protein, a homolog of dynamin required for vacuolar protein sorting in Saccharomyces cerevisiae, is a GTPase with two functionally separable domains. *The Journal of Cell Biology*, *119*(4), 773–86.

Vizeacoumar, F. J., Vreden, W. N., Fagarasanu, M., Eitzen, G. a, Aitchison, J. D., & Rachubinski, R. a. (2006). The dynamin-like protein Vps1p of the yeast Saccharomyces cerevisiae associates with peroxisomes in a Pex19p-dependent manner. *The Journal of Biological Chemistry*, *281*(18), 12817–23.

Wang, D., Sletto, J., Tenay, B., & Kim, K. (2011). Yeast dynamin implicated in endocytic scission and the disassembly of endocytic components. *Communicative & Integrative Biology*, *4*(2), 178–81.

Warren, D. T., Andrews, P. D., Gourlay, C. W., & Ayscough, K. R. (2002). Sla1p couples the yeast endocytic machinery to proteins regulating actin dynamics. *Journal of Cell Science*, *115*(Pt 8), 1703–15.

Weinberg, J., & Drubin, D. G. (2012). Clathrin-mediated endocytosis in budding yeast. *Trends in Cell Biology*, *22*(1), 1–13.

Wenger, J., Klinglmayr, E., Fröhlich, C., Eibl, C., Gimeno, A., Hessenberger, M., … Goettig, P. (2013). Functional mapping of human dynamin-1-like GTPase domain based on x-ray structure analyses. *PloS One*, *8*(8), e71835.

Wong, M. H., Meng, L., Rajmohan, R., Yu, S., & Thanabalu, T. (2010). Vrp1p-Las17p interaction is critical for actin patch polarization but is not essential for growth or fluid phase endocytosis in S. cerevisiae. *Biochimica et Biophysica Acta*, *1803*(12), 1332–46.

Youn, J.-Y., Friesen, H., Kishimoto, T., Henne, W. M., Kurat, C. F., Ye, W., … Andrews, B. J. (2010). Dissecting BAR domain function in the yeast Amphiphysins Rvs161 and Rvs167 during endocytosis. *Molecular Biology of the Cell*, *21*(17), 3054–69.

Yu, X., & Cai, M. (2004). The yeast dynamin-related GTPase Vps1p functions in the organization of the actin cytoskeleton via interaction with Sla1p. *Journal of Cell Science*, *117*(Pt 17), 3839–53.

Zeng, G., Yu, X., & Cai, M. (2001). Regulation of yeast actin cytoskeleton-regulatory complex Pan1p/Sla1p/End3p by serine/threonine kinase Prk1p. *Molecular Biology of the Cell*, *12*(12), 3759–72.